



저작자표시-비영리-변경금지 2.0 대한민국

이용자는 아래의 조건을 따르는 경우에 한하여 자유롭게

- 이 저작물을 복제, 배포, 전송, 전시, 공연 및 방송할 수 있습니다.

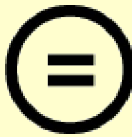
다음과 같은 조건을 따라야 합니다:



저작자표시. 귀하는 원저작자를 표시하여야 합니다.



비영리. 귀하는 이 저작물을 영리 목적으로 이용할 수 없습니다.



변경금지. 귀하는 이 저작물을 개작, 변형 또는 가공할 수 없습니다.

- 귀하는, 이 저작물의 재이용이나 배포의 경우, 이 저작물에 적용된 이용허락조건을 명확하게 나타내어야 합니다.
- 저작권자로부터 별도의 허가를 받으면 이러한 조건들은 적용되지 않습니다.

저작권법에 따른 이용자의 권리는 위의 내용에 의하여 영향을 받지 않습니다.

이것은 [이용허락규약\(Legal Code\)](#)을 이해하기 쉽게 요약한 것입니다.

[Disclaimer](#)

Ph.D. Dissertation of Science in Agricultural Biotechnology

**Functional beverages with antioxidant
and anti-obesity properties and
enhanced sensory quality using kimchi
lactic acid bacteria**

김치 유산균을 활용한 항산화 및 항비만 기능성
음료와 관능 품질 개선 음료 개발

February 2025

Graduate School of
Seoul National University
Department of Agricultural Biotechnology
Biomodulation Major

Moeun Lee

Functional beverages with antioxidant and anti-obesity properties and enhanced sensory quality using kimchi lactic acid bacteria

Advisor: Ki Won Lee

Submitting a Ph.D. Dissertation of
Agricultural Biotechnology

February 2025

Department of Agricultural Biotechnology
Seoul National University
Biomodulation Major

Moeun Lee

Confirming the Ph.D. Dissertation written by

Moeun Lee

February 2025

Chair	<u>Do Yup Lee</u>	(Seal)
Vice Chair	<u>Ki Won Lee</u>	(Seal)
Examiner	<u>Jung Han Yoon Park</u>	(Seal)
Examiner	<u>Do-Won Jeong</u>	(Seal)
Examiner	<u>Ji Yoon Chang</u>	(Seal)

Abstract

Moeun Lee

Department of Agricultural Biotechnology

The Graduate School

Seoul National University

Emerging probiotic food applications, such as plant-based products, beverages, and cereal, offer alternative means of delivering probiotics to consumers. This study explored the functional potential of kimchi-derived lactic acid bacteria (LAB) strains, focusing on antioxidant and anti-obesity properties, metabolite profiling, and sensory enhancements in fermented foods. Among 35,000 LAB strains isolated, *Companilactobacillus allii* WiKim39 and *Lactococcus lactis* WiKim0124 were identified as highly effective in antioxidant activities through transcriptomic and proteomic analyses, revealing mechanisms such as antioxidant production and reactive oxygen species regulation. Fermentation of vegetable juices (VJ) with these strains increased phenolic compounds and metabolites like d-leucic acid, indole-3-lactic acid, and 3-phenyllactic acid, correlating with improved antioxidant and anti-obesity effects *in vitro* and *in vivo*. The study further demonstrated that LAB-fermented VJ showed greater bioavailability of beneficial metabolites when incorporated into food matrices, highlighting the synergistic effects of probiotics and substrates. Enhanced sensory

attributes were achieved in malt beverages fermented with *Levilactobacillus brevis* WiKim0194, characterized by increased sourness, reduced bitterness, and improved aroma profiles. In malt beverages, sensory improvements were attributed to the reduction of off-flavors and the production of desirable flavor compounds, such as vanillin, citronellol, and β -damascenone, alongside decreased bitterness from compounds like chlorobenzene and 2-acetylpyridine. The study emphasizes the importance of selecting appropriate LAB strains to optimize fermentation processes for both health benefits and sensory qualities. By demonstrating the antioxidant, anti-obesity, and sensory improvement effects of specific LAB strains, such as WiKim39, WiKim0124, and WiKim0194, this research highlights their potential as starter cultures in various food applications. The integration of advanced metabolomics and sensory analysis technologies, including UPLC-QTOF-MS, GC-MS, electronic tongue, and electronic nose, provided valuable insights into the mechanisms underlying these benefits. By identifying strains with superior antioxidant and anti-obesity properties, such as WiKim39 and WiKim0124, alongside sensory-enhancing strains like WiKim0194, the study showcases the multifaceted applications of LAB in developing functional foods. These findings advocate for the strategic selection of LAB as functional supplements and starter cultures, offering a pathway to meet consumer demands for nutritious, flavorful, and health-promoting fermented products. This work contributes not only to academic advancements in probiotics and fermentation but also to the food industry's

efforts to innovate and expand the diversity of functional food offerings globally.

Keyword: Probiotics, starter culture, functional foods, metabolomics, sensory analysis

Student Number: 2021-38950

Contents

Abstract.....	i
Contents	iv
List of figures	xi
List of tables	xv
Chapter 1. Background.....	1
1.1. Probiotic foods and industrial trends.....	2
1.1.1. Challenges and opportunities for domestically developed LAB....	3
1.1.2. Strain-specific functionalities and screening methods for LAB	4
1.1.3. LAB isolated from kimchi.....	6
1.2. Functionalities of probiotic fermented products.....	10
1.2.1. Antioxidant properties	10
1.2.2. Antiobesity properties	12
1.3. Fermented plant-based beverages as suitable probiotic carrier.....	16
1.3.1. Fruits and vegetables.....	17
1.3.2. Cereals.....	18
1.4. Aroma and flavor production.....	19
1.5. Concluding remarks and future perspectives.....	20
1.6. Summary.....	24
1.7. References	25

Chapter 2. Transcriptome responses of lactic acid bacteria isolated from kimchi under hydrogen peroxide exposure	34
Abstract.....	35
2.1. Introduction	37
2.2. Material and methods	40
2.2.1. Bacterial strains and culture conditions	41
2.2.2. H ₂ O ₂ resistance of LAB strains.....	42
2.2.3. Measuring the antioxidant activity of LAB strains	42
2.2.3.1. Collection of intact cells and preparation of cell-free supernatant and cell-free extracts.....	42
2.2.3.2. 2,2-Diphenyl-1-picrylhydrazyl free radical scavenging activity	42
2.2.3.3. 2,2' -azino-bis(3-ethylbenzothiazoline-6-sulfonic acid) radical scavenging activity	43
2.2.3.4. Hydroxyl radical scavenging activity	44
2.2.3.5. Ferric reducing antioxidant power	45
2.2.3.6. Inhibition of lipid peroxidation	45
2.2.3.7. Antioxidant enzyme activity	46
2.2.4. Scanning electron microscopy	47
2.2.5. RNA isolation, sequencing, and analysis	47
2.2.5.1. RNA isolation and sequencing.....	47
2.2.5.2. Bioinformatics analysis.....	48
2.2.6. Protein extraction, two-dimensional polyacrylamide gel	

electrophoresis	48
2.2.6.1. Image data analysis and protein identification	49
2.2.6.2. Bioinformatics analysis.....	50
2.2.7. Statistical analyses.....	50
2.3. Results	52
2.3.1. H ₂ O ₂ tolerance and antioxidant activity	52
2.3.2. Antioxidant enzyme activity.....	55
2.3.3. Changes in bacterial morphology under oxidative stress.....	57
2.3.4. Transcriptomic signatures under oxidative stress.....	59
2.3.5. Proteomic signatures under oxidative stress	74
2.3.6. Proteins or genes associated with the stress response from three LAB strains	80
2.4. Discussion.....	81
2.5. Conclusion.....	86
2.6. References	87
Chapter 3. UPLC-QTOF-MS/MS and GC-MS Characterization of Metabolites in Vegetable Juice Fermented Using Lactic Acid Bacteria from Kimchi and Their Antioxidant Potential.....	95
Abstract.....	96
3.1. Introduction	97
3.2. Material and methods	99
3.2.1. Bacterial strains and culture conditions	99

3.2.2. Preparation and fermentation of VJ	99
3.2.3. Proximate composition and total phenolic and flavonoid concentrations.....	100
3.2.4. Antioxidant properties	101
3.2.4.1. 2,2-Diphenyl-1-Picrylhydrazyl radical scavenging activity	101
3.2.4.2. Hydroxyl radical scavenging activity	102
3.2.4.3. Ferric reducing antioxidant power	103
3.2.4.4. Inhibition rate of lipid peroxidation.....	103
3.2.5. VJ fermentation metabolite analysis	103
3.2.5.1. UPLC-QTOF-MS/MS profile.....	103
3.2.5.2. GC-MS profile	107
3.2.6. Statistical analysis	108
3.3. Results and discussion.....	109
3.3.1. Proximate composition and TP and TF content	109
3.3.2. Antioxidant capacity of fermented VJ.....	113
3.3.3. Phytochemical compounds formed during VJ fermentation.....	115
3.3.3.1. UPLC-QTOF-MS/MS characterization of fermented VJ	115
3.3.3.2. GC-MS characterization of fermented VJ	126
3.3.3.3. Comparative analysis of fermented VJ metabolites and their antioxidant properties	132
3.4. Conclusion.....	136
3.5. References	137

Chapter 4. Anti-obesity effect of vegetable juice fermented with lactic acid bacteria isolated from kimchi in C57BL/6J mice and human mesenchymal stem cells.....	145
Abstract.....	146
4.1. Introduction	148
4.2. Material and methods	151
4.2.1. Bacterial strains.....	151
4.2.2. Preparation and fermentation of VJ	151
4.2.3. Cell culture and adipogenic differentiation	152
4.2.4. <i>In vitro</i> cytotoxicity test	153
4.2.5. Antibody array analysis.....	153
4.2.6. Bioinformatic analysis	154
4.2.7. Animals.....	155
4.2.8. Dietary dosage information.....	156
4.2.9. Histological analysis	156
4.2.10. Plasma biochemical indicators	156
4.2.11. Quantitative reverse transcription-polymerase chain reaction	157
4.2.12. Statistical analysis	157
4.3. Results	158
4.3.1. Effects of LAB fermented VJ on the differentiated hMSCs and adipogenic proteins	158
4.3.2. Effects of LAB and LAB fermented VJs administration on body weight, plasma lipid profile, and adipocyte size in mice	167

4.3.3. Expression of adipogenic transcription factors and related genes ...	173
4.3.4. Inhibition of intracellular lipid accumulation of LAB fermented VJ metabolites in hMSCs.....	175
4.4. Discussion.....	177
4.5. Conclusion.....	181
4.6. References	182
Chapter 5. Kimchi lactic acid bacteria starter culture: Impact on fermented malt beverage volatile profile, sensory analysis, and physicochemical traits	189
Abstract.....	190
5.1. Introduction	192
5.2. Materials and Methods	195
5.2.1. Wort preparation and starter culture	195
5.2.2. Microbial growth.....	197
5.2.3. Chemical analyses	197
5.2.4. High-Performance Liquid Chromatography	197
5.2.5. Electronic tongue analysis.....	198
5.2.6. Electronic nose analysis	198
5.2.7. Statistical analysis	199
5.3. Results and discussion	200
5.3.1. Strain selection	200

5.3.2. Changes in sugar and organic acid concentrations throughout fermentation	203
5.3.3. Sensory characteristics of fermented malt beverage	206
5.3.3.1. E-tongue analysis	206
5.3.3.2. Key aroma compounds	209
5.4. Conclusion	212
5.5. References	213
Conclusions	220
국문초록	222

List of Figures

Fig. 1.1. Schematic illustration of kimchi LAB isolation and screening methods for strain-specific functionalities.	9
Fig. 1.2. Schematic illustration of oxidative stress, obesity, and microbiome interaction.	14
Fig. 1.3. Strain selection results based on preliminary experiments... 	23
Fig. 2.1. H₂O₂ resistance of five lactic acid bacteria (LAB) strains isolated from kimchi and a reference strain	53
Fig. 2.2. Antioxidant potential of five lactic acid bacteria (LAB) strains isolated from kimchi and a reference strain.....	54
Fig. 2.3. Surface analysis of LAB after H₂O₂ treatment	58
Fig. 2.4. Transcriptomic signatures of WiKim38, WiKim39, and WiKim0124 grown under oxidative stress	60
Fig. 2.5. Gene Ontology (GO) enrichments analysis of LAB strains exposed to 0 mM and 2.0 mM H₂O₂	61
Fig. 2.6. Gene ontology (GO) categorization of differentially expressed genes (DEGs) of WiKim38, WiKim39, and WiKim0124 grown under different levels of oxidative stress (1–3 mM H₂O₂) under biological processes.....	71
Fig. 2.7. Gene ontology (GO) categorization of differentially expressed	

genes (DEGs) of WiKim38, WiKim39, and WiKim0124 grown under different levels of oxidative stress (1–3 mM H ₂ O ₂) under cellular components.....	72
Fig. 2.8. Two-dimensional gel electrophoresis images of proteins extracted from WiKim38 grown under exposure to 2.5 mM H ₂ O ₂	73
Fig. 2.9. Two-dimensional gel electrophoresis images of proteins extracted from WiKim39 grown under exposure to 2.5 mM H ₂ O ₂	76
Fig. 2.10. Two-dimensional gel electrophoresis images of proteins extracted from WiKim0124 grown under exposure to 2.5 mM H ₂ O ₂	77
Fig. 2.11. Proteomic analysis of WiKim38, WiKim39, and WiKim0124 DEPs exposed to 2.5 mM H ₂ O ₂	78
Fig. 2.12. Proteomic analysis of WiKim38, WiKim39, and WiKim0124 DEPs exposed to 2.5 mM H ₂ O ₂	79
Fig. 3.1. Antioxidant capacities of vegetable juice fermented with lactic acid bacteria.....	114
Fig. 3.2. Identification of phytochemical profile in fermented or non-fermented vegetable juice.....	118
Fig. 3.3. Total Ion Chromatogram obtained using UPLC-QTOF-MS/MS in VJ.....	119
Fig. 3.4. Total Ion Chromatogram obtained using UPLC-QTOF-MS/MS in VJ+WiKim39.....	120
Fig. 3.5. Total Ion Chromatogram obtained using UPLC-QTOF-MS/MS	

in VJ+WiKim0124.....	121
Fig. 3.6. Total Ion Chromatogram obtained by UPLC-QTOF-MS/MS in VJ.....	122
Fig. 3.7. Total Ion Chromatogram obtained by UPLC-QTOF-MS/MS in VJ+WiKim39.....	123
Fig. 3.8. Total Ion Chromatogram obtained by UPLC-QTOF-MS/MS in VJ+WiKim0124.....	124
Fig. 3.9. Heatmap	134
Fig. 3.10. The production of key metabolites in VJ inoculated with other <i>Lactobacillaceae</i> strains.	135
Fig. 4.1. Effect of LAB and LAB fermented VJ on cell viability (a, c) and adipogenic differentiation (b, d)	160
Fig. 4.2. Identification of differentially expressed proteins (DEPs) in human mesenchymal stem cells treated with WiKim39 and WiKim0124 fermented vegetable juices using antibody array. Array map used in the panel	161
Fig. 4.3. Identification of differentially expressed proteins (DEPs) in human mesenchymal stem cells treated with WiKim39 and WiKim0124 fermented vegetable juices using antibody array. Human antibody array panel used in this study (Raw image files).....	162
Fig. 4.4 Analysis of the antibody array. Hierarchical cluster analysis of differentially expressed proteins (DEPs).....	165

Fig. 4.5 Analysis of the antibody array. Scatter plots of enriched GO pathways relevant to biological processes and molecular function.....	166
Fig. 4.6. Effects of WiKim39 and WiKim0124 fermented vegetable juice on high-fat diet-induced obese mice.....	168
Fig. 4.7. Effects of WiKim39 and WiKim0124 fermented vegetable juice on high-fat diet-induced obese mice.....	169
Fig. 4.8. Effects of WiKim39 and WiKim0124 fermented vegetable juice administration in high-fat diet-induced obese mice	171
Fig. 4.9. Effects of WiKim39 and WiKim0124 fermented vegetable juice administration in high-fat diet-induced obese mice	172
Fig. 4.10. Effects of WiKim39 and WiKim0124 fermented vegetable juices on the expression of genes related to lipid metabolism in the epididymal adipose tissues of high-fat diet-induced obese mice	174
Fig. 4.11. Effects of potential anti-adipogenic agents present in vegetable juice fermented products on human mesenchymal stem cells.....	176
Fig. 5.1. Properties of malt wort beverages during fermentation using eight LAB strains.....	202
Fig. 5.2. Metabolomic profiles of malt wort beverages	205
Fig. 5.3. Sensory attribute profiles of WiKim0194-fermented malt wort constructed by e-tongue.....	208
Fig. 5.4. Comparison of aroma compounds—e-nose signal values in WiKim0194-fermented malt wort	211

List of Tables

Table 2.1. Lactic acid bacteria strains used in this study	41
Table 2.2. Superoxide dismutase (SOD) and glutathione peroxidase (GPX) activities of lactic acid bacteria strains under different conditions	56
Table 2.3. Mass spectrometry identification and bioinformatic analysis of 20 differently expressed proteins of Wikim38	62
Table 2.4. Mass spectrometry identification and bioinformatic analysis of 21 differently expressed proteins of Wikim39	65
Table 2.5. Mass spectrometry identification and bioinformatic analysis of 14 differently expressed proteins of Wikim0124	68
Table 3.1. Detailed analytical conditions of UPLC-QTOF-MS/MS.....	106
Table 3.2. Proximate composition, TP and TF content of non-fermented or fermented vegetable juice with LAB.....	112
Table 3.3. Tentatively identified compounds from probiotic vegetable juice samples by UPLC-QTOF-MS/MS under negative ion mode.....	117
Table 3.4. Quantitative characterization of significant phytochemical compounds in VJ samples by UPLC-QTOF-MS/MS	125
Table 3.5. Tentatively identified compounds from probiotic vegetable juice samples by GC-MS.....	129

Table 4.1. Organ and adipose tissue weights of mice fed high-fat diet and
LAB-fermented VJs for 8 weeks 170

Table 5.1. Lactic acid bacteria strains used in this study 196

Chapter 1. Background

Background

1.1. Probiotic foods and industrial trends

In recent years, probiotic foods have drawn attention for their health benefits, undergoing multidimensional studies for various technological and industrial applications. In 2021, the worldwide market for probiotic ingredients, supplements, and foods attained a value of USD 61.15 billion, with estimates suggesting it will escalate at a compound annual growth rate of 7.7% by 2027 throughout the forecast period (<https://www.polarismarketresearch.com/industry-analysis/probiotics-market>, accessed on 04 June 2024). The growing demand for probiotic products is due to their well-established effectiveness in addressing digestive health and alleviating related disorders (Spacova et al., 2023).

Probiotics, as functional foods, are gaining prominence in both basic and clinical research. Their rising popularity has also made them a profitable area of economic interest (Sakandar & Zhang, 2021). The well-known definition of probiotics suggests their use by healthy individuals to prevent certain conditions or enhance diverse physiological functions (Sanders & Marco, 2010). Currently, probiotics are derived from various genera and species, including yeast and bacteria such as bacilli, bifidobacteria, and lactic acid bacteria (LAB) (Behnsen, Deriu, Sassone-Corsi, & Raffatellu,

2013). They're incorporated into a variety of foods, including cheese, ice cream, yogurt, nutrition bars, snacks, breakfast cereals, and infant formula, and are also available as freeze-dried capsules (Suez, Zmora, Segal, & Elinav, 2019).

The status of a microorganism as a probiotic is determined only once its potential health benefits are confirmed through comprehensive, stringent, and well-structured research involving both animal and human subjects. Consequently, it's crucial to consistently study and gather additional insights regarding how probiotics impacts specific biomarkers. The effects of probiotics administered as freeze-dried pills or powders on chronic health conditions have been widely researched. However, there is a lack of sufficient studies focusing on probiotic fermented products (Ma et al., 2020). Therefore, further research is necessary to advance the commercial application of probiotic products as natural remedies for health-related concerns.

1.1.1. Challenges and opportunities for domestically developed LAB

LAB have been studied to a limited extent, with only a few strains successfully commercialized. Furthermore, their application across various food matrices remains challenging. The limited presence of domestically developed LAB can be attributed to several biological, economic, and

research-related factors. First, although traditional Korean fermented foods contain LAB, with only a few dominant strains. This suggests a limited diversity of LAB available for commercial application (Lee et al., 2017). Second, technical limitations present another barrier. While some domestic LAB strains may demonstrate excellent functionality, they often fail to meet commercial criteria, such as scalability in mass culture or storage stability. Moreover, there is a lack of genomic information and functional analysis data for many domestic strains, making them less competitive in global research and commercialization (Cha et al., 2024). Finally, consumer perception plays a role. Many consumers in Korea have a preference for well-known international LAB strains, such as *Lactobacillus rhamnosus* GG, which can limit the market demand for domestic strains (Ananthan et al., 2024).

To address these challenges, it is crucial to expand research on LAB derived from traditional Korean fermented foods and increase investments in research and development by both the government and private sector. Enhancing cultivation, mass production, and storage technologies for domestic strains is essential. With these measures, domestically developed LAB can become more competitive in the global market.

1.1.2. Strain-specific functionalities and screening methods for LAB

The functionality of LAB is highly strain-specific, meaning each strain possesses unique physiological and functional characteristics. Even within the same species, individual strains can exhibit distinct properties, such as antimicrobial activity, immunomodulation, gastrointestinal survival, or flavor enhancement (Peluzio, Martinez, & Milagro, 2021). Therefore, tailored screening methods must be applied to select LAB strains that meet specific functional goals. Strain-specific screening is critical for identifying LAB strains that exhibit targeted functionalities for use in probiotics, fermentation, or other industrial applications. LAB strains differ significantly in their abilities to perform under specific conditions, such as pH levels, temperature, and nutrient availability, further emphasizing the need for precise selection processes (Yang et al., 2018).

In probiotic fermented beverage applications, the screening of LAB focuses on their viability in food matrices, growth potential, and dominance. These traits are essential for ensuring the survival of LAB and their effective interaction with substrates in the food matrix (Amenu & Bacha, 2023). In the context of food fermentation, LAB strains are evaluated for their ability to produce flavor-enhancing compounds, such as organic acids, esters, and peptides, which contribute to improved taste, aroma, and texture (Yang et al., 2024). Additionally, LAB strains are screened for the production of bioactive compounds, including antioxidants, exopolysaccharides, which are linked to functional benefits such as stress reduction and anti-obesity effects

(Choi et al., 2021). To refine and enhance the screening process, modern technologies like genomics, metabolomics, and proteomics are employed to identify genetic and metabolic traits associated with these functionalities (Ning et al., 2021). This allows for the precise selection of LAB strains tailored for specific industrial, nutritional, and health-related applications.

1.1.3. Lactic acid bacteria isolated from kimchi

Kimchi is a traditional Korean side dish with functional properties, and certain LAB are utilized as health-promoting organisms. While various microorganisms participate in the fermentation of kimchi, LAB are the predominant fermentative microbes (Lee, Song, Park, & Chang, 2019). Natural fermentation can often produce end products with inconsistent quality. To address these challenges, the use of starter cultures has been proposed as a viable solution. The goals of incorporating starter cultures into fermented products include enhancing sensory qualities, regulating fermentation levels, and ensuring functional properties and consistent quality (Lee, Song, Shim, & Chang, 2020)

To elevate the functional properties of fermented products, researchers have explored the use of kimchi-derived LAB starter cultures. Certain studies have demonstrated that inoculating with these starter cultures can offer health benefits by boosting antioxidant and anticancer activities. Starter cultures that produce γ -amino butyric acid (GABA) and anti-obesity

compounds have also been utilized. Some LAB strains isolated from kimchi have been found to catalyze the decarboxylation of glutamate, producing GABA and CO₂ as byproducts (Seok et al., 2008). For instance, *Leuconostoc mesenteroides* KCKM0828, isolated from kimchi, has been shown to reduce intracellular lipid accumulation and regulate obesity-related gene expression in mice on a high-fat diet (Yun et al, 2024).

A strategy utilizing an enzymatic reaction from starter cultures has been suggested to boost oligosaccharide production and ensure an optimal level of sweetness. The LAB strain *Leuconostoc citreum* KACC 91035, known for its highly active glycosyltransferases, has been employed to produce beneficial oligosaccharides (Yim et al., 2008). Furthermore, incorporating a sucrose-maltose blend as donor and acceptor with the starter culture has been demonstrated to provide the desired sweetness by releasing fructose and inhibiting unwanted polymer formation through isomaltooligosaccharide production. When *Leuconostoc* spp. are used as a starter culture, free sugar consumption starts earlier and leads to a moderate increase in the production of lactic acid, acetic acid, and mannitol. This indicates that fermentation is completed more quickly and with a higher yield of metabolites compared to fermentation without a starter culture. *Leuconostoc* species are extensively studied as starter cultures due to their anticipated positive impact on sensory characteristics (Lee et al., 2015). The time required to reach the optimal fermentation state can be shortened with

the addition of a starter; however, the development of technologies for maintaining quality over the long term after reaching the optimal fermentation stage through rapid fermentation needs to be considered.

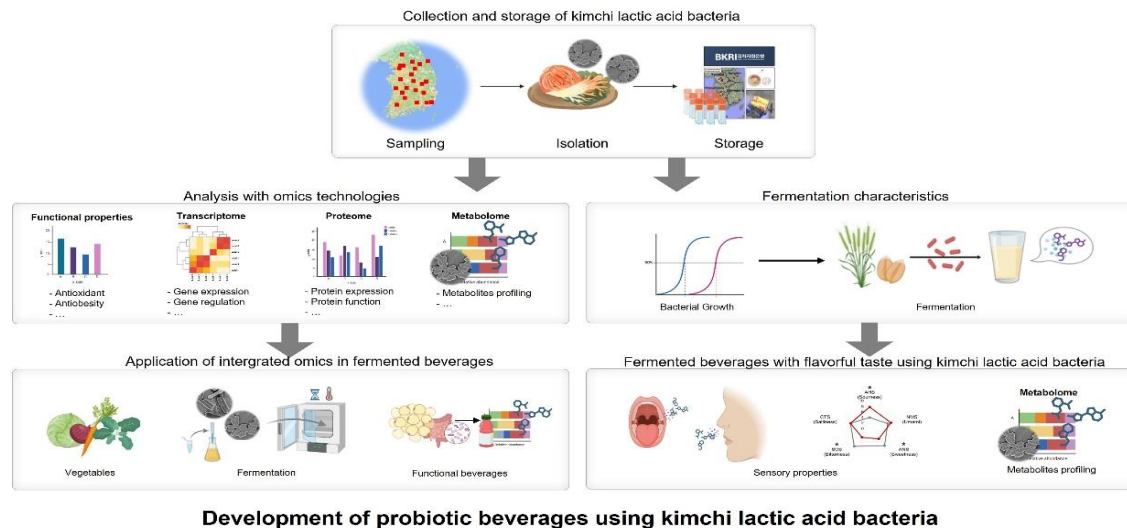


Fig. 1.1. Schematic illustration of kimchi LAB isolation and screening methods for strain-specific functionalities. The figure outlines the process of isolating LAB from kimchi, focusing on screening methods to evaluate strain-specific functionalities. Screening methods are applied to assess functionalities such as antioxidant activity, anti-obesity effects, and flavor enhancement, including survival in the food matrix and metabolite production analysis. Advanced tools such as genomics, metabolomics, and proteomics are used to identify and characterize key traits.

1.2. Functionalities of probiotic fermented products

The exploration of functional food is shifting towards the creation of dietary supplements that incorporate probiotics, nutraceuticals, and prebiotics. These elements have the capacity to impact both the composition and functions of gut microbiota (Lau, Chan, Tan, & Kwek, 2013). Functional foods are ideal for enhancing the health perception of probiotics, especially considering that fermented foods, particularly dairy products, already carry a positive health connotation (Saxelin, Tynkkynen, Mattila-Sandholm, & de Vos, 2005). Consumers are aware that fermented foods contain live microorganisms. Therefore, using probiotics as starter cultures combines the positive effects of both fermentation and probiotic products. The antioxidant and anti-inflammatory properties of LAB, along with their probiotic potential in conditions such as obesity, cancer, atopic dermatitis, and immune-related disorders, underscore the significance of kimchi LAB for human health. The isolation and effectiveness of numerous potential probiotic strains from kimchi microbiota have been widely reported (Cha et al., 2023). Thus, screening kimchi LAB can ensure the identification of functional LAB and enhance competitiveness within the fermented food industry.

1.2.1. Antioxidant properties

Antioxidants can stabilize free radicals by donating an electron, thereby halting the chain reaction caused by these unstable molecules. Free radicals

are known to contribute to the aging process (Alenisan, Alqattan, Tolbah, & Shori, 2017). Free radicals, when present in high concentrations, can mediate oxidative damage to essential biological molecules, including DNA, lipids, and proteins (Valko, Rhodes, Moncol, Izakovic, & Mazur, 2006). This process leads to an elevated susceptibility to degenerative conditions such as cancer, cardiovascular disease, atherosclerosis, arthritis, and neurodegenerative disorders (Shori, Aljohani, Al-zahrani, Al-sulbi, & Baba, 2022). Microbial species, including LAB, possess antioxidant defense mechanisms. These comprise intracellular redox processes involving thiols (like glutathione) and enzymes that defend against oxidation (catalase and superoxide dismutase). These systems collaborate to eliminate ROS synergistically, safeguarding cells from oxidative stress by minimizing damage to large molecules and maintaining optimal redox conditions. Additionally, they offer protection against various environmental stressors (Bryukhanov, Klimko, & Netrusov, 2022). That is, probiotic LAB strains offer a chance to enhance the host's cellular antioxidant defense.

LAB serve as effective carriers for delivering antioxidant enzymes to the gastrointestinal tract, aiming to prevent or treat various inflammatory conditions (LeBlanc et al., 2011). However, it's important to note that various types of antioxidant activities typically vary among strains. Therefore, to optimize the efficacy of using LAB as probiotic supplements, comprehensive studies across a wide range of strains are essential. These

studies would identify essential properties in vitro and evaluate their potential benefits.

1.2.2. Antiobesity properties

Obesity has become a significant global health concern due to its profound impact on human health. It is closely linked with metabolic syndrome and various related conditions including hypertension, diabetes, fatty liver disease, and cardiovascular disease, among others (Nova, Perez de Heredia, Gomez-Martinez, & Marcos, 2016). Probiotic LAB resources have been extensively researched and utilized globally for several years. Many natural probiotics exhibit numerous beneficial functions and hold promise as potential therapeutic strategies for reducing obesity and associated chronic diseases. Scientific evidences indicate that numerous probiotic LAB can potentially prevent and improve obesity and obesity-related chronic diseases. They achieve this by regulating lipid and cholesterol metabolism, reducing oxidative stress, enhancing gut microbiota composition, and suppressing chronic inflammation (Tang, Kong, Shan, Lu, & Lu, 2021). However, investigating gene pathways linked to obesity and targeting these genes for weight loss represent both a challenging and prominent area of research. Future studies are needed to elucidate the regulatory effects on important mechanisms involved in lactic acid fermentation and food matrices, particularly when applied to and delivered

through fermented foods.

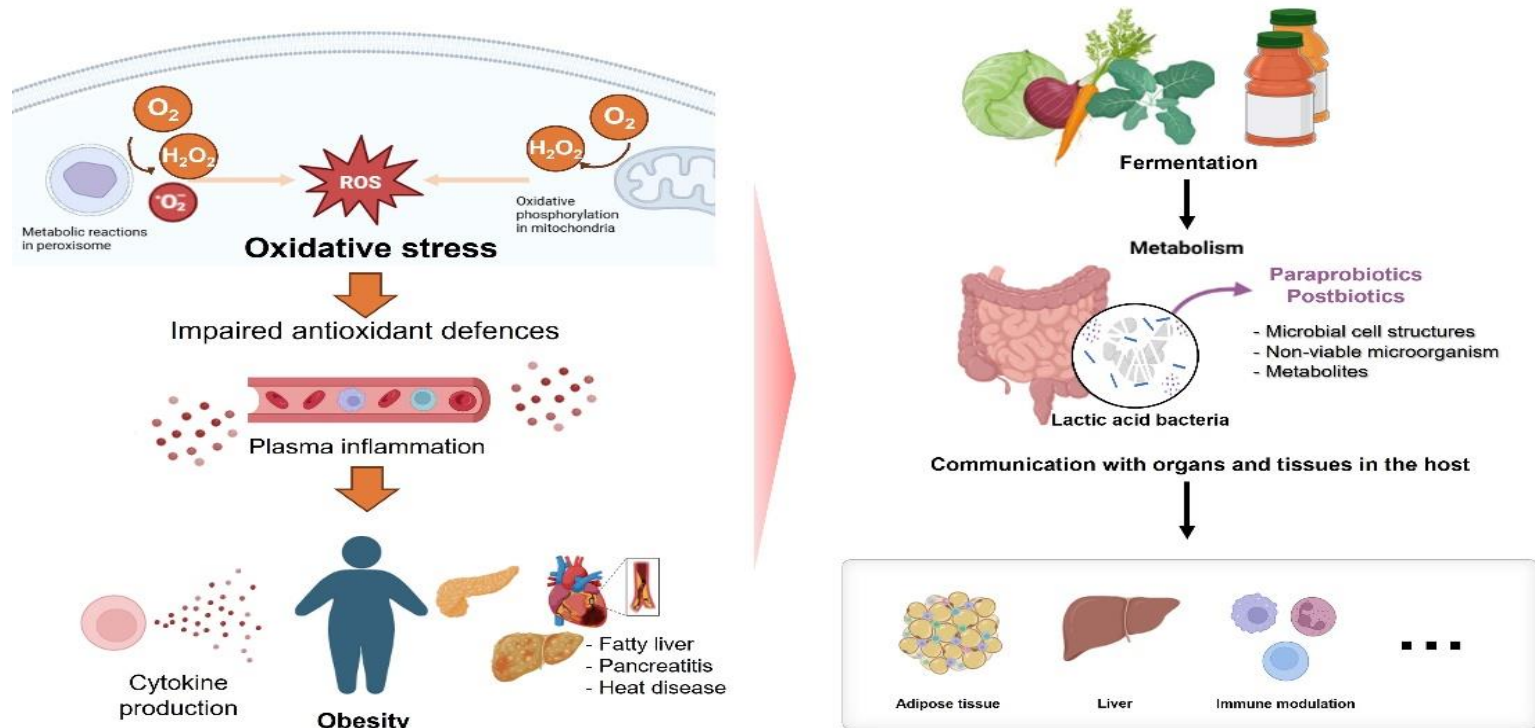


Fig. 1.2. Schematic illustration of oxidative stress, obesity, and microbiome interaction. The diagram highlights the interconnection between oxidative stress, obesity, and the gut microbiome. Oxidative stress contributes to inflammation and

metabolic dysfunction, which promote obesity. In turn, obesity can further exacerbate oxidative stress through increased adipose tissue and systemic inflammation. The gut microbiome plays a regulatory role by influencing oxidative stress levels, energy metabolism, and host immune responses, potentially mitigating or aggravating obesity-related effects. Arrows indicate the directional relationships and interactions among these factors.

1.3. Fermented plant-based beverages as suitable probiotic carrier

To obtain the claimed benefits from probiotic fermented products, it's crucial that the probiotics are viable and sufficiently abundant upon consumption. However, the presence of various adverse environmental factors may compromise the viability of probiotics.

Most probiotic foods currently on the market are dairy-based, making them unsuitable for individuals with milk protein allergies or severe lactose intolerance. The survival of probiotics within the food matrix is contingent upon various factors including pH, storage temperature, and the existence of competing microorganisms and inhibitors (Tripathi & Giri, 2014). Therefore, ensuring the stability of probiotics during storage in LAB products applied to non-dairy items like cereals and beverages is crucial.

Evolving food applications, including plant-based products, beverages, offer different avenues for delivering probiotics to consumers. Research focus on probiotics is shifting towards identifying and characterizing specific secondary metabolites known as postbiotics (Prajapati et al., 2023). These postbiotics exhibit stability through processing, preparation, storage, and digestion, showcasing various physiological advantages like lowering blood pressure, reducing inflammation, modulating the immune system, providing antioxidants, and preventing cancer (Peluzio, Martinez, & Milagro, 2021; Sabahi et al., 2023). Notably, the food matrix could either enhance or diminish the potential effects of probiotics. Therefore, it's crucial to evaluate the composition of food matrices that transport probiotics before

implementing them. This presents numerous opportunities to design novel health-enhancing foods and supplements for pharmaceutical and clinical applications using probiotics and postbiotics.

1.3.1. Fruits and vegetables

Fruits and vegetables are ideal food matrices for delivering probiotics due to their favorable structural attributes and nutritional composition, which promote probiotic survival (Prado, Parada, Pandey, & Soccol, 2008). There is growing interest in crafting fruit-juice-based functional beverages enriched with probiotics and prebiotics. These beverages offer taste profiles that appeal to people of all ages and are viewed as both healthy and refreshing options (Szutowska, 2020).

Consuming fruits and vegetables help mitigate the risk of various diseases by providing bioactive compounds that combat chronic conditions, cancer, coronary heart disease, and strokes. Fruit and vegetable juices are low in sodium and potassium, aiding in the maintenance of healthy blood pressure, while their absence of fat benefits cardiovascular health (Aune et al., 2017). Particular, phenolic compounds, abundant in vegetables and fruits, encompass a diverse range of bioactive molecules produced by plants as secondary metabolites. This extensive group of polyphenols is recognized for their antioxidant, anticarcinogenic, and hypoglycemic effects (Rodríguez et al., 2021).

Microbial enzymes like β -glucosidases, phenolic acid reductases and

decarboxylases play crucial roles in phenolic metabolism. LAB have the ability to break down and alter these secondary metabolites during fermentation (Lee & Paik, 2017). This modification of phenolic compounds during fermentation significantly enhances the bioavailability and/or functionality of the resulting products (Pontonio et al., 2019). Utilizing fruits and vegetables as food matrices to create fermented functional foods is highly recommended for their nutritional benefits.

In recent years, LAB have been applied as starter cultures for fermenting vegetables and fruits to enhance their antioxidant properties through phenolic metabolism. Indeed, alterations in phenolic content during fermentation are influenced by various factors, including microbial strains and matrices (Liu et al., 2019). Consequently, both increases and decreases in total phenolic content have been observed in fruit juice fermentations (Markkinen, Laaksonen, Nahku, Kuldjärv, & Yang, 2019). The bioconversion of phenolic compounds is influenced by the specific strain of LAB involved, although certain pathways remain unclear. Therefore, there is a necessity to carefully select LAB strains capable of generating bioactive compounds during plant fermentation that are beneficial for human health.

1.3.2. Cereals

Cereals provide a favorable environment for the growth of probiotic LAB and can also serve as sources of prebiotics and synbiotics (Charalampopoulos, Wang, Pandiella, & Webb, 2002). Cereal grains contain

higher levels of specific essential vitamins, prebiotic dietary fiber, and minerals, yet they contain lower amounts of easily fermentable carbohydrates (Gupta & Abu-Ghannam, 2012). Cereals have been assessed as favorable mediums for cultivating probiotic strains. Utilizing these grains for the production of nutritious or functional foods such as bread, traditional beverages, or flakes is becoming increasingly popular (Coda, Di Cagno, Gobbetti, & Rizzello, 2014). The fermentation process, carried out by lactic acid bacteria such as *Leuconostoc* spp., *Lactococcus* spp, and *Lactobacillus* spp., serves to reduce anti-nutritional components in raw materials while enhancing flavor (Litwinek et al., 2022; Xu et al., 2020). The robust growth of LAB in cereals suggests that introducing a probiotic strain into a cereal base under controlled conditions could yield a fermented food with distinct and reliable attributes, potentially offering health benefits by combining probiotic and prebiotic elements (Milanović et al., 2020). However, probiotics have been found to produce off-flavors, which can often lead to consumer dissatisfaction (Luckow, Sheehan, Fitzgerald, & Delahunty, 2006). A sensory study of cereal-based beverages showed that consumers prefer the sensory properties of conventional juices over those containing probiotics, regardless of their functional properties (Luckow & Delahunty, 2004).

1.4. Aroma and flavor production

Taste, specifically sensory perception, stands out as the primary aspect of quality evaluation in a consumer's decision-making process for purchases

(Shori, Peng, Bagheri, & Baba, 2021).

LAB play a significant role in enhancing the aroma and flavor of fermented products. They acidify the food, imparting a tangy lactic acid taste, and frequently perform proteolytic and lipolytic activities. Additionally, they produce aromatic compounds by converting amino acids and other substances (Williams, Noble, & Banks, 2001; Yvon & Rijnen, 2001). Additionally, wild strain starter cultures are crucial for flavor development due to their high biosynthetic capacity and ability to produce unique aromatic compounds (Weerkamp, Klijn, Neeter, & Smit, 1996). Homofermentative LAB convert nearly all available sugars into lactic acid through pyruvate to generate energy while also producing various other metabolites, including acetate, ethanol, diacetyl, and acetaldehyde (Kleerebezemab, Hols, & Hugenholtz, 2000). Proper fermentation control via LAB starter cultures can regulate the production of some of these volatile substances. Ensuring both nutritional quality and desirable sensory qualities presents significant challenges in the development of effective probiotic food products. Further research is imperative to address these challenges.

1.5. Concluding remarks and future perspectives

To address the growing global demand for probiotic-fortified products, it is essential to develop reliable methods that ensure a stable and high-quality outcome. The optimal strategy involves using carefully selected

starter strains and managing fermentation under controlled conditions. The industry's interest in employing suitable starters is driven by their ability to enhance sensory qualities and provide health benefits in fermented products. Starter cultures are known to generate higher amounts of lactic acid, acetic acid, and mannitol from free sugars, thereby expediting the fermentation process. Many studies have demonstrated that probiotic-fortified products with starter cultures exhibit superior health-promoting properties, including antioxidant, anticancer, and anti-obesity effects, compared to conventional products. However, some studies have highlighted that the use of LAB starters may result in less precise control over the entire fermentation process.

Currently, the availability of genomic sequences for numerous microorganisms enables researchers to quickly assess the metabolic capabilities of specific strains. The genomes of various LAB strains isolated from kimchi have been sequenced and are expected to offer valuable insights for optimizing starter cultures. Despite extensive research on the use of starter cultures for fermentation, a comprehensive understanding of the effectiveness and applicability of this approach has not yet fully materialized.

Several practical issues must be addressed to enhance product quality with starter cultures. These include: (1) the limited availability due to the lack of diverse commercial starters, (2) the rise in production costs associated with the use of starters, and (3) the absence of developed

methods for optimizing fermentation conditions in raw materials. To address these challenges and advance the quality of probiotic-fortified products, especially on an industrial scale, additional research and development will be necessary.

Therefore, in this study, 35,000 LAB strains were isolated from kimchi. Through preliminary research, 30 strains were initially selected based on their survival rate and dominance in a vegetable beverage food matrix. Further sensory evaluation with a panel of 10 members led to the selection of 5 strains. The goal was to utilize these strains to produce antioxidant and anti-obesity functional beverages, as well as beverages aimed at improving sensory quality. Figure 1.3 presents the results of strain selection based on preliminary experiments.

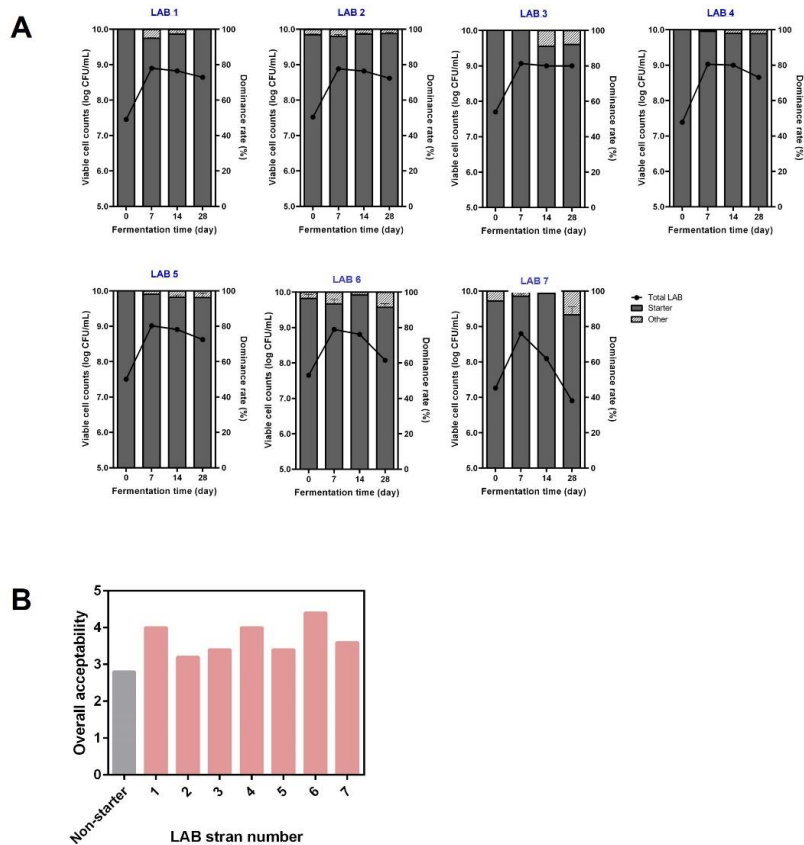


Fig. 1.3. Strain selection results based on preliminary experiments. LAB isolated from kimchi were screened based on survival rate and dominance (<75% cutoff throughout the fermentation period). Activated strains in de Man, Rogosa, and Sharpe broth were inoculated into vegetable beverages and monitored for fermentation for up to 28 days (A). Among the selected strains, those demonstrating superior sensory quality (overall acceptability) compared to the non-inoculated control were finally chosen and used in this study.

1.6. Summary

Probiotic fortified-products have emerged as significant contributors to the food industry, driven by growing consumer awareness of their health benefits and the expanding scientific understanding of their mechanisms. The use of Kimchi LAB not only enhances the flavor but also contributes to its health-promoting properties, including antioxidant and anti-inflammatory effects. The LAB fermentation process not only enhances the nutritional profile of foods but also improves their bioavailability and sensory qualities. However, challenges remain in optimizing probiotic application conditions and mitigating off-flavors associated with fermentation, which are critical considerations for consumer acceptance. Moving forward, continued research is essential to unlock the full potential of probiotics, particularly in non-dairy products like cereals and beverages, which are increasingly popular among consumers seeking alternative dietary options. Advances in probiotic strain selection, fermentation techniques, and food matrix interactions will drive the development of novel, health-enhancing products. This study aims to analyze the characteristics of LAB isolated from the kimchi microbial community to explore new possibilities for use and enhance the competitiveness of the fermented food industry. Using Kimchi LAB, the objective is to produce fermented products that not only enhance taste but also provide health-promoting effects such as antioxidants and anti-obesity properties.

1.7. References

- Alenisan, M. A., Alqattan, H. H., Tolbah, L. S., & Shori, A. B. (2017). Antioxidant properties of dairy products fortified with natural additives: A review. *Journal of the Association of Arab Universities for Basic and Applied Sciences*, 24, 101-106.
- Ananthan, A., Balasubramanian, H., Rath, C., & Others. (2024). Lactobacillus rhamnosus GG as a probiotic for preterm infants: A strain-specific systematic review and meta-analysis. *European Journal of Clinical Nutrition*, 78, 830–846.
- Amenu, D., & Bacha, K. (2023). Probiotic potential and safety analysis of lactic acid bacteria isolated from Ethiopian traditional fermented foods and beverages. *Annals of Microbiology*, 73(37).
- Aune, D., Giovannucci, E., Boffetta, P., Fadnes, L. T., Keum, N., Norat, T., Greenwood, D. C., Riboli, E., Vatten, L. J., & Tonstad, S. (2017). Fruit and vegetable intake and the risk of cardiovascular disease, total cancer and all-cause mortality-a systematic review and dose-response meta-analysis of prospective studies. *Int J Epidemiol*, 46(3), 1029-1056.
- Behnsen, J., Deriu, E., Sassone-Corsi, M., & Raffatellu, M. (2013). Probiotics: properties, examples, and specific applications. *Cold*

Spring Harb Perspect Med, 3 (3), a010074.

Bryukhanov, A., Klimko, A., & Netrusov, A. (2022). Antioxidant properties of lactic acid bacteria. *Microbiology*, 91 (5), 463-478.

Cha, J., Kim, Y. B., Park, S.-E., Lee, S. H., Roh, S. W., Son, H.-S., & Whon, T. W. (2023). Does kimchi deserve the status of a probiotic food? *Critical reviews in food science and nutrition*, 1-14.

Charalampopoulos, D., Wang, R., Pandiella, S. S., & Webb, C. (2002). Application of cereals and cereal components in functional foods: a review. *Int J Food Microbiol*, 79 (1-2), 131-141.

Choi, I. S., Ko, S. H., Lee, M. E., Kim, H. M., Yang, J. E., Jeong, S. G., & Park, H. W. (2021). Production, characterization, and antioxidant activities of an exopolysaccharide extracted from spent media wastewater after *Leuconostoc mesenteroides* WiKim32 fermentation. *ACS Omega*, 6(12), 8171–8178.

Coda, R., Di Cagno, R., Gobbetti, M., & Rizzello, C. G. (2014). Sourdough lactic acid bacteria: Exploration of non-wheat cereal-based fermentation. *Food microbiology*, 37, 51-58.

Gupta, S., & Abu-Ghannam, N. (2012). Probiotic fermentation of plant based products: possibilities and opportunities. *Crit Rev Food Sci Nutr*, 52 (2), 183-199.

Kleerebezemab, M., Hols, P., & Hugenholtz, J. (2000). Lactic acid bacteria as a cell factory: rerouting of carbon metabolism in *Lactococcus lactis* by metabolic engineering. *Enzyme and microbial technology*,

26 (9-10), 840-848.

- Lau, T.-C., Chan, M.-W., Tan, H.-P., & Kwek, C.-L. (2013). Functional food: a growing trend among the health conscious. *Asian Social Science*, 9 (1), 198.
- LeBlanc, J. G., del Carmen, S., Miyoshi, A., Azevedo, V., Sesma, F., Langella, P., Bermúdez-Humarán, L. G., Watterlot, L., Perdigon, G., & de LeBlanc, A. d. M. (2011). Use of superoxide dismutase and catalase producing lactic acid bacteria in TNBS induced Crohn's disease in mice. *Journal of Biotechnology*, 151 (3), 287-293.
- Lee, M. E., Jang, J. Y., Lee, J. H., Park, H. W., Choi, H. J., & Kim, T. W. (2015). Starter cultures for kimchi fermentation. *Journal of Microbiology and Biotechnology*, 25 (5), 559-568.
- Lee, M., Song, J. H., Park, J. M., & Chang, J. Y. (2019). Bacterial diversity in Korean temple kimchi fermentation. *Food Res Int*, 126, 108592.
- Lee, M., Song, J. H., Shim, W. B., & Chang, J. Y. (2020). DNAzyme-based quantitative loop-mediated isothermal amplification for strain-specific detection of starter kimchi fermented with *Leuconostoc mesenteroides* WiKim32. *Food chemistry*, 333, 127343.
- Lee, M., Song, J. H., Jung, M. Y., Lee, S. H., & Chang, J. Y. (2017). Large-scale targeted metagenomics analysis of bacterial ecological changes in 88 kimchi samples during fermentation. *Food Microbiology*, 66, 173-183.
- Lee, N. K., & Paik, H. D. (2017). Bioconversion Using Lactic Acid

Bacteria: Ginsenosides, GABA, and Phenolic Compounds. *J Microbiol Biotechnol*, 27 (5), 869-877.

Litwinek, D., Boreczek, J., Gambuś, H., Buksa, K., Berski, W., & Kowalczyk, M. (2022). Developing lactic acid bacteria starter cultures for wholemeal rye flour bread with improved functionality, nutritional value, taste, appearance and safety. *Plos one*, 17 (1), e0261677.

Liu, Y., Cheng, H., Liu, H., Ma, R., Ma, J., & Fang, H. (2019). Fermentation by Multiple Bacterial Strains Improves the Production of Bioactive Compounds and Antioxidant Activity of Goji Juice. *Molecules*, 24 (19).

Luckow, T., & Delahunty, C. (2004). Which juice is 'healthier'? A consumer study of probiotic non-dairy juice drinks. *Food Quality and Preference*, 15 (7-8), 751-759.

Luckow, T., Sheehan, V., Fitzgerald, G., & Delahunty, C. (2006). Exposure, health information and flavour-masking strategies for improving the sensory quality of probiotic juice. *Appetite*, 47 (3), 315-323.

Ma, C., Huo, D., You, Z., Peng, Q., Jiang, S., Chang, H., Zhang, J., & Zhang, H. (2020). Differential pattern of indigenous microbiome responses to probiotic *Bifidobacterium lactis* V9 consumption across subjects. *Food Res Int*, 136, 109496.

Markkinen, N., Laaksonen, O., Nahku, R., Kuldjärv, R., & Yang, B. (2019). Impact of lactic acid fermentation on acids, sugars, and phenolic

- compounds in black chokeberry and sea buckthorn juices. *Food chemistry*, 286, 204-215.
- Milanović, V., Osimani, A., Garofalo, C., Belleggia, L., Maoloni, A., Cardinali, F., Mozzon, M., Foligni, R., Aquilanti, L., & Clementi, F. (2020). Selection of cereal-sourced lactic acid bacteria as candidate starters for the baking industry. *Plos one*, 15 (7), e0236190.
- Ning, Y., Fu, Y., Hou, L., Ma, M., Wang, Z., Li, X., & Jia, Y. (2021). iTRAQ-based quantitative proteomic analysis of synergistic antibacterial mechanism of phenyllactic acid and lactic acid against *Bacillus cereus*. *Food Research International*, 139, 109562.
- Nova, E., Perez de Heredia, F., Gomez-Martinez, S., & Marcos, A. (2016). The Role of Probiotics on the Microbiota: Effect on Obesity. *Nutr Clin Pract*, 31 (3), 387-400.
- Peluzio, M. d. C. G., Martinez, J. A., & Milagro, F. I. (2021). Postbiotics: Metabolites and mechanisms involved in microbiota-host interactions. *Trends in Food Science & Technology*, 108, 11-26.
- Pontonio, E., Montemurro, M., Pinto, D., Trani, A., Mazzeo, A., Gobbetti, M., & Rizzello, C. (2019). Lactic acid fermentation of pomegranate juice as a tool to improve antioxidant activity. *Frontiers in Microbiology*, 10, 460471.
- Prado, F. C., Parada, J. L., Pandey, A., & Soccol, C. R. (2008). Trends in non-dairy probiotic beverages. *Food Research International*, 41 (2), 111-123.

- Prajapati, N., Patel, J., Singh, S., Yadav, V. K., Joshi, C., Patani, A., Prajapati, D., Sahoo, D. K., & Patel, A. (2023). Postbiotic production: harnessing the power of microbial metabolites for health applications. *Frontiers in Microbiology, 14*, 1306192.
- Rodríguez, L. G. R., Gasga, V. M. Z., Pescuma, M., Van Nieuwenhove, C., Mozzi, F., & Burgos, J. A. S. (2021). Fruits and fruit by-products as sources of bioactive compounds. Benefits and trends of lactic acid fermentation in the development of novel fruit-based functional beverages. *Food Research International, 140*, 109854.
- Sabahi, S., Homayouni Rad, A., Aghebati-Maleki, L., Sangtarash, N., Ozma, M. A., Karimi, A., Hosseini, H., & Abbasi, A. (2023). Postbiotics as the new frontier in food and pharmaceutical research. *Critical reviews in food science and nutrition, 63* (26), 8375-8402.
- Sakandar, H. A., & Zhang, H. (2021). Trends in Probiotic (s)-Fermented milks and their in vivo functionality: A review. *Trends in Food Science & Technology, 110*, 55-65.
- Sanders, M. E., & Marco, M. L. (2010). Food formats for effective delivery of probiotics. *Annu Rev Food Sci Technol, 1*, 65-85.
- Saxelin, M., Tynkkynen, S., Mattila-Sandholm, T., & de Vos, W. M. (2005). Probiotic and other functional microbes: from markets to mechanisms. *Curr Opin Biotechnol, 16* (2), 204-211.
- Seok J. H., Park K. B., Kim Y. H., Bae M. O., Lee M. K., & Oh S. H. (2008). Production and characterization of kimchi with enhanced levels of γ -

aminobutyric acid. *Food Sci. Biotechnol.* 17, 940-946.

Sharma, A., Lee, S., & Park, Y. S. (2020). Molecular typing tools for identifying and characterizing lactic acid bacteria: A review. *Food Science and Biotechnology*, 29, 1301–1318.

Shori, A. B., Aljohani, G. S., Al-zahrani, A. J., Al-sulbi, O. S., & Baba, A. S. (2022). Viability of probiotics and antioxidant activity of cashew milk-based yogurt fermented with selected strains of probiotic *Lactobacillus* spp. *Lwt*, 153, 112482.

Shori, A. B., Peng, C. W., Bagheri, E., & Baba, A. S. (2021). Physicochemical analysis, proteolysis activity and exopolysaccharides production of herbal yogurt fortified with plant extracts. *International Journal of Food Engineering*, 17 (3), 227-236.

Spacova, I., Binda, S., Ter Haar, J. A., Henoud, S., Legrain-Raspaud, S., Dekker, J., Espadaler-Mazo, J., Langella, P., Martín, R., & Pane, M. (2023). Comparing technology and regulatory landscape of probiotics as food, dietary supplements and live biotherapeutics. *Frontiers in Microbiology*, 14, 1272754.

Suez, J., Zmora, N., Segal, E., & Elinav, E. (2019). The pros, cons, and many unknowns of probiotics. *Nature Medicine*, 25 (5), 716-729.

Szutowska, J. (2020). Functional properties of lactic acid bacteria in fermented fruit and vegetable juices: A systematic literature review. *European Food Research and Technology*, 246 (3), 357-372.

Tang, C., Kong, L., Shan, M., Lu, Z., & Lu, Y. (2021). Protective and

- ameliorating effects of probiotics against diet-induced obesity: A review. *Food Research International*, *147*, 110490.
- Tripathi, M. K., & Giri, S. K. (2014). Probiotic functional foods: Survival of probiotics during processing and storage. *Journal of functional foods*, *9*, 225-241.
- Valko, M., Rhodes, C. J., Moncol, J., Izakovic, M., & Mazur, M. (2006). Free radicals, metals and antioxidants in oxidative stress-induced cancer. *Chem Biol Interact*, *160* (1), 1-40.
- Weerkamp, A., Klijn, N., Neeter, R., & Smit, G. (1996). Properties of mesophilic lactic acid bacteria from raw milk and naturally fermented raw milk products.
- Williams, A. G., Noble, J., & Banks, J. (2001). Catabolism of amino acids by lactic acid bacteria isolated from Cheddar cheese. *International Dairy Journal*, *11* (4-7), 203-215.
- Xu, Y., Zhou, T., Tang, H., Li, X., Chen, Y., Zhang, L., & Zhang, J. (2020). Probiotic potential and amylolytic properties of lactic acid bacteria isolated from Chinese fermented cereal foods. *Food Control*, *111*, 107057.
- Yang, E., Fan, L., Yan, J., & Park, Y. S. (2018). Influence of culture media, pH, and temperature on growth and bacteriocin production of bacteriocinogenic lactic acid bacteria. *AMB Express*, *8*, 10.
- Yang, X., Hong, J., Wang, L., Cai, C., Mo, H., Wang, J., & Liao, Z. (2024). Effect of lactic acid bacteria fermentation on plant-based products.

Fermentation, 10(1), 48.

- Yim C. Y., Eom H. J., J Q, Kim S.Y., Han N. S. (2008). Characterization of low temperature-adapted *Leuconostoc citreum* HJ-P4 and its dextransucrase for the use of kimchi starter. *Food Science and Biotechnology*, 17:1391-1395.
- Yun, Y. R., Kwon, M. S., Lee, H. J., Lee, W., Lee, J. E., & Hong, S. W. (2024). Anti-obesity activity of lactic acid bacteria-starter-based kimchi in high-fat diet-induced obese mice. *Journal of Functional Foods*, 112, 105966.
- Yvon, M., & Rijnen, L. (2001). Cheese flavour formation by amino acid catabolism. *International Dairy Journal*, 11 (4-7), 185-201.

This chapter comprises articles, published in *Food research international* with minor modification as a partial fulfillment of Moeun Lee's Ph.D. program

Chapter 2.

Transcriptome responses of lactic acid bacteria isolated from kimchi under hydrogen peroxide exposure

Abstract

In this study, five species of lactic acid bacteria (LAB) isolated from kimchi were analyzed in terms of their potential antioxidant activity. *Latilactobacillus curvatus* WiKim38, *Companilactobacillus allii* WiKim39, and *Lactococcus lactis* WiKim0124 exhibited higher radical scavenging activity, reducing power, and lipid peroxidation inhibition than the reference strain and tolerated hydrogen peroxide (H₂O₂) exposure up to a concentration of 2.5 mM. To investigate the antioxidant mechanism of LAB strains, transcriptomic and proteomic signatures were compared between the H₂O₂-exposed and untreated group using RNA sequencing and two-dimensional protein gel electrophoresis. Across all LAB strains, cell membrane responses and metabolic processes were the most prominent in the main categories of gene ontology classification, indicating that cellular components and interactions play an important role in oxidative stress responses. Thus, LAB strains isolated from kimchi could be considered for potential use in functional food production and in antioxidant starter cultures.

Keywords: *Latilactobacillus curvatus* WiKim38, *Companilactobacillus allii* WiKim39, *Lactococcus lactis* WiKim0124, antioxidant starter

culture, RNA sequencing, two-dimensional protein gel electrophoresis

2.1. Introduction

Oxidants are produced via the intracellular metabolism of mitochondria and peroxisomes as well as various cytoplasmic enzymatic systems (Nakagawa & Miyazaki, 2017). Weakened host defenses can increase the production of reactive oxidizing species (ROS), resulting in redox imbalance and oxidative damage to macromolecules such as DNA, RNA, lipids, and proteins (Qian, Wang, Zhuang, Zhang, & Yan, 2020).

Intestinal ROS can be produced either endogenously or exogenously. Excessive amounts of ROS cause oxidative stress and lead to various intestinal diseases, inflammation, and dysfunction (Wu et al., 2022). Many lactic acid bacteria (LAB) have been reported to produce antioxidant enzymes and metabolites that eliminate ROS, with several associated health benefits (Koller et al., 2008).

Kimchi, a popular traditional Korean fermented side dish, is currently being studied as a health food because of its synbiotic properties (Kim, Yang, Kim, Lee, & Lee, 2018). Additionally, kimchi LAB produce biologically active compounds that enhance the flavor of various food matrices and improve the quality of fermented products without side effects (Lee, Song, Park, & Chang, 2019). Therefore, kimchi LAB are closely linked to antioxidant (Lee et al., 2021), antitumor (Kim & Park, 2018), antimicrobial (Toushik et al., 2021), viral inhibitory (Seo, Jung, Jung, Yeo, & Choi, 2020),

and immunomodulatory effects (Yun, Lee, Song, Choi, & Chang, 2022). Commercial food products can thus be supplemented with kimchi LAB to improve their quality and provide various health benefits (Lee, Song, Shim, & Chang, 2020).

As the functional food market is expanding, so is the demand for LAB-supplemented products. Therefore, the potential use and value of kimchi LAB as a functional probiotic is continuously being studied (Won, Chen, Park, & Yoon, 2020). In particular, LAB strains isolated from kimchi can strongly adhere to the epithelial cells of the gastrointestinal tract and can survive in adverse conditions, such as low pH and bile salts, which is advantageous for probiotics (Han, Lee, Lee, & Paik, 2020).

Probiotic LAB, which exhibit significant antioxidant activity, contribute to the amelioration of oxidative stress-induced damage by promoting the production of antioxidant enzymes and detoxifying ROS in the intestine. Thus, some LAB strains can protect human cells from oxidative stress-induced damage (Lin et al., 2018). As additive antioxidants, LAB can alleviate oxidative stress by strengthening antioxidant defense systems (Wu, Zhang, Ye, & Wang, 2021).

Although the antioxidant potential of LAB has been globally investigated *in vitro* and *in vivo*, the mechanisms modulating oxidative stress resistance have not been sufficiently studied. Thus, the purpose of this study was to determine the antioxidant effect of kimchi LAB strains and analyze the possible mechanisms of oxidative stress resistance in relation to hydrogen

peroxide (H₂O₂) exposure at the transcriptomic and proteomic levels.

2.2. Material and Methods

2.2.1. Bacterial strains and culture conditions

Five LAB strains isolated from kimchi were used in this study (Table 2.1). *Lacticaseibacillus rhamnosus* GG KCTC 5033 (LGG) was purchased from the Korean Collection for Type Cultures (KCTC; Jeollabuk-do, Korea) and used as a reference strain. The LAB strains isolated from kimchi were cultured in de Man, Rogosa, and Sharpe (MRS) medium (BD Difco, Rockville, MD, USA) at 30 °C for 24 h before use.

Table 2.1. Lactic acid bacteria strains used in this study.

Strain	Gene bank ac no.	Code
<i>Leuconostoc mesenteroides</i> WiKim32	NZ_CP037752.1	WiKim32
<i>Latilactobacillus sakei</i> WiKim34	OL638252.1	WiKim34
<i>Latilactobacillus curvatus</i> WiKim38	KU936208.1	WiKim38
<i>Companilactobacillus allii</i> WiKim39	NR_159087.1	WiKim39
<i>Lactococcus lactis</i> WiKim0124	MZ424472.1	WiKim0124
<i>Lacticaseibacillus rhamnosus</i> GG		LGG

2.2.2. H₂O₂ resistance of LAB strains

First, 1% (v/v) of the Kimchi LAB culture was added to 10 mL MRS broth containing 0, 1.0, 1.5, 2.0, 2.5, 3.0, and 4.0 mM H₂O₂ and incubated for 0–72 h at 30 °C. Bacterial populations were then measured on MRS agar plates after incubation for 48 h at 30 °C.

2.2.3. Measuring the antioxidant activity of LAB strains

2.2.3.1. Collection of intact cells and preparation of cell-free supernatant and cell-free extracts

After incubation, the intact bacterial cells were collected via centrifugation at 10,000 ×g for 10 min at 4 °C and adjusted their concentration to 1×10⁹ CFU/mL. The cell-free supernatant was subsequently filtered by a 0.45 µm filter membrane. To prepare cell-free extracts, the 10⁹ CFU/mL bacterial cell suspensions were subjected to ultrasonic disruption (comprising ten 1 min strokes at 1 min intervals in an ice bath), after which the cell debris was removed via centrifugation at 10,000 ×g for 10 min at 4 °C. The three types of LAB samples that were prepared were then used for the antioxidant assay.

2.2.3.2. 2,2-Diphenyl-1-picrylhydrazyl free radical scavenging activity

The free radical scavenging activity of 2,2-diphenyl-1-picrylhydrazyl (DPPH) was measured as described in a previous study (Lee et al., 2021),

with some modifications. To establish the sample group, 20 μL of the sample was added to 180 μL of an ethanolic 0.2 mM DPPH solution and incubated in the dark at 25 $^{\circ}\text{C}$ for 30 min. The control and blank groups contained equal volumes of distilled water and ethanol, respectively, instead of LAB samples. Absorbance was measured at 571 nm after centrifugation at 10,000 $\times g$ for 10 min. The free radical scavenging activity of DPPH was calculated using the following equation:

$$\text{DPPH free radical scavenging activity (\%)} = [1 - (A_{\text{Sample}} - A_{\text{Blank}})/A_{\text{Control}}] \times 100$$

where A_{Sample} , A_{Control} , and A_{Blank} are the absorbance of the sample, control, and blank groups, respectively.

2.2.3.3. 2,2'-azino-bis (3-ethylbenzothiazoline-6-sulfonic acid) radical scavenging activity

A 2,2'-azino-bis(3-ethylbenzothiazoline-6-sulfonic acid) (ABTS) cation assay was conducted using a modified method described in a previous study (Zheng, Zhao, Xiao, Zhao, & Su, 2016). Briefly, 7.0 mM ABTS⁺ solution was added to a 2.4 mM potassium persulfate. The mixture was stored overnight in the dark before use. To prepare the working solution, the ABTS radical solution was diluted with 50 mM phosphate buffer to adjust the absorbance at 734 nm to 0.8. Then, 180 μL of the working solution was added to 20 μL of the sample, and the absorbance of the mixture was

recorded after 30 min. The control and blank groups contained the same volume of distilled water and 50 mM phosphate buffer, respectively, instead of LAB samples. The radical scavenging activity of ABTS was calculated using the following equation:

$$\text{ABTS radical scavenging activity (\%)} = [1 - (A_{\text{Sample}} - A_{\text{Blank}})/A_{\text{Control}}] \times 100$$

where A_{Sample} , A_{Blank} , and A_{Control} are the absorbance of the sample, blank, and control groups, respectively.

2.2.3.4. Hydroxyl radical scavenging activity

To measure hydroxyl (OH) radical scavenging activity, an assay was performed using a method described in a previous study (Lee et al., 2021). First, 1 mL of the sample was mixed with 1 mL each of H₂O₂ (0.025%, w/v), sodium salicylate (9 mM), and FeSO₄ (9 mM). The mixture was stored at 37 °C for 1 h. The control and blank groups consisted of 1 mL of distilled water and X mL of Y, respectively. The absorbance of each of these three groups was measured at 536 nm, and the OH radical scavenging activity was calculated using the following equation:

$$\text{OH radical scavenging activity (\%)} = (A_{\text{Sample}} - A_{\text{Control}})/(A_{\text{Blank}} - A_{\text{Control}}) \times 100$$

where A_{Sample} , A_{Control} , and A_{Blank} are the absorbance of the sample, control, and blank groups, respectively.

2.2.3.5. Ferric reducing antioxidant power

A ferric reducing antioxidant power (FRAP) assay was performed using a commercial assay kit (Abcam, Hong Kong, China), following the manufacturer's instructions. Briefly, a FRAP working solution was prepared by mixing the TPTZ solution, ferric chloride solution, and acetate buffer. The samples were diluted in acetate buffer, and 10 μL of the sample was added to a 96-well plate. Next, 200 μL of the FRAP working solution was added to each well, and the samples were incubated at 37 $^{\circ}\text{C}$ for 30 min. Then, FRAP was quantified using a ferrous sulfate calibration curve, and the results were expressed as equivalent Fe^{2+} concentrations (μM).

2.2.3.6. Inhibition of lipid peroxidation

The inhibition of lipid peroxidation in the LAB samples was determined based on the ability of biological fluids to inhibit the production of thiobarbituric acid reactive substances using a modified thiobarbituric acid method (Ghani, Barril, Bedgood Jr, & Prenzler, 2017). The reaction mixture comprised 0.5 mL of distilled water, 1.0 mL of FeSO_4 (1%), and 1.0 mL of linoleic acid emulsion (0.5%). The reaction mixture was combined with 1.0 mL of the sample and incubated in a water bath at 37 $^{\circ}\text{C}$ for 2 h. Then, 0.2 mL of trichloroacetic acid (4%) and 2 mL of thiobarbituric acid (0.8%) were added to the sample mixture, which was subsequently incubated at 100 $^{\circ}\text{C}$ for 30 min. After centrifugation at 4,000 $\times g$ for 15 min, the absorbance of the supernatant was measured at 532 nm. The blank group

contained 1.0 mL of distilled water instead of the sample. The inhibition of lipid peroxidation was calculated using the following equation:

Inhibition of lipid peroxidation (%) =

$$(A_{\text{Blank}} - A_{\text{Sample}}/A_{\text{Blank}}) \times 100$$

where A_{Blank} and A_{Sample} are the absorbance of the blank and sample groups, respectively.

2.2.3.7. Antioxidant enzyme activity

The activities of superoxide dismutase (SOD) and glutathione peroxidase (GPX) in LAB samples were measured using commercial assay kits (Abcam) following the manufacturer's instructions. The samples were diluted in assay buffer and added to a 96-well plate. For SOD activity, a reaction mixture and WST-1 were added, and the samples were incubated for 20 min. Then, the stop solution was added, and the absorbance was read at 450 nm. For GPX activity, a reaction mixture, co-substrate mixture, and NADPH mixture were added, and the samples were incubated for 10 min. The stop solution was added, and the absorbance was measured at 340 nm. To calculate SOD and GPX activity, standard curves generated from known SOD and GPX concentrations were used. The activities of SOD and GPX were expressed in U/mg protein.

2.2.4. Scanning electron microscopy

The LAB strains were treated with MRS broth containing 2.5 mM H₂O₂ for 24 h, and the non-treated group was analyzed using field emission scanning electron microscopy (FE-SEM). Cells were collected via centrifugation and washed twice. Cell pellets were treated with fixing solution at 4 °C for 4 h, dehydrated with ethanol solution, and dried using an HCP-2 critical point dryer (Hitachi, Tokyo, Japan). The samples were then coated with gold and observed using FE-SEM (Helios G3 CX; FEI, Hillsboro, OR, USA) at 1.00 kV.

2.2.5. RNA isolation, sequencing, and analysis

2.2.5.1. RNA isolation and sequencing

Ribosomal RNA depletion was conducted using an Epicenter RiboZero rRNA removal kit (Illumina, San Diego, CA, USA) according to the manufacturer's instructions. Libraries for Illumina sequencing were generated using the TruSeq Stranded mRNA sample preparation kit (Illumina) following the manufacturer's protocol. Library quality was measured using an Agilent Bioanalyzer 2100 (Agilent Technologies, Santa Clara, CA, USA). Libraries were sequenced on the Illumina HiSeq 2500 platform using paired-end 100 bp sequencing. The reference genomes for the sequenced data were obtained from the National Center for Biotechnology Information (NCBI) database (<https://www.ncbi.nlm.nih.gov/>).

2.2.5.2. Bioinformatics analysis

Trimmed reads were aligned with the reference genome sequence using Bowtie2 software. Relative transcript abundance was measured in fragments per kilobase of exon sequence per million mapped sequence reads (FPKM). Data were normalized using the Z-score obtained from their FPKM values. A \log_2 fold change $\geq |2.0|$ was used to filter significant upregulation and downregulation. The Gene Ontology (GO) database was used for pathway analysis. Differentially expressed gene (DEG) analysis of the mapping results was performed using the DESeq CLRNASeqTM program (ChunLab, Seoul, South Korea). The GO enrichment analysis was performed using the R GOseq package based on Wallenius's noncentral hypergeometric distribution (Garcia-Moreno et al., 2022). The resulting *p*-value was adjusted with a false discovery rate (cutoff of $p < 0.01$). A hierarchical clustering heatmap analysis of the top 50 DEGs was performed using the R pheatmap package.

2.2.6. Protein Extraction, two-dimensional polyacrylamide gel electrophoresis (2DE)

Two-dimensional polyacrylamide gel electrophoresis (2-DE) was performed following the steps described in a previous study (Park et al., 2002). Samples in a buffer of 7 M urea, 2 M thiourea, 4.5% 3-[(3-cholamidopropyl) dimethylammonio]-1-propanesulfonate, 100 mM

dithioerythritol, and 40 mM **tris**(hydroxymethyl)aminomethane (pH 8.8) were applied to the immobilized nonlinear gradient strips with a pH of 3–10 (Amersham Biosciences, Uppsala, Sweden). Isoelectric focusing was performed at 80,000 Vh. The second dimension was analyzed on 9–16% linear gradient polyacrylamide gels (18 cm × 20 cm × 1.5 mm) at a constant current of 40 mA per gel for approximately 5 h. After protein fixation in 40% methanol and 5% phosphoric acid for 1 h, the gels were stained with Coomassie brilliant blue G-250 for 12 h.

2.2.6.1. Image data analysis and protein identification

The gels were de-stained with distilled water, scanned in a Bio-Rad (Richmond, CA, USA) GS710 densitometer, and converted into digital data, which were analyzed using the Image Master Platinum 5.0 program (Amersham Biosciences, Amersham, UK). Differentially expressed proteins (DEPs) were manually extracted from the preparative gel, digested using trypsin and peptide, and extracted as described in a previous study (Sghaier-Hammami, S, Baazaoui, Gomez-Diaz, & Jorrin-Novo, 2020). Nano-scale liquid chromatography coupled with tandem mass spectrometry (LC-MS/MS) was conducted using an Easy n-LC and LTQ Orbitrap XL mass spectrometer (Thermo Fisher, San Jose, CA, USA) equipped with a nano-electrospray source. A C18 nanobore column (150 × 0.1 mm, 3 µm pore size; Agilent Technologies) was used for sample separation. Mass spectra were obtained using data-dependent acquisition via a full mass scan (380–

1,700 m/z) and 10 MS/MS scans. The peptide sequences present in the protein sequence database were identified using the Mascot algorithm (Matrix Science, Chicago, IL, USA). Database search parameters included the following: taxonomic restriction to *Latilactobacillus curvatus*, *Companilactobacillus allii*, and *Lactococcus lactis*; fixed modification via cysteine carbamidomethylation; variable modification via methionine oxidation; a maximum missed cleavage threshold of 10 ppm; and a MS/MS tolerance of 0.8 Da. Peptides were filtered using a significance threshold of $p < 0.05$. Proteins with a sequence coverage over 40% were then identified.

2.2.6.2. Bioinformatics analysis

Proteins with a \log_2 fold change $\geq |1.0|$ fold from the non-treated group (0 mM) to the 2.5 mM H₂O₂ treated group were considered DEPs. The UniProt (<https://www.uniprot.org/>) and NCBI (<https://www.ncbi.nlm.nih.gov/>) databases were used to obtain information on all proteins identified in this study. These DEPs were retrieved from the GO database (<http://geneontology.org/>) to evaluate their functional classification.

2.2.7. Statistical analyses

Tukey's honest significant difference test was employed to determine the statistical significance in comparisons between the five LAB strains and reference strain via the R agricolae package. Results with a p -value < 0.05

were considered statistically significant. All experiments were performed in triplicate, and the results were expressed as the mean \pm standard deviation.

2.3. Results

2.3.1. H₂O₂ tolerance and antioxidant activity

The five kimchi LAB strains grew in media with different H₂O₂ concentrations, thereby exhibiting H₂O₂ resistance. Bacterial growth was inhibited in an H₂O₂ dose-dependent manner, and the lagging phase was prolonged (Fig. 2.1). Bacterial cells survived in the presence of 2.5 mM H₂O₂. WiKim32, WiKim38, and WiKim0124 exhibited a slow decrease in the number of CFUs at H₂O₂ concentrations of 3.0 and 4.0 mM. In contrast, WiKim39 survived up to a H₂O₂ concentration of 3.0 mM. In terms of the antioxidant activity of LAB strains, cell-free supernatants, intact cells, and cell-free extracts inhibited the formation of DPPH, ABTS, and OH radicals (Fig. 2.2). Cell-free supernatants were stronger than intact cells and cell-free extracts. Similar to the radical scavenging activity, the FRAP and lipid peroxidation inhibition of kimchi LAB strains were higher than those of the reference strain. Overall, WiKim0124, WiKim39, and WiKim38 exhibited the highest antioxidant capacities.

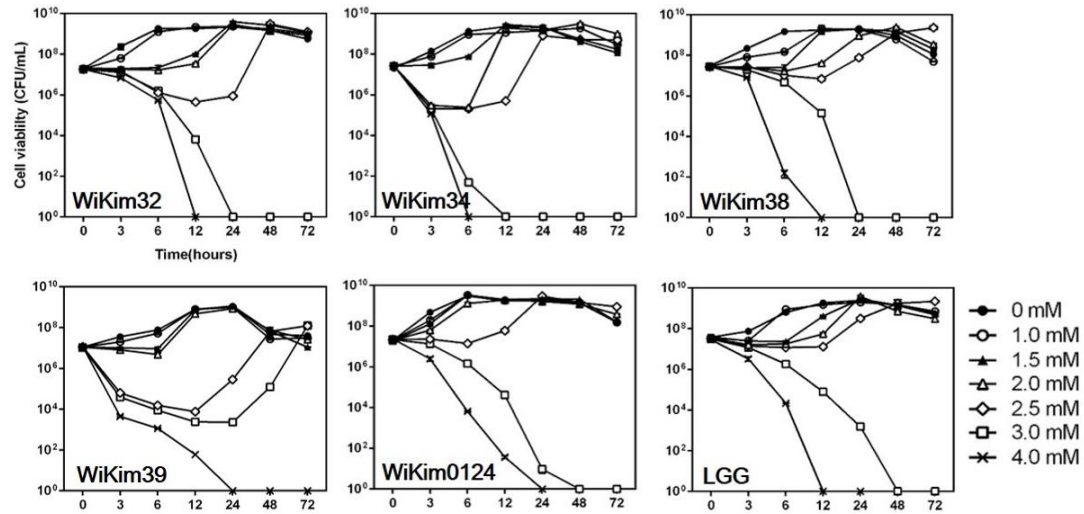


Fig. 2.1. H₂O₂ resistance of five lactic acid bacteria (LAB) strains isolated from kimchi and a reference strain. Growth curves in de Man, Rogosa, and Sharpe (MRS) broth with different hydrogen peroxide (H₂O₂) concentrations (0–4 mM).

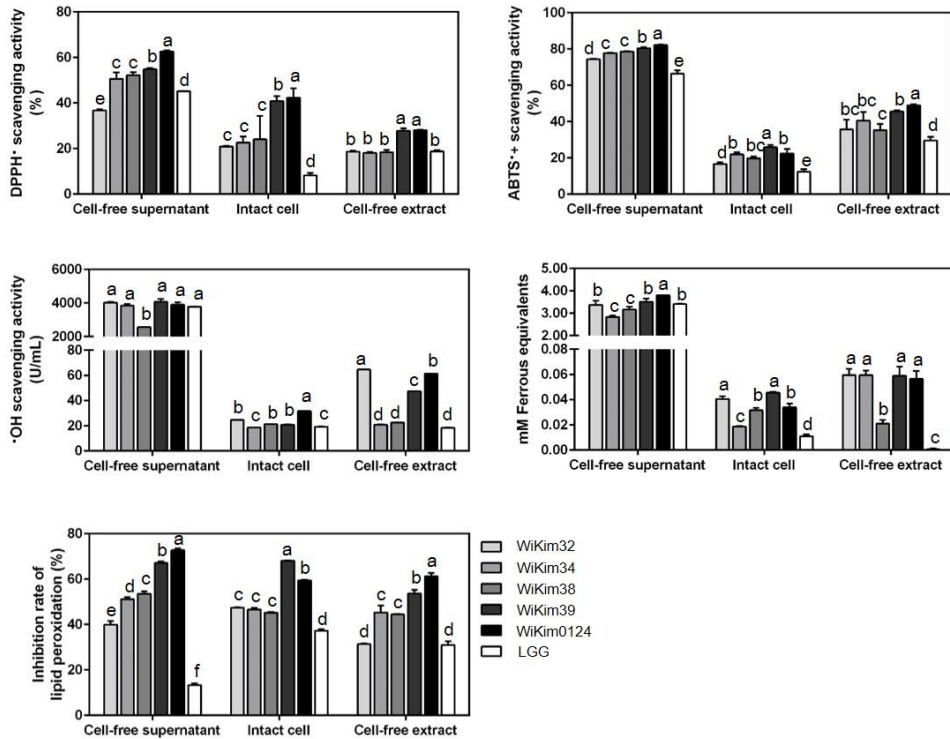


Fig. 2.2. Antioxidant potential of five lactic acid bacteria (LAB) strains isolated from kimchi and a reference strain. 2,2-Diphenyl-1-picrylhydrazyl (DPPH), 2,2'-azino-bis(3-ethylbenzothiazoline-6-sulfonic acid) (ABTS), and hydroxyl (OH) radical scavenging activity, reducing power, and lipid peroxidation inhibition. Superscript letters indicate significant differences between the LAB strains and the reference strain (Tukey's honest significant difference; $p < 0.05$).

2.3.2. Antioxidant enzyme activity

The SOD and GPX potential of the LAB strains showed the same trend as radical scavenging activity. Cell-free supernatants exhibited the highest activity by a wide margin, followed by cell-free extracts, whereas intact cells showed the lowest activity (Table 2.2). Most LAB strains showed higher SOD and GPX activity than LGG in cell-free supernatants and cell-free extracts. Based on these results, the WiKim32, WiKim39, WiKim38, and WiKim0124 strains were selected for further study.

Table 2.2. Superoxide dismutase (SOD) and glutathione peroxidase (GPX) activities of lactic acid bacteria strains under different conditions.

Subjects		WiKim32	WiKim34	WiKim38	WiKim39	WiKim0124	LGG
SOD activity (Inhibition ratio, %)	Cell-free supernatant	60.85 ± 0.19 ^b	48.83 ± 0.61 ^d	65.14 ± 0.41 ^a	51.65 ± 0.32 ^c	39.61 ± 0.00 ^e	51.48 ± 0.00 ^c
	Intact cell	12.29 ± 4.81 ^b	10.32 ± 0.74 ^b	15.13 ± 4.31 ^b	18.99 ± 3.76 ^b	42.99 ± 0.11 ^a	12.29 ± 1.13 ^b
	Cell-free extract	41.59 ± 0.21 ^b	39.05 ± 0.64 ^c	37.20 ± 0.00 ^c	37.99 ± 0.19 ^c	79.23 ± 0.84 ^a	37.38 ± 0.40 ^c
GPX activity (U/mg protein)	Cell-free supernatant	161.46 ± 22.84 ^d	197.67 ± 1.96 ^c	202.61 ± 23.09 ^c	315.72 ± 8.35 ^a	226.41 ± 11.41 ^b	218.34 ± 23.01 ^b
	Intact cell	46.42 ± 5.82	49.22 ± 2.81	43.59 ± 1.84	47.97 ± 7.23	59.51 ± 3.79	54.28 ± 6.17
	Cell-free extract	74.24 ± 7.91 ^{ab}	56.11 ± 3.63 ^{abc}	80.79 ± 3.44 ^a	52.01 ± 1.77 ^{bc}	72.05 ± 11.29 ^{ab}	42.22 ± 5.39 ^c

All values are shown as the mean ± standard deviation of three replicate experiments. Different letters in the same row are significantly different ($p < 0.05$).

2.3.3. Changes in bacterial morphology under oxidative stress

Based on SEM results, WiKim0124 exhibited a smooth surface and an intact cell wall (Fig. 2.3). In contrast, WiKim39 exhibited slight distortion and shrinkage, WiKim32 and WiKim38 were distorted, and WiKim32 exhibited the most visible damage.

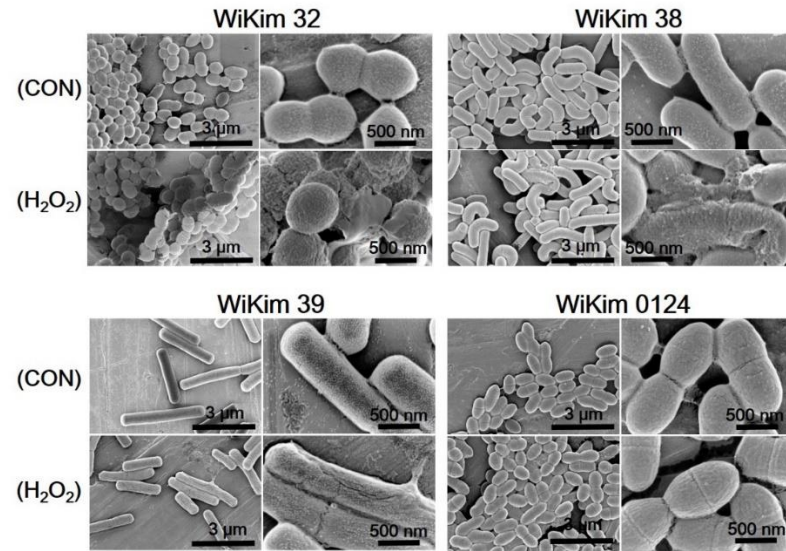


Fig. 2.3. Surface analysis of LAB after H₂O₂ treatment. Surface expressed LAB were visualized by scanning electron microscopy (SEM). CON, non-treated, H₂O₂, 2.5 mM H₂O₂ treated for 24 hours.

2.3.4. Transcriptomic signatures under oxidative stress

To analyze the gene expression profiles during oxidative stress exposure, RNA sequencing data were generated for WiKim38, WiKim39, and WiKim0124 cells. After filtering the initial reads, 20,035 valid reads and 958 DEGs were identified. Overall, the number of upregulated genes increased with increasing H₂O₂ concentration (Fig. 2.4a–c). A hierarchical clustering heat map was constructed based on the 50 most enriched DEGs to visualize the transcriptomic differences among the experimental groups (Fig. 2.4d–f). These heat maps were classified according to the H₂O₂ concentration to compare the five strains with the reference strain. Based on the GO enrichment analysis, all LAB strains, particularly WiKim39, exhibited significant differences in color distribution and the concentration of cell components (CCs), including the membrane part, membrane, and cell part. Biological processes (BPs), including single-organism, metabolic, and cellular processes and biological regulation, were the dominant factors in WiKim38 and WiKim0124 (Fig. 2.5 and Table 2.3). Additionally, the number of DEGs involved in CCs increased with increasing H₂O₂ concentration in WiKim38 and WiKim39, whereas DEGs associated with BPs exhibited no H₂O₂ concentration-dependent trend (Fig. 2.6-2.7).

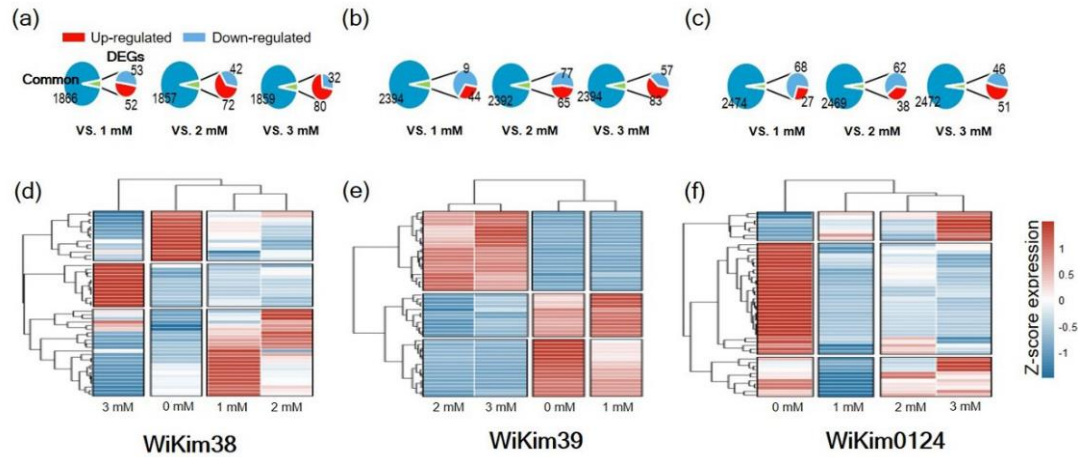


Fig. 2.4. Transcriptomic signatures of WiKim38, WiKim39, and WiKim0124 grown under oxidative stress. (a–c) Expression map of the differentially expressed genes (DEGs) of (a) WiKim38, (b) WiKim39, and (c) WiKim0124. (d–f) Heat map and cluster analysis of the 50 most enriched DEGs. The X-axis represents the experimental groups, and the Y-axis represents the DEGs. Red represents up-regulated DEGs, while blue represents down-regulated DEGs.

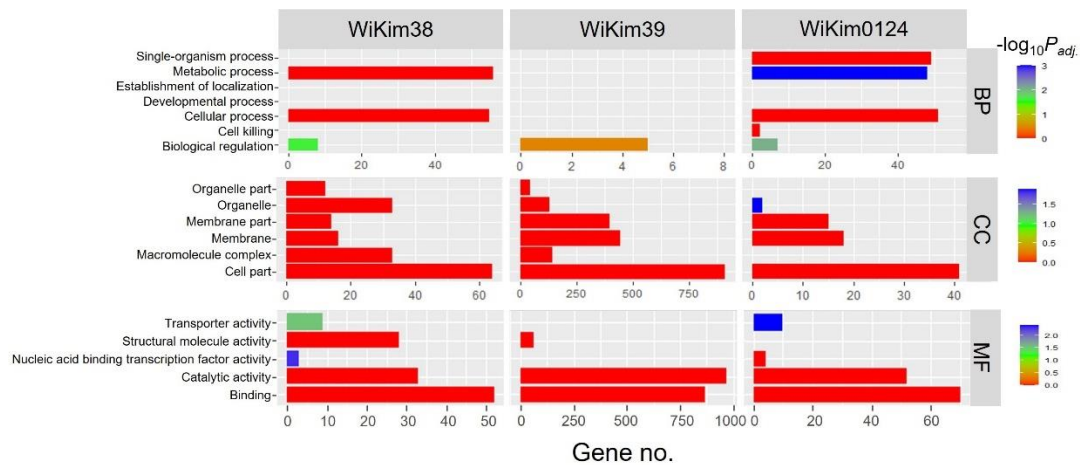


Fig. 2.5. Gene Ontology (GO) enrichment analysis of LAB strains exposed to 0 mM and 2.0 mM H₂O₂. The color represents the negative log₁₀ (P-value), corresponding to the false discovery rate and indicating the significance of enrichment. CC: cellular component; MF: molecular function; BP: biological process.

Table 2.3. Mass spectrometry identification and bioinformatic analysis of 20 differently expressed proteins of Wikim38.

	Spot no. ¹⁾	Log ₂ FC	Monoisotopic mass (Mr)	Mascot score	Coverage (%)	calc. pI	UniProtKB	NCBI accession	Protein	Gene	Organism	GO ID	MF	GO ID	BP	GO ID	CC
down	329	-2.7	22209	497	40	4.84	A0A1X7QLG0	gi 490392004	nitroreductase family protein	<i>nfrA</i>	<i>Latilactobacillus curvatus</i>	GO:0016491	oxidoreductase activity				
												GO:0042602	riboflavin reductase (NADPH) activity				
down	193	-2.6	33766	646	33	5.13	A0A0B2XJ47	gi 734892767	alcohol dehydrogenase GroES-like domain protein	<i>adh2</i>	<i>Latilactobacillus curvatus</i>	GO:0046872	metal ion binding				
												GO:0016491	oxidoreductase activity				
down	282	-1.7	24232	628	43	9.22	A0A0B2XQ77	gi 490391748	50S ribosomal protein L1	<i>rplA</i>	<i>Latilactobacillus curvatus</i>	GO:0019843	rRNA binding	GO:0006417	regulation of translation	GO:0005840	ribosome
												GO:0003723	RNA binding	GO:0006412	translation		
												GO:0000049	tRNA binding				
down	253	-1.7	25838	606	39	5.13	A0A1B2A445	gi 734894178	2,3-bisphosphoglycerate-dependent phosphoglycerate mutase	<i>gpm1</i>	<i>Latilactobacillus curvatus</i>	GO:0046538	2,3-bisphosphoglycerate-dependent phosphoglycerate mutase activity	GO:0006096	glycolytic process		
												GO:0016853	isomerase activity	GO:0006094	gluconeogenesis		
down	89	-1.5	52393	628	22	5.37	A0A1B2A4E0	gi 490385653	Inosine-5'-monophosphate dehydrogenase	<i>guaB</i>	<i>Latilactobacillus curvatus</i>	GO:0003938	IMP dehydrogenase activity	GO:0006164	purine nucleotide biosynthetic process		
												GO:0046872	metal ion binding	GO:0006177	GMP biosynthetic process		
												GO:0016491	oxidoreductase activity				
												GO:0000166	nucleotide binding				
down	342	-1.5	19389	692	45	9.07	A0A1B2A4X2	gi 1036231757	50S ribosomal protein L6	<i>rplF</i>	<i>Latilactobacillus curvatus</i>	GO:0000049	tRNA binding	GO:0006412	translation	GO:0005840	ribosome
												GO:0019843	rRNA binding				
down	392	-1.3	17157	242	33	6.59	A0A0B2XM17	gi 734892574	3-hydroxyacyl-ACP dehydratase	<i>fabA_1</i>	<i>Latilactobacillus curvatus</i>						
down	373	-1.2	17608	510	45	9.47	A0A0B2XP96	gi 490390744	30S ribosomal protein S5	<i>rpsE</i>	<i>Latilactobacillus curvatus</i>	GO:0003735	structural constituent of ribosome	GO:0006412	translation	GO:0005737	cytoplasm
												GO:0019843	rRNA binding			GO:1990904	ribonucleo protein complex
												GO:0003723	RNA binding			GO:0005840	ribosome
down	294	x	22835	442	20	10.02	A0A0B2XKM0	gi 490391527	30S ribosomal protein S4	<i>rpsD</i>	<i>Latilactobacillus curvatus</i>	GO:0019843	rRNA binding	GO:0006412	translation	GO:0005840	ribosome
												GO:0003723	RNA binding			GO:0043229	intracellular organelle

Table 2.3. Continued.

Spot no. ¹⁾	Log ₂ FC	Monoisotopic mass (Mr)	Mascot score	Coverage (%)	calc. pI	UniProtKB	NCBI accession	Protein	Gene	Organism	GO ID	MF	GO ID	BP	GO ID	CC	
up	59	1.9	57243	1136	30	4.67	A0A0B2XPV1	gij490385535	60 kDa chaperonin	<i>groEL</i>	<i>Latilactobacillus curvatus</i>	GO:0051082	unfolded protein binding	GO:0042026	protein refolding	GO:0005737	cytoplasm
												GO:0005524	ATP binding				
												GO:0000166	nucleotide binding				
up	183	1.7	35336	1068	55	4.98	A0A0B2XLJ2	gij734892333	L-lactate dehydrogenase	<i>ldh</i>	<i>Latilactobacillus curvatus</i>	GO:0004459	L-lactate dehydrogenase activity	GO:0006096	glycolytic process	GO:0005737	cytoplasm
												GO:0003824	catalytic activity	GO:0008152	metabolic process		
												GO:0016491	oxidoreductase activity				
up	159	1.6	35694	774	35	5.18	A0A358LUT2	gij490391914	Type I glyceraldehyde-3-phosphate dehydrogenase	DEB54_02440	<i>Lactobacillus</i> sp.	GO:0016491	oxidoreductase activity				
up	444	1.5	13496	202	23	10.67	A0A1B2A555	gij490390750	30S ribosomal protein S13		<i>Latilactobacillus curvatus</i>	GO:0019843	rRNA binding	GO:0006412	translation	GO:0005840	ribosome
												GO:0003735	structural constituent of ribosome				
												GO:0003723	RNA binding				
												GO:0000166	nucleotide binding				
												GO:0000049	tRNA binding				
up	427	1.4	13215	453	53	11.47	A0A0B2XBN3	gij490385974	50S ribosomal protein L19	<i>rplS</i>	<i>Latilactobacillus curvatus</i>			GO:0006412	translation	GO:0005840	ribosome
up	102	1.4	50435	971	35	5.06	A0A2Z6FE34	gij1063819698	Methionine aminopeptidase	<i>pepM</i>	<i>Latilactobacillus curvatus</i>	GO:0046914	transition metal ion binding	GO:0006464	cellular protein modification process		
												GO:0004177	aminopeptidase activity	GO:0070084	protein initiator methionine removal		
												GO:0046872	metal ion binding	GO:0006508	proteolysis		
												GO:0016787	hydrolase activity				

Table 2.3. Continued.

Spot no. ¹⁾	Log ₂ FC	Monoisotopic mass (Mr)	Mascot score	Coverage (%)	calc. pI	UniProtKB	NCBI accession	Protein	Gene	Organism	GO ID	MF	GO ID	BP	GO ID	CC	
up	40	1.4	63013	1895	52	5.23	A0A1X7QIH3	gi 734892239	pyruvate kinase	<i>pyk</i>	<i>Latilactobacillus curvatus</i>	GO:0004743	pyruvate kinase activity	GO:0006096	glycolytic process		
												GO:0046872	metal ion binding				
												GO:0000166	nucleotide binding				
												GO:0016740	transferase activity				
												GO:0016310	phosphorylation				
												GO:0005524	ATP binding				
												GO:0016301	kinase activity				
up	202	1.3	35162	1090	47	4.89	A0A1X7QJM0	gi 490391618	Alpha-ketoacid dehydrogenase subunit beta	<i>pdhB</i>	<i>Latilactobacillus curvatus</i>	GO:0016491	oxidoreductase activity				
up	27	1.3	76861	1317	30	4.71	A0A0B2XL15	gi 490390758	Elongation factor G	<i>fusA</i>	<i>Latilactobacillus curvatus</i>	GO:0003746	translation elongation factor activity	GO:0006412	translation	GO:0005737	cytoplasm
												GO:0000166	nucleotide binding	GO:0006414	translational elongation		
												GO:0005525	GTP binding				
up	169	1.3	35242	1003	45	4.81	A0A0B2XNU8	gi 490391508	Rod shape-determining protein MreD	<i>mreD</i>	<i>Latilactobacillus curvatus</i>			GO:0008360	regulation of cell shape	GO:0005886	plasma membrane
																GO:0016021	integral component of membrane
																GO:0016020	membrane
up	166	1.3	35694	911	43	5.18	A0A358LUT2	gi 490391914	Type I glyceraldehyde-3-phosphate dehydrogenase	DEB54_02440	<i>Lactobacillus</i> sp.	GO:0016491	oxidoreductase activity				

¹⁾ Spots are assigned numbers as indicated in Figure 2.6, 2.7, 2.8.

²⁾ Log₂FC: Log₂ fold change is the ratio of the H₂O₂-treated group to the non-treated group.

²⁾ Best protein accession is according to the NCBI.

³⁾ Thero.kDa and Thero.pI are the theoretical values of molecular weight (Mr, kDa) and pI for the identified proteins, respectively.

⁴⁾ Percentage coverage (%) of matched peptides in the whole protein sequence.

⁵⁾ The *p*-value is the highest score expected for the matched peptides.

Table 2.4. Mass spectrometry identification and bioinformatic analysis of 21 differently expressed proteins of Wikim39.

Spot no.	Log ₂ FC	Monoisotopic mass (Mr)	Mascot score	Coverage (%)	calc. pI	UniProtKB	NCBI accession	Protein	Gene	Organism	GO ID	MF	GO ID	BP	GO ID	CC	
down	127	-1.7	52801	1340	48	5.18	A0A1P8Q3X2	APX72547.1	6-phosphogluconate dehydrogenase, decarboxylating	BTM29_08285	<i>Companilactobacillus allii</i>	GO:0016491	oxidoreductase activity	GO:0016054	organic acid catabolic process		
													GO:0006740	NADPH regeneration			
													GO:0019521	D-gluconate metabolic process			
down	155	-4	42851	1737	54	5.48	A0A1P8Q3D8	APX72358.1	Phosphoglycerate kinase	<i>pgk</i>	<i>Companilactobacillus allii</i>	GO:0000166	nucleotide binding	GO:0006096	glycolytic process	GO:0005737	cytoplasm
												GO:0016740	transferase activity	GO:0016310	phosphorylation		
												GO:0016301	kinase activity				
down	196	-2.1	36274	1308	52	5.73	A0A1P8Q3E8	APX72357.1	Glyceraldehyde-3-phosphate dehydrogenase	BTM29_07190	<i>Companilactobacillus allii</i>	GO:0016491	oxidoreductase activity				
												GO:0000166	nucleotide binding				
down	202	-6.2	36274	1308	52	5.73	A0A1P8Q3E8	APX72357.1	Glyceraldehyde-3-phosphate dehydrogenase	BTM29_07190	<i>Companilactobacillus allii</i>	GO:0016491	oxidoreductase activity				
												GO:0000166	nucleotide binding				
down	245	-1.4	31676	1717	62	5.08	A0A1P8Q453	APX72624.1	Elongation factor Ts	<i>tsf</i>	<i>Companilactobacillus allii</i>	GO:0003746	translation elongation factor activity	GO:0006414	translational elongation	GO:0110165	cellular anatomical entity
														GO:0006412	translation	GO:0005737	cytoplasm
down	265	-1.4	31777	470	20	5.25	A0A1P8Q4C2	APX72677.1	2,5-diketo-D-gluconic acid reductase	BTM29_08990	<i>Companilactobacillus allii</i>	GO:0016491	oxidoreductase activity				
down	270	-1.5	29159	348	26	4.98	A0A1P8Q3F3	APX72375.1	Exodeoxyribonuclease III	BTM29_07285	<i>Companilactobacillus allii</i>	GO:0003824	catalytic activity				
down	134	-1.1	49363	1321	43	4.99	A0A1P8Q5Y9	APX73251.1	Glucose-6-phosphate isomerase	<i>pgi</i>	<i>Companilactobacillus allii</i>	GO:0004347	glucose-6-phosphate isomerase activity	GO:0006094	gluconeogenesis	GO:0005737	cytoplasm
												GO:0016853	isomerase activity	GO:0006096	glycolytic process		
												GO:0016874	ligase activity	GO:0006412	translation	GO:0043231	intracellular membrane-bounded organelle
up	99	1.8	52287	534	31	5.11	A0A1P8Q2P3	APX72130.1	Glutamyl-tRNA(Gln) amidotransferase subunit A	<i>gatA</i>	<i>Companilactobacillus allii</i>	GO:0000166	nucleotide binding			GO:0005737	cytoplasm
												GO:0016740	transferase activity				
												GO:0005524	ATP binding				
												GO:0003824	catalytic activity				

Table 2.4. Continued.

Spot no.	Log ₂ FC	Monoisotopic mass (Mr)	Mascot score	Coverage (%)	calc. pI	UniProtKB	NCBI accession	Protein	Gene	Organism	GO ID	MF	GO ID	BP	GO ID	CC	
up	185	2.1	35139	941	47	4.75	A0A1P8Q5D0	APX73064.1	Cell shape-determining protein MreB	<i>mreB</i>	<i>Companilactobacillus allii</i>	GO:0005524	ATP binding	GO:0000902	cell morphogenesis	GO:0005737	cytoplasm
												GO:0000166	nucleotide binding	GO:0008360	regulation of cell shape		
up	186	1.7	36274	1422	47	5.73	A0A1P8Q3E8	APX72357.1	Glyceraldehyde-3-phosphate dehydrogenase	BTM29_07190	<i>Companilactobacillus allii</i>	GO:0016491	oxidoreductase activity				
												GO:0000166	nucleotide binding				
up	190	1.8	36274	1188	51	5.73	A0A1P8Q3E8	APX72357.1	Glyceraldehyde-3-phosphate dehydrogenase	BTM29_07190	<i>Companilactobacillus allii</i>	GO:0016491	oxidoreductase activity				
												GO:0000166	nucleotide binding				
up	210	1.4	36345	852	41	5.67	A0A1P8Q5H2	APX73091.1	Threonylcarbamoyl-AMP synthase	BTM29_11255	<i>Companilactobacillus allii</i>	GO:0016740	transferase activity	GO:0008033	tRNA processing	GO:0005737	cytoplasm
												GO:0000166	nucleotide binding				
												GO:0005524	ATP binding				
up	242	1.5	35427	778	38	5.94	A0A1P8PZX9	APX71119.1	EIIAB-Man	BTM29_00500	<i>Companilactobacillus allii</i>	GO:0016740	transferase activity	GO:0008643	carbohydrate transport	GO:0005886	plasma membrane
															GO:0016020	membrane	
up	264	1.3	29649	408	35	4.82	A0A1P8Q0Y8	APX71544.1	Bifunctional hydroxymethyl pyrimidine kinase/phosphomethyl-pyrimidine kinase	BTM29_02765	<i>Companilactobacillus allii</i>	GO:0016301	kinase activity	GO:001631	phosphorylation	GO:0005737	cytoplasm
up	326	1.4	26430	1018	44	5.84	A0A1P8Q444	APX72625.1	Uridylate kinase	<i>pyrH</i>	<i>Companilactobacillus allii</i>	GO:0033862	UMP kinase activity	GO:0008152	metabolic process	GO:0005737	cytoplasm
												GO:0003824	catalytic activity	GO:001631	phosphorylation		
												GO:0016740	transferase activity				
												GO:0000166	nucleotide binding				
												GO:0005524	ATP binding				
up	339	1.4	24052	787	54	8.57	A0A1P8PZS0	APX71095.1	50S ribosomal protein L1	<i>rplA</i>	<i>Companilactobacillus allii</i>	GO:0003723	RNA binding	GO:0006412	translation	GO:0015934	large ribosomal subunit
														GO:0006417	regulation of translation	GO:0005840	ribosome
up	372	1.4	24467	1129	69	5.89	A0A1P8Q458	APX72641.1	Protein GrpE	<i>grpE</i>	<i>Companilactobacillus allii</i>		GO:0006457	protein folding	GO:0005737	cytoplasm	

Table 2.4. Continued.

Spot no.	Log ₂ FC	Monoisotopic mass (Mr)	Mascot score	Coverage (%)	calc. pI	UniProtKB	NCBI accession	Protein	Gene	Organism	GO ID	MF	GO ID	BP	GO ID	CC
Up	456	1.3	15384	173	20	5.45	A0A1P8Q1D7	APX71693.1	Galactose-6-phosphate isomerase	BTM29_03600	<i>Companilactobacillus allii</i>	GO:0016853	isomerase activity	GO:0005988	lactose metabolic process	
up	639	1.4	21366	705	54	6.85	A0A1P8Q2R0	APX72125.1	Xanthine phosphoribosyltransferase	<i>xpt</i>	<i>Companilactobacillus allii</i>	GO:0016740	transferase activity		GO:0005737	cytoplasm
up	645	1.4	17266	338	63	4.47	A0A1P8Q3X7	APX72556.1	Transcription elongation factor GreA	<i>greA</i>	<i>Companilactobacillus allii</i>	GO:0003677	DNA binding	GO:0006414	translational elongation	
												GO:0070063	RNA polymerase binding			

Table 2.5. Mass spectrometry identification and bioinformatic analysis of 14 differently expressed proteins of Wikim0124.

	Spot no.	Log ₂ FC	Monoisotopic mass (Mr)	Mascot score	Coverage (%)	calc. pI	UniProtKB	NCBI accession	Protein	Gene	Organism	GO ID	MF	GO ID	BP	GO ID	CC
down	120	-2	44683	1293	45	4.99	A0A2A9IN45	QQF00899.1	30S ribosomal protein S1	<i>rpsA</i>	<i>Lactococcus lactis</i>					GO:0005840	ribosome
												GO:0003746	translation elongation factor activity				
												GO:0005525	GTP binding			GO:0005737	cytoplasm
down	418	-2	43185	560	25	4.89	A0A089XR72	RQE03428.1	Elongation factor Tu		<i>Lactococcus lactis</i>	GO:0016787	hydrolase activity				
												GO:0000166	nucleotide binding				
												GO:0003746	translation elongation factor activity	GO:0006414	translational elongation		
												GO:0005525	GTP binding	GO:0006412	translation		
down	129	-1.3	46128	1086	42	5.15	A0A2A8DCG2	RQE00445.1	Arginine deiminase	<i>arcA</i>	<i>Lactococcus lactis</i>	GO:0016990	arginine deiminase activity	GO:0006527	arginine catabolic process	GO:0005737	cytoplasm
												GO:0016787	hydrolase activity	GO:0006525	arginine metabolic process		
														GO:0019547	arginine catabolic process to ornithine		
down	226	-1.2	33912	743	40	4.86	A0A2A8DDV5	GFO78898.1	tagatose-6-phosphate kinase	<i>pfkB</i>	<i>Lactococcus lactis</i>	GO:0016772	transferase activity	GO:0016310	phosphorylation		
												GO:0009024	tagatose-6-phosphate kinase activity	GO:2001059	D-tagatose 6-phosphate catabolic process		
												GO:0008662	1-phosphofructokinase activity	GO:0005988	lactose metabolic process		
												GO:0000166	nucleotide binding	GO:0016310	phosphorylation		
												GO:0005524	ATP binding				
												GO:0016301	kinase activity				
down	248	-1.1	28517	550	30	5.09	A0A2A9HL64	QQF00028.1	30S ribosomal protein S2	<i>rpsB</i>	<i>Lactococcus lactis</i>			GO:0006412	translation	GO:0005840	ribosome
down	166	-1.1	36647	1275	55	4.92	A0A089ZFY8	QQF00027.1	Elongation factor Ts	<i>tsf</i>	<i>Lactococcus lactis</i>	GO:0003746	translation elongation factor activity	GO:0006414	translational elongation	GO:0110165	cellular anatomical entity
																GO:0005737	cytoplasm

Table 2.5. Continued.

Spot no.	Log ₂ FC	Monoisotopic mass (Mr)	Mascot score	Coverage (%)	calc. pI	UniProtKB	NCBI accession	Protein	Gene	Organism	GO ID	MF	GO ID	BP	GO ID	CC	
down	137	-1.1	43185	1516	44	4.89	A0A089XR72	RQE03428.1	Elongation factor Tu	<i>Lactococcus lactis</i>	GO:0003746	translation elongation factor activity					
											GO:0005525	GTP binding		GO:0005737	cytoplasm		
											GO:0016787	hydrolase activity					
											GO:0000166	nucleotide binding					
											GO:0003746	translation elongation factor activity	GO:0006414	translational elongation			
down	74	-1.1	46943	936	32	4.42	A0A2A9IQR2	QQF00568.1	Trigger factor	<i>tig</i>	<i>Lactococcus lactis</i>	GO:0016853	isomerase activity	GO:0007049	cell cycle	GO:0005737	cytoplasm
														GO:0051301	cell division		
														GO:0006457	protein folding		
														GO:0015031	protein transport		
down	426	-1.1	20761	330	26	4.82	A0A089XP37	QQF00437.1	Alkyl hydroperoxide reductase C	<i>ahpC</i>	<i>Lactococcus lactis</i>	GO:0016209	antioxidant activity	GO:0006979	response to oxidative stress	GO:0005737	cytoplasm
												GO:0051920	peroxiredoxin activity				
												GO:0004601	peroxidase activity				
												GO:0016491	oxidoreductase activity				
up	257	2.2	32110	569	24	4.66	A0A2A9IB80	RQE01453.1	Glucose-1-phosphate thymidyltransferase	<i>rfaA</i>	<i>Lactococcus lactis</i>	GO:0008879	glucose-1-phosphate thymidyltransferase activity	GO:0045226	extracellular polysaccharide biosynthetic process		
												GO:0046872	metal ion binding				
												GO:0016779	nucleotidyltransferase activity				
												GO:0016740	transferase activity				

Table 2.5. Continued.

Spot no.	Log ₂ FC	Monoisotopic mass (Mr)	Mascot score	Coverage (%)	calc. pI	UniProtKB	NCBI accession	Protein	Gene	Organism	GO ID	MF	GO ID	BP	GO ID	CC
up	343	1.4	25624	312	22	6.43	A0A2A8DG91	QQF00843.1	3-oxoacyl-[acyl-carrier-protein] reductase	<i>Lactococcus lactis</i>	GO:0051287	NAD binding	GO:0006633	fatty acid biosynthetic process		
											GO:0004316	3-oxoacyl-[acyl-carrier-protein] reductase (NADPH) activity	GO:0006629	lipid metabolic process		
											GO:0016746	acyltransferase activity	GO:0006631	fatty acid metabolic process		
											GO:0016740	transferase activity				
											GO:0016491	oxidoreductase activity				
up	359	2	46940	664	25	4.68	A0A2A9ISE0	QQF00661.1	Phosphopyruvate hydratase	<i>eno</i> <i>Lactococcus lactis</i>	GO:0004634	phosphopyruvate hydratase activity	GO:0006096	glycolytic process	GO:0005576	extracellular region
											GO:0046872	metal ion binding			GO:0005737	cytoplasm
											GO:0016829	lyase activity			GO:0009986	cell surface
											GO:0000287	magnesium ion binding				
up	429	1.3	19496	248	30	5.43	A0A6M0M974	PAL02118.1	DUF536 domain-containing protein	GTP08_09695	<i>Lactococcus lactis</i>					
up	430	1	18440	817	56	4.79	A0A0A7T232	RQE03401.1	Asp23/Gis24 family envelope stress response protein							

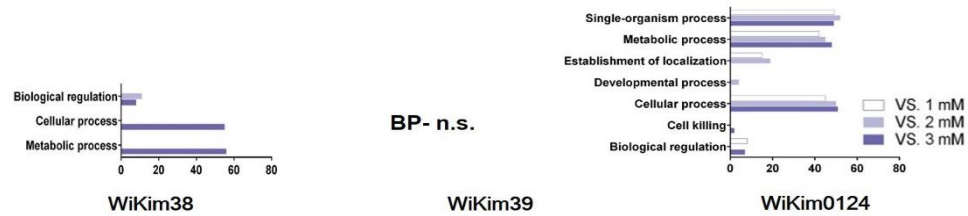


Fig. 2.6. Gene ontology (GO) categorization of differentially expressed genes (DEGs) of WiKim38, WiKim39, and WiKim0124 grown under different levels of oxidative stress (1–3 mM H₂O₂) under biological processes.

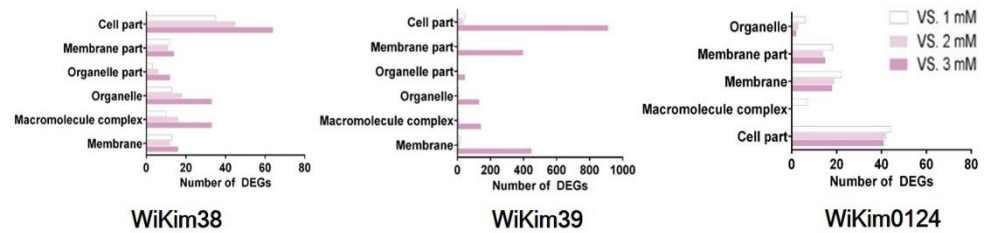


Fig. 2.7. Gene ontology (GO) categorization of differentially expressed genes (DEGs) of WiKim38, WiKim39, and WiKim0124 grown under different levels of oxidative stress (1–3 mM H₂O₂) under cellular components.

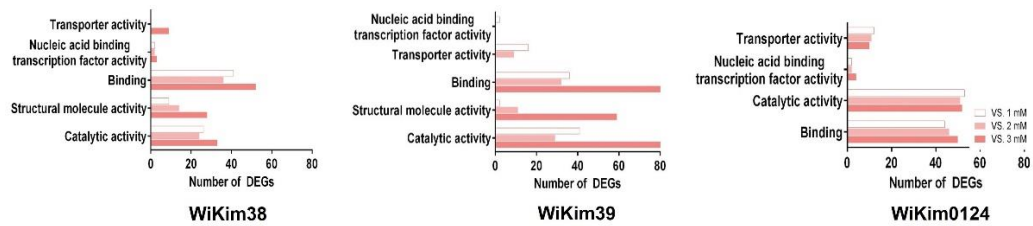


Fig. 2.8. Gene ontology (GO) categorization of differentially expressed genes (DEGs) of WiKim38, WiKim39, and WiKim0124 grown under different levels of oxidative stress (1–3 mM H₂O₂) under molecular function.

2.3.5. Proteomic signatures under oxidative stress

Changes in protein expression levels during oxidative stress exposure were measured using 2-DE protein separation. In total, 55 DEPs were detected in each gel. Treatment with 2.5 mM H₂O₂ resulted in 12 and 10 instances of upregulated and downregulated protein expression, respectively, in WiKim38, 8 and 13 instances of upregulated and downregulated protein expression, respectively, in WiKim39, and 9 and 5 instances of upregulated and downregulated protein expression, respectively, in WiKim0124. Some proteins were observed in multiple spots on the same gel. These proteins can arise from different protein isoforms, post-translational modifications, or degradation (Jiang et al., 2020). Representative gel images and detailed information on each spot obtained via MS are shown in Figure 2.8-2.10, and Tables 2.3–2.5, respectively. All identified protein spots were subjected to functional annotation analysis using the GO pathway database. Consistent with the analysis of RNA sequencing data, all samples showed significantly upregulated DEPs in the cytoplasm associated with CCs, whereas DEPs associated with BPs were upregulated in translation and translational elongation. Additionally, DEPs associated with MFs demonstrated increased activity in nucleotide binding (GO:0000166) and transferase activity proteins (GO:0016740) (Fig. 2.11). Numerous DEPs of glycolysis or metabolic processes, such as ATP binding (GO:0005524), L-lactate dehydrogenase activity (GO:0004459), oxidoreductase activity (GO:0016491), and catalytic activity (GO:0003824), were highly

upregulated.

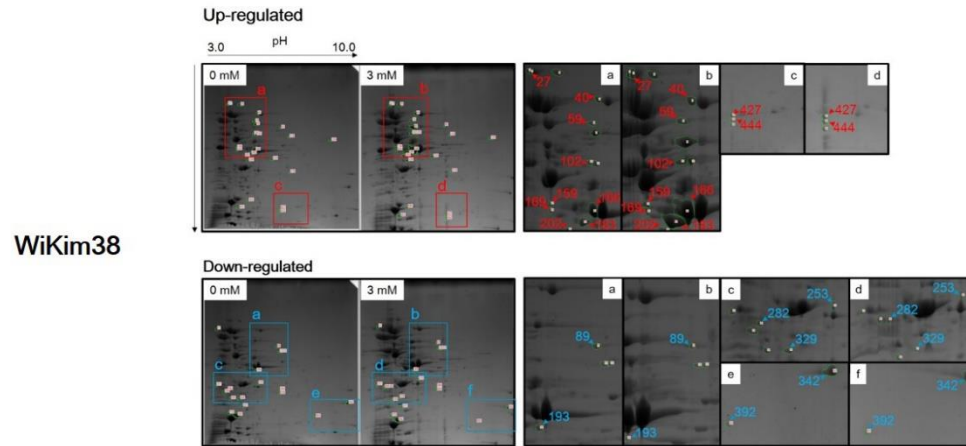
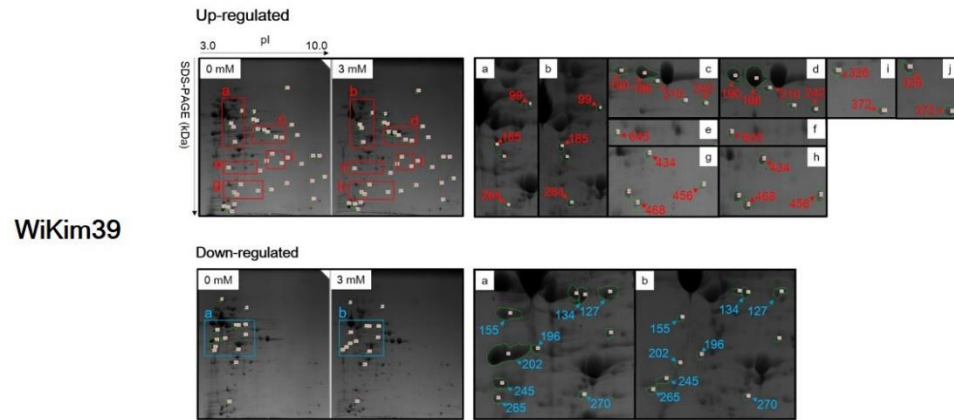


Fig. 2.9. Two-dimensional gel electrophoresis images of proteins extracted from WiKim38 grown under exposure to 2.5 mM H₂O₂. Coomassie blue-stained 2-DE pattern of the WiKim38 proteome analyzed using nonlinear gradient strips with a pH range of 3–10 and 9–16% linear gradient polyacrylamide gels in SDS-PAGE. Spots were excised from the gels for MS/MS analysis. Each spot labeled with a red or blue number represents up-regulated or down-regulated gel spots selected for MS/MS analysis.



WiKim39

Fig. 2.10. Two-dimensional gel electrophoresis images of proteins extracted from WiKim39 grown under exposure to 2.5 mM H₂O₂. Coomassie blue-stained 2-DE pattern of the WiKim39 proteome analyzed using nonlinear gradient strips with a pH range of 3–10 and 9–16% linear gradient polyacrylamide gels in SDS-PAGE. Spots were excised from the gels for MS/MS analysis. Each spot labeled with a red or blue number represents up-regulated or down-regulated gel spots selected for MS/MS analysis.

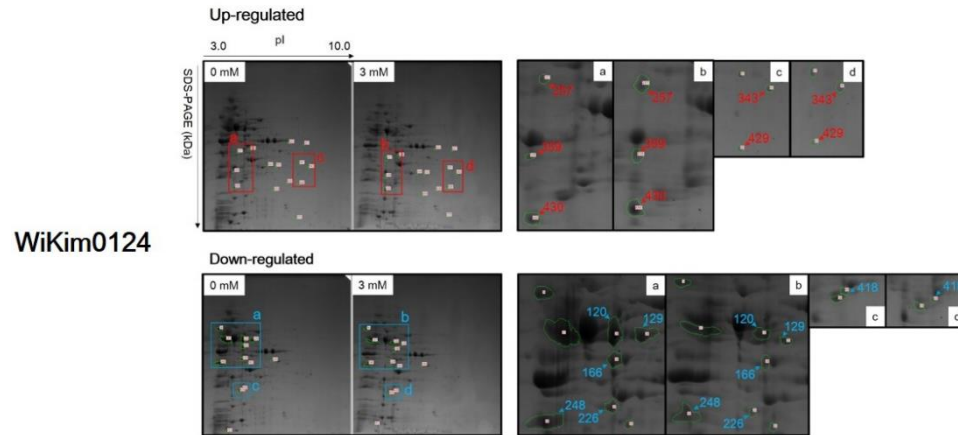


Fig. 2.11. Two-dimensional gel electrophoresis images of proteins extracted from WiKim0124 grown under exposure to 2.5 mM H₂O₂. Coomassie blue-stained 2-DE pattern of the WiKim0124 proteome analyzed using nonlinear gradient strips with a pH range of 3–10 and 9–16% linear gradient polyacrylamide gels in SDS-PAGE. Spots were excised from the gels for MS/MS analysis. Each spot labeled with a red or blue number represents up-regulated or down-regulated gel spots selected for MS/MS analysis.

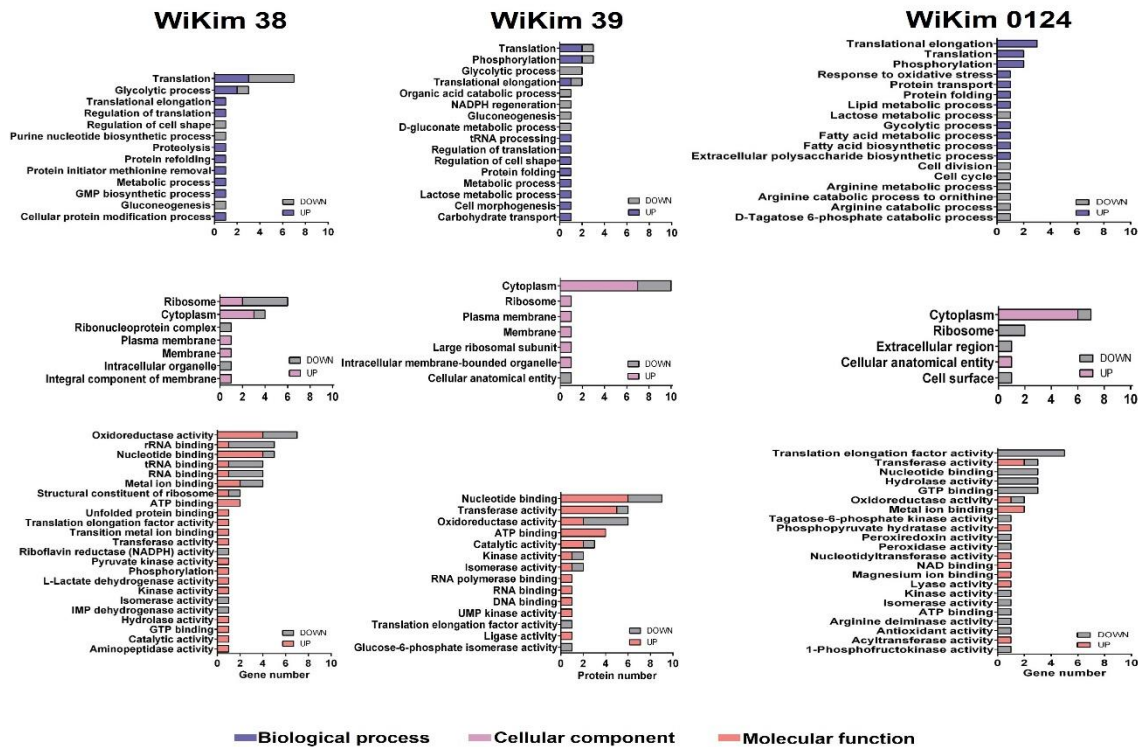


Fig. 2.12. Proteomic analysis of WiKim38, WiKim39, and WiKim0124 DEPs exposed to 2.5 mM H₂O₂. Gene ontology (GO) categorization of differentially expressed proteins (DEPs) under biological processes, cellular components and molecular function.

2.3.6. Proteins or genes associated with the stress response from three LAB strains

By comparing the proteome profiles of three different lactic acid bacteria with previously reported stress genes, a total of five genes (*adh2*, *groEL*, *ldh*, *nfrA*, *pepM*) were identified in WiKim38, and two genes (*mreB*, *tsf*) were identified in WiKim39. Only one gene associated with the stress response (*tsf*) was identified in WiKim0124. These findings suggest that the identified genes could play a role in stress response and resistance in these bacterial strains.

2.4. Discussion

Although H₂O₂ has relatively low toxicity and reactivity, it can cause oxidative damage by reacting with Fe²⁺ salts to generate toxic OH radical ions via the Fenton reaction (Mbye et al., 2020). In this study, all LAB strains, including LGG, were resistant to H₂O₂ at a concentration of 2.5 mM. Furthermore, WiKim32, WiKim38, WiKim39, and WiKim0124 survived for 6 h in the presence of 4 mM H₂O₂, with WiKim39 showing the highest resistance. Large amounts of H₂O₂ can arrest cell growth because OH radicals can easily diffuse into the cell membranes of LAB. Therefore, LAB likely have mechanisms ensuring survival during oxidative stress.

The cell-free supernatant had the highest DPPH, ABTS, and hydroxyl radical scavenging activity, which could be due to the promotion of biologically active compounds by LAB growth. In a recent study, WiKim39 and WiKim0124 exhibited enhanced radical scavenging activity because of the increased production of functional organic acids and phenolic compounds in fermented vegetable juices (Lee et al., 2021). In contrast to LGG, intact cells and cell-free extracts across all five LAB strains exhibited strong antioxidant activity. Oxidative stress often presents symptoms associated with membrane lipid peroxidation, which can lead to accumulation of ROS and malondialdehyde (Jiang et al., 2020). Proteins,

polysaccharides, peptidoglycans, lipoteichoic acid, and exopolysaccharides (EPS) on LAB surfaces exhibit free radical scavenging activity and inhibit lipid peroxidation (Kim, Yang, & Paik, 2021). In a previous study, we found that EPS in WiKim32 exhibited reducing potential and antioxidant activity by inhibiting lipid peroxidation (Choi et al., 2021). Moreover, intracellular components, amino acids, and peptides are responsible for antioxidant activity and can chelate iron to reduce Fe^{2+} levels (Feng & Wang, 2020). The reducing potential and inhibition of lipid peroxidation in cell-free extracts and intact LAB cells were significantly higher than those of LGG. This may be due to the enhanced activity of intracellular antioxidants and cell wall components in LAB.

Although H_2O_2 -degrading enzymes such as catalase and peroxidase are rarely produced in LAB, they have other antioxidant mechanisms. Specifically, SOD catalyzes the conversion of superoxide anions to oxygen and thus controls H_2O_2 -induced cell damage. Furthermore, glutathione–glutaredoxin systems (including glutathione reductase and GPX), which oxidize glutathione to glutathione disulfide to reduce H_2O_2 , play a major role in protecting against oxidative damage (Vázquez et al., 2017). The higher antioxidant enzyme levels of WiKim38, WiKim39, and WiKim0124 suggest strong antioxidant properties. However, the antioxidant mechanisms of probiotic LAB are complex and vary between strains.

In this study, slight cell-surface damage was observed in WiKim39 and WiKim0124, whereas the cell walls of WiKim32 showed severe damage.

Some WiKim38 cells were completely ruptured. This is consistent with the enzyme activity results and suggests that some cell wall components may be responsible for the antioxidant potential of LAB.

Based on the transcriptional responses of WiKim38, WiKim39, and WiKim0124 under different H₂O₂ conditions, upregulated gene expression patterns changed in a concentration-dependent manner. The GO pathway enrichment analysis of DEGs was mainly influenced by CCs, and the highly enriched GO terms were the cell part, membrane, and membrane part, particularly in the WiKim39 group exposed to 3 mM H₂O₂. In terms of BPs, most DEGs were involved in cellular and metabolic processes. Thus, H₂O₂ oxidative stress may be less affected by BPs than CCs. Cell envelopes and membranes are the first barriers to environmental stress, and the related genes may play important roles in stress responses (Zhao et al., 2020). In the case of damaged cells, membrane repair must be rapid so that cells can recover from stress-induced damage (Lan & Shi, 2022). In the MF category, genes associated with the GO terms catalytic activity and binding were abundantly expressed, indicating active metabolic processes and regulatory networks under oxidative stress conditions. Additionally, genes related to structural molecule activity were most abundant in WiKim38, suggesting the activation of functions that maintain cellular structure and stability (Papadimitriou et al., 2016). These findings suggest that the strain actively contributes to various processes, including metabolic activity, cellular structure maintenance, and gene expression regulation. Our DEG

distribution results indicate that membrane damage was repaired first during recovery to combat oxidative stress. Oxidative damage results in metabolic dysfunction, cell destruction, or mutations (Li et al., 2020). Metabolic and cellular processes were significantly upregulated in WiKim38 and WiKim0124. This indicates that cells can use ATP, regulate metabolic abnormalities, and repair DNA damage, thereby maintaining stable ROS scavenging activity (Shimizu, Yoshida, Suda, & Minamino, 2014).

Consistent with the RNA sequencing results, H₂O₂ stress also significantly upregulated cytoplasmic and CC-related proteins. In addition, most DEPs were significantly upregulated in translation, translational elongation, and glycolytic processes within the BP category. The loss of bacterial membrane integrity occurs when cells are subjected to sublethal stress in response to damage (Hon & Pyun, 2001). In general, glycolytic enzymes are expressed to generate energy to sustain growth and maintenance in response to damage (Liu, Chan, Chen, Solem, & Jensen, 2019). Up regulation of nucleotide binding and transferase activity indicates that under stress conditions (e.g., H₂O₂ exposure), the cells are activating key physiological responses such as energy metabolism, signal transduction, and gene expression regulation, particularly as mechanisms to repair damaged cellular functions caused by oxidative stress or to enhance cellular defense systems (Sujitha et al., 2023). Consistent with previous studies, there was an overall shift toward energy and protein production during H₂O₂ exposure, with the upregulation of genes involved in cellular respiration and

protein biosynthesis. Among the gene profiles of the three LAB strains, several genes related to stress response were identified, including *adh2*, *groEL*, *ldh*, *mreB*, *nfrA*, *pepM*, and *tsf*. *Ldh* encodes lactate dehydrogenase, which helps maintain redox balance and prevent oxidative stress damage by generating NAD⁺ (Rico, Yebra, Pérez-Martínez, Deutscher, & Monedero, 2008). *Adh2* plays a positive role in oxidative stress response by reducing toxic aldehydes (Hu et al., 2019), and *groEL* is a chaperonin that protects against oxidative stress (Hosseini Nezhad, Hussain, & Britz, 2015). *MreB* is involved in resisting oxidative stress and maintaining cell morphology (Domínguez-Escobar et al., 2011), whereas *nfrA* reduces ROS and prevents oxidative damage (Streker, Freiberg, Labischinski, Hacker, & Ohlsen, 2005). *PepM* plays a role in protein degradation, and its overexpression can reduce the toxic effects of oxidative stress (Kaur, Ali, Kumar, Mohanty, & Behare, 2017). *Tsf* is involved in protein synthesis, cell division, and cell wall synthesis (Mangalappalli-Illathu & Korber, 2006).

2.5. Conclusions

The objective of this study was to determine whether five LAB strains isolated from kimchi exhibited antioxidant activity and provide insights into the related mechanism of H₂O₂-induced oxidative stress regulation. The LAB strains exhibited DPPH, ABTS, and OH radical scavenging activity. Furthermore, they exhibited strong reducing potential, lipid peroxidation inhibitory effects, and antioxidant enzyme activity. Transcriptomic and proteomic profiles during H₂O₂ exposure indicated that the cell membrane, intracellular metabolism, and cellular processes were activated in response to oxidative damage. These results support the hypothesis that LAB strains isolated from kimchi have antioxidant effects. This suggests that LAB isolated from kimchi could be used as a functional supplement and starter culture in the fermented food industry to enhance the antioxidant properties of different products. Further research is required to investigate these antioxidant mechanisms and bacterial cell-wall components.

2.6. References

- Choi, I. S., Ko, S. H., Lee, M. E., Kim, H. M., Yang, J. E., Jeong, S.-G., Lee, K. H., Chang, J. Y., Kim, J.-C., & Park, H. W. (2021). Production, characterization, and antioxidant activities of an exopolysaccharide extracted from spent media wastewater after *Leuconostoc mesenteroides* WiKim32 fermentation. *ACS Omega*, 6 (12), 8171-8178.
- Domínguez-Escobar, J., Chastanet, A., Crevenna, A. H., Fromion, V., Wedlich-Söldner, R., & Carballido-López, R. (2011). Processive movement of MreB-associated cell wall biosynthetic complexes in bacteria. *Science*, 333 (6039), 225-228.
- Feng, T., & Wang, J. (2020). Oxidative stress tolerance and antioxidant capacity of lactic acid bacteria as probiotic: a systematic review. *Gut Microbes*, 12 (1), 1801944.
- García-Moreno, A., López-Domínguez, R., Villatoro-García, J. A., Ramírez-Mena, A., Aparicio-Puerta, E., Hackenberg, M., Pascual-Montano, A., & Carmona-Saez, P. (2022). Functional enrichment analysis of regulatory elements. *Biomedicines*, 10 (3), 590.
- Ghani, M. A., Barril, C., Bedgood Jr, D. R., & Prenzler, P. D. (2017). Measurement of antioxidant activity with the thiobarbituric acid

reactive substances assay. *Food chemistry*, 230, 195-207.

Han, K. J., Lee, J.-E., Lee, N.-K., & Paik, H.-D. (2020). Antioxidant and anti-inflammatory effect of probiotic *Lactobacillus plantarum* KU15149 derived from Korean homemade diced-radish kimchi.

Hon, S. I., & Pyun, Y. R. (2001). Membrane damage and enzyme inactivation of *Lactobacillus plantarum* by high pressure CO₂ treatment. *Int J Food Microbiol*, 63 (1-2), 19-28.

Hosseini Nezhad, M., Hussain, M. A., & Britz, M. L. (2015). Stress responses in probiotic *Lactobacillus casei*. *Critical reviews in food science and nutrition*, 55 (6), 740-749.

Hu, Z., Jia, P., Bai, Y., Fan, T.-p., Zheng, X., & Cai, Y. (2019). Characterisation of five alcohol dehydrogenases from *Lactobacillus reuteri* DSM20016. *Process Biochemistry*, 86, 73-79.

Jiang, J., Ren, X., Li, L., Hou, R., Sun, W., Jiao, C., Yang, N., & Dong, Y. (2020). H₂S Regulation of Metabolism in Cucumber in Response to Salt-Stress Through Transcriptome and Proteome Analysis. *Front Plant Sci*, 11, 1283.

Kaur, G., Ali, S. A., Kumar, S., Mohanty, A. K., & Behare, P. (2017). Label-free quantitative proteomic analysis of *Lactobacillus fermentum* NCDC 400 during bile salt exposure. *Journal of proteomics*, 167, 36-45.

Kim, H.-Y., & Park, K.-Y. (2018). Clinical trials of kimchi intakes on the regulation of metabolic parameters and colon health in healthy

- Korean young adults. *Journal of Functional Foods*, 47, 325-333.
- Kim, K.-T., Yang, S. J., & Paik, H.-D. (2021). Probiotic properties of novel probiotic *Levilactobacillus brevis* KU15147 isolated from radish kimchi and its antioxidant and immune-enhancing activities. *Food Science and Biotechnology*, 30 (2), 257-265.
- Kim, M. S., Yang, H. J., Kim, S. H., Lee, H. W., & Lee, M. S. (2018). Effects of Kimchi on human health: A protocol of systematic review of controlled clinical trials. *Medicine (Baltimore)*, 97 (13), e0163.
- Koller, V. J., Marian, B., Stidl, R., Nersesyan, A., Winter, H., Simic, T., Sontag, G., & Knasmuller, S. (2008). Impact of lactic acid bacteria on oxidative DNA damage in human derived colon cells. *Food Chem Toxicol*, 46 (4), 1221-1229.
- Lan, L., & Shi, H. (2022). New insights into the formation and recovery of sublethally injured *Escherichia coli* O157: H7 induced by lactic acid. *Food Microbiology*, 102, 103918.
- Lee, M., Song, J. H., Choi, E. J., Yun, Y. R., Lee, K. W., & Chang, J. Y. (2021). UPLC-QTOF-MS/MS and GC-MS Characterization of Phytochemicals in Vegetable Juice Fermented Using Lactic Acid Bacteria from Kimchi and Their Antioxidant Potential. *Antioxidants (Basel)*, 10 (11).
- Lee, M., Song, J. H., Park, J. M., & Chang, J. Y. (2019). Bacterial diversity in Korean temple kimchi fermentation. *Food Res Int*, 126, 108592.
- Lee, M., Song, J. H., Shim, W. B., & Chang, J. Y. (2020). DNAzyme-based

quantitative loop-mediated isothermal amplification for strain-specific detection of starter kimchi fermented with *Leuconostoc mesenteroides* WiKim32. *Food Chem*, 333, 127343.

Li, T., Lin, X., Yu, L., Lin, S., Rodriguez, I. B., & Ho, T.-Y. (2020). RNA-seq profiling of *Fugacium kawagutii* reveals strong responses in metabolic processes and symbiosis potential to deficiencies of iron and other trace metals. *Science of the Total Environment*, 705, 135767.

Lin, X., Xia, Y., Wang, G., Yang, Y., Xiong, Z., Lv, F., Zhou, W., & Ai, L. (2018). Lactic acid bacteria with antioxidant activities alleviating oxidized oil induced hepatic injury in mice. *Frontiers in microbiology*, 9, 2684.

Liu, J., Chan, S. H. J., Chen, J., Solem, C., & Jensen, P. R. (2019). Systems Biology - A Guide for Understanding and Developing Improved Strains of Lactic Acid Bacteria. *Front Microbiol*, 10, 876.

Mangalappalli-Illathu, A. K., & Korber, D. R. (2006). Adaptive resistance and differential protein expression of *Salmonella enterica* serovar Enteritidis biofilms exposed to benzalkonium chloride. *Antimicrobial agents and chemotherapy*, 50 (11), 3588-3596.

Mbye, M., Baig, M. A., AbuQamar, S. F., El-Tarabily, K. A., Obaid, R. S., Osaili, T. M., Al-Nabulsi, A. A., Turner, M. S., Shah, N. P., & Ayyash, M. M. (2020). Updates on understanding of probiotic lactic acid bacteria responses to environmental stresses and highlights on

proteomic analyses. *Comprehensive Reviews in Food Science and Food Safety*, 19 (3), 1110-1124.

Nakagawa, H., & Miyazaki, T. (2017). Beneficial effects of antioxidative lactic acid bacteria. *AIMS Microbiol*, 3 (1), 1-7.

Papadimitriou, K., Alegría, Á., Bron, P. A., de Angelis, M., Gobbetti, M., Kleerebezem, M., Lemos, J. A., Linares, D. M., Ross, P., Stanton, C., Turróni, F., van Sinderen, D., Varmanen, P., Ventura, M., Zúñiga, M., Tsakalidou, E., & Kok, J. (2016). Stress physiology of lactic acid bacteria. *Microbiology and Molecular Biology Reviews*, 80(3), e00076-15.

Park, K.-S., Kim, H., Kim, N.-G., Cho, S. Y., Choi, K.-H., Seong, J. K., & Paik, Y.-K. (2002). Proteomic analysis and molecular characterization of tissue ferritin light chain in hepatocellular carcinoma. *Hepatology*, 35 (6), 1459-1466.

Qian, J., Wang, C., Zhuang, H., Zhang, J., & Yan, W. (2020). Oxidative stress responses of pathogen bacteria in poultry to plasma-activated lactic acid solutions. *Food Control*, 118, 107355.

Rico, J., Yebra, M. J., Pérez-Martínez, G., Deutscher, J., & Monedero, V. (2008). Analysis of *ldh* genes in *Lactobacillus casei* BL23: role on lactic acid production. *Journal of Industrial Microbiology and Biotechnology*, 35 (6), 579-586.

Seo, D. J., Jung, D., Jung, S., Yeo, D., & Choi, C. (2020). Inhibitory effect of lactic acid bacteria isolated from kimchi against murine norovirus.

Food Control, 109, 106881.

- Sghaier-Hammami, B., S, B. M. H., Baazaoui, N., Gomez-Diaz, C., & Jorrin-Novo, J. V. (2020). Dissecting the Seed Maturation and Germination Processes in the Non-Orthodox *Quercus ilex* Species Based on Protein Signatures as Revealed by 2-DE Coupled to MALDI-TOF/TOF Proteomics Strategy. *Int J Mol Sci*, 21 (14).
- Shimizu, I., Yoshida, Y., Suda, M., & Minamino, T. (2014). DNA damage response and metabolic disease. *Cell metabolism*, 20 (6), 967-977.
- Streker, K., Freiberg, C., Labischinski, H., Hacker, J. r., & Ohlsen, K. (2005). *Staphylococcus aureus* NfrA (SA0367) is a flavin mononucleotide-dependent NADPH oxidase involved in oxidative stress response. *Journal of bacteriology*, 187 (7), 2249-2256.
- Sujitha, D., Kumar, H. J., Thapliyal, G., Pal, G., Vanitha, P. A., Uttarkar, A., & Vemanna, R. S. (2023). Transcription factors controlling the expression of oxidative stress-associated genes in rice (*Oryza sativa* L.). *Plant Biotechnology Reports*, 17(6), 835-851.
- Toushik, S. H., Kim, K., Ashrafudoulla, M., Mizan, M. F. R., Roy, P. K., Nahar, S., Kim, Y., & Ha, S.-D. (2021). Korean kimchi-derived lactic acid bacteria inhibit foodborne pathogenic biofilm growth on seafood and food processing surface materials. *Food Control*, 129, 108276.
- Vázquez, J., González, B., Sempere, V., Mas, A., Torija, M. J., & Beltran, G. (2017). Melatonin reduces oxidative stress damage induced by

- hydrogen peroxide in *Saccharomyces cerevisiae*. *Frontiers in microbiology*, 8, 1066.
- Won, S.-M., Chen, S., Park, K. W., & Yoon, J.-H. (2020). Isolation of lactic acid bacteria from kimchi and screening of *Lactobacillus sakei* ADM14 with anti-adipogenic effect and potential probiotic properties. *LWT*, 126, 109296.
- Wu, J., Tian, X., Xu, X., Gu, X., Kong, J., & Guo, T. (2022). Engineered Probiotic *Lactococcus lactis* for Lycopene Production against ROS Stress in Intestinal Epithelial Cells. *ACS Synth Biol*, 11 (4), 1568-1576.
- Wu, J., Zhang, Y., Ye, L., & Wang, C. (2021). The anti-cancer effects and mechanisms of lactic acid bacteria exopolysaccharides in vitro: A review. *Carbohydr Polym*, 253, 117308.
- Yun, Y.-R., Lee, M., Song, J. H., Choi, E. J., & Chang, J. Y. (2022). Immunomodulatory effects of *Companilactobacillus allii* WiKim39 and *Lactococcus lactis* WiKim0124 isolated from kimchi on lipopolysaccharide-induced RAW264. 7 cells and dextran sulfate sodium-induced colitis in mice. *Journal of Functional Foods*, 90, 104969.
- Zhao, H., Liu, L., Yuan, L., Hu, K., Peng, S., Li, H., & Wang, H. (2020). Mechanism analysis of combined acid-and-ethanol shock on *Oenococcus oeni* using RNA-Seq. *European Food Research and Technology*, 246 (8), 1637-1646.

Zheng, L., Zhao, M., Xiao, C., Zhao, Q., & Su, G. (2016). Practical problems when using ABTS assay to assess the radical-scavenging activity of peptides: Importance of controlling reaction pH and time. *Food chemistry*, 192, 288-294.

This chapter comprises articles, published in *Antioxidants* with minor modification as a partial fulfillment of Moeun Lee's Ph.D. program

Chapter 3.

UPLC-QTOF-MS/MS and GC-MS characterization of bioactive compounds in vegetable juice fermented using lactic acid bacteria from kimchi and their antioxidant potential

Abstract

This study aims to investigate fermentative metabolites in probiotic vegetable juice from four crop varieties (*Brassica oleracea* var. *capitata*, *B. oleracea* var. *italica*, *Daucus carota* L., and *Beta vulgaris*) and their antioxidant properties. Vegetable juice was inoculated with two lactic acid bacteria (LAB) (*Companilactobacillus allii* WiKim39 and *Lactococcus lactis* WiKim0124) isolated from kimchi and their properties were evaluated using untargeted UPLC-QTOF-MS/MS and GC-MS. The samples were also evaluated for radical (DPPH• and OH•) scavenging activities, lipid peroxidation, and ferric reducing antioxidant power. The fermented vegetable juices exhibited high antioxidant activities and increased amounts of total phenolic compounds. Fifteen compounds and thirty-two volatiles were identified using UPLC-QTOF-MS/MS and GC-MS, respectively. LAB fermentation significantly increased the contents of d-leucic acid, indole-3-lactic acid, 3-phenyllactic acid, pyroglutamic acid, γ -aminobutyric acid, and gluconic acid. Thus, vegetable juices fermented with WiKim39 and WiKim0124 can be considered as novel bioactive health-promoting sources.

Keywords: antioxidant activities; *Companilactobacillus allii* WiKim39; *Lactococcus lactis* WiKim0124; fermented vegetable juice

3.1. Introduction

The use of food to improve health and reduce disease risk has gained importance in nutritional science and clinical studies and is important when considering the increasing cost of healthcare, steady increase in lifespan, and the desire to improve quality of life (Nguyen, et al., 2019). The functional food market is expanding, with a significant demand for prebiotics, probiotics, synbiotics, and products fortified with probiotics (Manga, Zangué, Tatsadjeu, Zargar, Albert, & Bayat, 2019). Although fermented dairy products are the most representative probiotics on the food market, interest in developing functional non-dairy probiotics as an alternative for consumers who wish to limit dairy consumption, such as people with lactose intolerance or vegan diets (Dias, Scariot, Amboni, & Arisi, 2020), has grown.

Kimchi, a traditional Korean fermented vegetable product, is a great source of probiotic LAB (Lee, Song, Jung, Lee, & Chang, 2017); its health-related benefits are globally acknowledged (Lee, Song, Lee, Jung, & Chang, 2018). The potential use of kimchi LAB as functional probiotics is continuously being investigated; kimchi LAB can be a good source from a pharmaceutical perspective by increasing its antioxidant and anticancer activities (Lee, Jang, Lee, Park, Choi, & Kim, 2015).

Vegetables juices are a tasty and healthy option for people of all ages. Vegetables are a good source for LAB strains (Li, Jiang, Liu, Wu, Xu, & Lei, 2021). We prepared vegetable juice (VJ) from cabbage (*Brassica oleracea* var. *capitata*), broccoli (*B. oleracea* var. *italica*), carrot (*Daucus carota* L.), and beetroot (*Beta vulgaris*), which are good sources of dietary fiber, sugars, metabolites, ascorbate, and phenolic compounds. These ingredients have been reported as biologically active compounds and encourage LAB growth (Carrillo, Wilches-Pérez, Hallmann, Kazimierczak, & Rembiałkowska, 2019; Kusznierevich, Smiechowska, Bartoszek, & Namiesnik, 2008; Latté, Appel, & Lampen, 2011; Liu, et al., 2020; Yu, Zhou, & Parry, 2005). Because vegetables contain beneficial nutrients, VJ may serve as an ideal food matrix for developing probiotic products. Furthermore, VJs fortified with LAB have enhanced flavor and functionally bioactive substances (Soares, et al., 2019).

A comprehensive evaluation of the fermentation activity promoted by LAB and the total metabolites in VJ are unknown. We fermented VJ using *Companilactobacillus allii* WiKim39 or *Lactococcus lactis* WiKim0124 isolated from kimchi. A metabolomics approach, using ultra performance liquid chromatography quadrupole time-of-flight tandem mass spectrometry (UPLC-QTOF-MS/MS) and gas chromatography-mass spectrometry (GC-MS), was employed for the first time to identify, quantify, and compare the metabolites present in VJ fermented by LAB, and to analyze the correlation between these metabolites and their *in vitro* antioxidant properties.

3.2. Material and Methods

3.2.1. Bacterial strains and culture conditions

The LAB strains *C. alli* WiKim39 (GenBank ID: NR_159087.1) and *L. lactis* WiKim0124 (GenBank ID: MZ424472.1) isolated from kimchi were evaluated in this study. The strains were stored at $-80\text{ }^{\circ}\text{C}$ in De Man, Rogosa, and Sharpe (MRS) agar (Difco; De-troit, MI, USA) containing 15% glycerol (v/v). For activation, 1% (v/v) of the culture was added to 10 mL of MRS broth and incubated at $30\text{ }^{\circ}\text{C}$ for 24 h. The resulting suspension was used as an inoculum for 50 mL of MRS broth and incubated at $30\text{ }^{\circ}\text{C}$ for 24 h. The cells were collected by centrifugation ($6000\times\text{ g}$, 10 min, $4\text{ }^{\circ}\text{C}$) for further use.

3.2.2. Preparation and fermentation of VJ

The VJ was prepared using cabbage (*B. oleracea* var. *capitata*), broccoli (*B. oleracea* var. *italica*), carrot (*D. carota* L.), and beetroot (*B. vulgaris*), harvested from Jeju (Korea) in 2020. The vegetables were washed with tap water and completely dried. The VJ samples were prepared by mixing crushed vegetables and purified water (w/v) in the following ratio: 12% cabbage, 12% carrot, 12% broccoli, 10% beetroot, and 54% purified

water. This formulation was determined by a preliminary sensory analysis based on taste (data not shown). The samples were extracted using pressurized hot water extraction at 107 °C for 2 h in a 5-ton stainless steel tank and then filtered with a 50- μ m housing filter (Woosung Magnet Co., Ltd., Gimhae, Korea). The initial °Brix of the VJ samples was adjusted—5.5 °Brix for *C. allii* WiKim39 (VJ + WiKim39) and 10.0 °Brix for *L. lactis* WiKim0124 (VJ + WiKim0124) fermentation, respectively, with food-grade glucose according to optimal cell productivity (CFU/mL, data not shown). The VJ samples were sterilized at 98 °C for 10 min and filtered through a 100- μ m filter (Woosung Magnet Co., Ltd.). After the VJ had cooled to room temperature, 10^7 CFU/mL of each strain was used to inoculate the sterilized VJ and fermented at 30 °C for 48 h. For the in vitro experiments, the fermented samples were heat-killed at 95 °C for 10 min. This suspension was freeze-dried and stored at -70 °C until use. The non-inoculated VJ (pH 5.3 ± 0.2 , 5.0 °Brix) was used as the control. All the samples were prepared in GMP (Good-Manufacturing-Practice) compliant systems, which are the most suitable for food and drug applications.

3.2.3. Proximate composition and total phenolic and flavonoid concentrations

The moisture, ash, crude protein, crude fat, and crude fiber content of the fermented and unfermented VJ samples were determined using the method recommended by the AOAC (2000). The carbohydrate content was

calculated using the following formula: carbohydrates (%) = 100% – (moisture content (%) + crude fat content (%) + crude protein content (%) + ash content (%) + crude fiber (%)). The total phenolics (TP) were analyzed spectrophotometrically using the modified Folin–Ciocalteu method. The concentration of total phenolic compounds was expressed as gallic acid equivalent ($\mu\text{g GAE/mg}$). The total flavonoids (TF) were determined using the aluminum chloride colorimetric method with slight modifications and were expressed as catechin equivalent ($\mu\text{g CE/mg}$) [17].

3.2.4. Antioxidant properties

3.2.4.1. 2,2-Diphenyl-1-picrylhydrazyl radical scavenging activity

The activity of 2,2-diphenyl-1-picrylhydrazyl radical (DPPH•) scavenging was determined as described in previous studies [18,19], with slight modifications. The samples (VJ, VJ + WiKim39, and VJ + WiKim0124) were dissolved in distilled water to a concentration of 100 mg/mL (initial concentration). Next, 10 μL of sample was added to the 180 μL of 0.2 mM DPPH solution and kept in the dark at 25 °C for 30 min. The absorbance was measured at 517 nm with ascorbic acid as the standard antioxidant (50 $\mu\text{g/mL}$, initial concentration). All the measurements were performed in triplicate. The DPPH• scavenging activity was calculated using the equation below:

$$\text{DPPH}\bullet \text{ scavenging activity} = (A_{\text{Blank}} - A_{\text{Sample}})/A_{\text{Blank}} \times 100$$

where A_{Sample} is the absorbance in the presence of the sample and A_{Blank} is the absorbance of the distilled water control in the absence of the sample. DPPH radical scavenging activity was expressed as IC_{50} value and with ascorbic acid (vitamin C) comparison. All the measurements were performed in triplicate.

3.2.4.2. Hydroxyl radical scavenging activity

The assay was conducted based on the production of the hydroxyl radical ($OH\bullet$) from a fenton reaction between ferrous ions and hydrogen peroxide [20]. A total of 1 mL of sample (100 mg/mL, initial concentration) was mixed with 1 mL H_2O_2 (0.025%, w/v), 1 mL sodium salicylate (9 mM), and 1 mL $FeSO_4$ (9 mM). The reaction mixture was incubated at 37 °C for 1 h and cooled. The absorbance was measured at 536 nm with ascorbic acid as the standard antioxidant (50 $\mu\text{g/mL}$, initial concentration) and distilled water was used as a negative control. The $OH\bullet$ scavenging activity was calculated using the following equation:

$$\% \text{ OH}\bullet \text{ scavenging rate} = \frac{(A_{\text{Sample}} - A_{\text{Control}})}{(A_{\text{Blank}} - A_{\text{Control}})} \times 100$$

where A_{Sample} is the absorbance in the presence of the sample, A_{Control} is the absorbance of the control in the absence of the sample, and A_{Blank} is the absorbance without the sample and the Fenton reaction system. All the measurements were performed in triplicate.

3.2.4.3. Ferric reducing antioxidant power

The ferric reducing antioxidant power (FRAP) assay was performed using a commercial kit (ab234626; Abcam, Hong Kong, China). After ferric-tripyridyltriazine (Fe^{+3} -TPTZ) in the reaction mixture was converted to Fe^{+2} in an acidic environment (pH 3.6), the absorbance was measured at 594 nm. The quantification was performed using a calibration curve of ferrous sulfate and the results were expressed as Fe^{2+} equivalents (μM).

3.2.4.4. Inhibition rate of lipid peroxidation

The inhibition rate of lipid peroxidation in the samples was evaluated as the ability of biological fluids to inhibit the production of thiobarbituric acid reactive substances (TBARS) using the thiobarbituric acid (TBA) method, as described [21]. Butylated hydroxytoluene (BHT) (3 mM, initial concentration) was used as the reference. The inhibition rate of lipid peroxidation was calculated using the formula:

Inhibition rate of lipid peroxidation (%) =

$$(\text{A}_{\text{Blank}} - \text{A}_{\text{Sample}}/\text{A}_{\text{Blank}}) \times 100$$

where A_{Sample} is the absorbance in the presence of the sample and A_{Blank} is the absorbance of the control in the absence of the sample. All the measurements were performed in triplicate.

3.2.5. VJ Fermentation metabolite analysis

3.2.5.1. UPLC-QTOF-MS/MS profile

Sample replicates from VJ fermentation were purified using the Sep-Pak C18 cartridge (Waters, Dublin, Ireland), as described (de Souza, da Silva, da Silva, Camara, & Silva, 2018). Next, the solutions were filtered through a 0.22- μm syringe filter. The purified samples were screened using UPLC-QTOF-MS/MS. The UPLC-QTOF-MS/MS system consisted of the Vanquish UPLC system (Thermo Fisher Scientific, San Jose, CA, USA) with a Waters COR-TECS T3, C₁₈ column (2.1 \times 150 mm, 1.6 μm ; Waters, Milford, MA, USA) connected to the TSQ Altis triple quadrupole mass spectrometer (Thermo Scientific, San Jose, CA, USA). Via an electrospray ionization (ESI) interface, the QTOF-MS/MS was used to complete the high-resolution experiment in the negative ion mode. The analytical detector was a Waters Acquity PDA detector, which was set to a wavelength range of 200–400 nm. The elution program for the UPLC separation used 10 mM ammonium acetate in water as eluent A and methanol as eluent B. The gradient elution program was as follows: 0–0.4 min; 15% B, 0.5–7 min; 15% B, 7–7.5 min; 15–100% B, 7.5–8 min; 100–15% B, and equilibration with 15% B for 5 min at a flow rate of 0.2 mL/min. The column was set at 45 °C, and the auto sampler was maintained at 4 °C. The injection volume of each sample solution was 3 μL . The detailed experimental conditions are listed in Table 3.1. The data acquisition and analysis were performed using Thermo Xcalibur™ software (Thermo Fisher Scientific, San Jose, CA, USA). The standard solutions of d-leucic acid (d-LA), indole-3-lactic acid (ILA), and 3-phenyllactic acid (3-PLA) were obtained from Sigma Aldrich

(St. Louis, MO, USA).

Table 3.1. Detailed analytical conditions of UPLC-QTOF-MS/MS.

Instrument	TSQ Altis triple-quadrupole mass spectrometer (Thermo Scientific, USA)
Ionization	Electrospray ionisation (H-ESI)
Negative Ion / Positive Ion (V)	2500 / 3500
Sheath Gas (Arb)	50
Aux Gas (Arb)	10
Sweep Gas (Arb)	1
Ion Transfer Tube Temp (°C)	325
Vaporizer Temp (°C)	350
Scan type	Selected reaction monitoring (SRM)
Polarity	Negative / Positive

3.2.5.2. GC-MS profile

For the derivatization, 100 μL of 20,000 ppm pyridine were added to 5 mg of each lyophilized sample and incubated at 30 $^{\circ}\text{C}$ for 90 min. Next, 100 μL of N,O-bis(trimethylsilyl)trifluoroacetamide with 1% trimethylchlorosilane solution and 20 μL of internal standard (1000 ppm fluoranthene) were added to the sample vial and incubated at 60 $^{\circ}\text{C}$ for 30 min. The samples were analyzed through GC-MS. GC chromatographic separations were achieved on a Thermo Scientific TRACE™ 1310 Gas Chromatograph with a single quadrupole mass spectrometer. The GC was equipped with a capillary column (Agilent, Palo Alto, CA, USA; DB-5MS 60 m \times 0.25 mm \times 0.25 μm) and run in full scan mode (scan range 40–700 m/z with detector voltage 2160 V). The gas carrier was helium, with a flow rate of 1.5 mL/min. The transfer line was settled at 310 $^{\circ}\text{C}$ and 1 μL of the sample was injected. The oven temperature was fixed at 50 $^{\circ}\text{C}$ for 2 min, increased to 180 $^{\circ}\text{C}$ (rate 5 $^{\circ}\text{C}/\text{min}$), held for 5 min, increased to 325 $^{\circ}\text{C}$ (rate 5 $^{\circ}\text{C}/\text{min}$), and held for 10 min. The ion source was settled at 270 $^{\circ}\text{C}$ and the solvent delay was 4.5 min. Mass spectra were recorded in electronic impact mode at 70 eV, scanning within the 35–650 m/z range for the selection of appropriate electronic impact mass fragments for each analyte, with a scan rate of 6 scans/s. The standard solutions (pyroglutamic acid, γ -aminobutyric acid, and gluconic acid) were obtained from Sigma Aldrich (St. Louis, MO, USA).

3.2.6. Statistical Analysis

The statistical analysis was performed using Tukey's honest significant difference (HSD) test carried out in the "agricolae" package of R (v3.3.2; <https://www.r-project.org/>, 31.12.2016) for group comparisons.

3.3. Results and Discussion

3.3.1. Proximate composition and TP and TF content

The moisture, ash, crude protein, crude fat, crude fiber, carbohydrate, TP, and TF content of freeze-dried fermented VJ are shown in Table 3.2. The fermented VJ contained high levels of carbohydrate (86.23–88.17%); moderate levels of moisture (6.66–7.05%); and low levels of crude protein (2.24–3.60%), ash (1.60–1.68%), crude fat (0.49–0.69%), and crude fiber (0.45–0.85%). Due to fermentation, the crude protein content was significantly higher in VJ + WiKim39 (3.20%) and VJ + WiKim0124 (3.06%). The increase in protein content may be due to proteolytic enzymes produced during microbial fermentation or a result of synthesizing proteins by fermenting substrates that may result in amino acid production (Ogodo, Ugbo, Onyeagba, & Okereke, 2018). Crude fiber and fat content significantly increased in LAB-fermented VJs; VJ + WiKim0124 showed the highest content, followed VJ + WiKim39, at 0.85% and 0.79%, respectively. VJ had a carbohydrate content of 88.17%, followed by VJ + WiKim0124 (87.07%) and VJ + WiKim39 (86.23%). This may be due to the possible bioconversion of carbohydrates to crude fiber or crude fat (Jeff-Agboola & Oguntuase, 2006; Olukomaiya, Adiamo, Fernando, Mereddy, Li, & Sultanbawa, 2020). Crude fiber content was significantly increased in

LAB-fermented groups; however, the VJ samples were filtered using a 50 μm filter, which may have affected the fiber content in the filtrate, and therefore, the same cannot be commented upon in this study.

The TP and TF content in samples are crucial because of their positive effect on physiological processes, including antioxidant activities, anti-inflammatory properties, and cancer-risk reduction activity (Surveswaran, Cai, Corke, & Sun, 2007). The TP ranged from 206.29 to 255.69 $\mu\text{g GAE/g}$. VJ + WiKim39 contained the highest level of TP, at 255.69 $\mu\text{g GAE/g}$, whereas VJ presented the lowest content, at 206.29 $\mu\text{g GAE/g}$. The TF ranged from 11.62 to 16.75 $\mu\text{g CE/g}$. The highest level of TF was found in VJ + WiKim39, at 16.75 $\mu\text{g CE/g}$, whereas VJ + WiKim0124 presented the lowest TF content, at 11.62 $\mu\text{g CE/g}$. The significant increase in TP in the LAB-fermented samples may have been due to the hydrolytic enzymes in the LAB strains that hydrolyze complex metabolites into simpler forms. The differences in metabolite concentrations between LAB strains (WiKim39 and WiKim0124) may have been due to their individual adaptability and their ability to produce more hydrolytic enzymes (Kwaw, et al., 2018). An increase in TF was observed in VJ + WiKim39, which may be due to the enzymatic breakdown of complex polyphenols into simpler flavonol compounds during fermentation (Landete, Curiel, Rodríguez, de las Rivas, & Muñoz, 2014). A significant decrease in TF was observed in VJ + WiKim0124, probably because of the depolymerization of high molecular

weight phenolic compounds by polyphenol oxidase in the LAB strain (Li, Jiang, Liu, Wu, Xu, & Lei, 2021).

Table 3.2. Proximate composition, TP and TF content of non-fermented or fermented vegetable juice with LAB.

Parameters (g/100g)	VJ	VJ+WiKim39	VJ+WiKim0124
Moisture	7.05±0.25 ^a	7.01±0.15 ^a	6.66±0.21 ^b
Ash	1.60±0.12	1.68±0.11	1.67±0.15
Crude protein	2.24±0.01 ^c	3.60±0.05 ^a	3.06±0.02 ^b
Crude fat	0.49±0.15 ^a	0.69±0.12 ^b	0.69±0.01 ^a
Carbohydrate*	88.173±0.16	86.23±0.14	87.07±0.05
Crude fiber	0.45±0.15 ^b	0.79±0.01 ^b	0.85±0.01 ^a
TP (ug Garlic acid equivalents)	206.29±1.44 ^c	255.69±2.44 ^a	240.52±0.72 ^b
TF (ug Catechin equivalents)	12.67±0.09 ^b	16.75±0.13 ^a	11.62±0.15 ^c

Values are given as mean ± standard deviation (n = 3) in dry matter basis. Different superscripts in the same row are significantly different ($p < 0.05$, ANOVA, Tukey-HSD).

* Carbohydrate (%) = 100 - (% ash + % crude protein + % crude fat + % crude fiber).

3.3.2. Antioxidant capacity of fermented VJ

Metal ions (Fe^{3+}) and free radicals are important oxidants involved in the pathogenic process of many chronic diseases, and good antioxidants should not only reduce oxidants, but also scavenge free radicals. Lipid oxidation is problematic in food systems. Lipid oxidation proceeds through a free-radical chain mechanism and is an indicator of oxidative damage in physiological systems, as many end products produce toxic compounds and are a major cause of diseases, such as atherosclerosis (Ghani, Barril, Bedgood, & Prenzler, 2017). To evaluate the antioxidant capacity of fermented and non-fermented VJs, DPPH• and OH• scavenging, FRAP, and TBARS assays were used. We found distinct effects of fermentation on antioxidant activities. Compared to the non-fermented samples, the LAB-fermented samples generally displayed higher antioxidant capacities. As shown in Figure 3.1, VJ was more susceptible to lipid peroxidation than VJ + WiKim39 and VJ + WiKim0124 and featured lower DPPH• and OH• scavenging capacity. The quantification of antioxidant capacity with FRAP showed an increase in antioxidant capacity in VJ + WiKim39 and VJ + WiKim0124. The increased antioxidant activity may have been due to the ability to release active compounds from the VJ matrix during fermentation, which is thought to be associated with the production of phenolic compounds (Li, Teng, Lyu, Hu, Zhao, & Wang, 2019). However, metabolites other than TP can also contribute to antioxidant activities. Therefore, we performed high-resolution LC-MS/MS and GC-MS to

explore identify metabolites in fermented VJs.

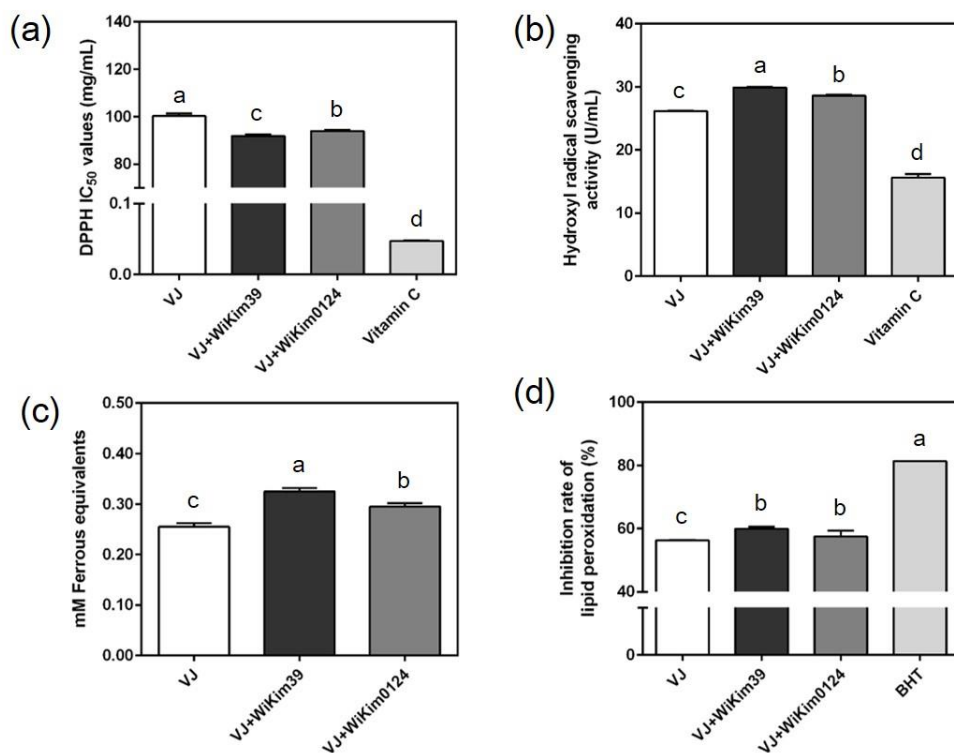


Fig. 3.1. Antioxidant capacities of vegetable juice fermented with lactic acid bacteria. (a) DPPH radical scavenging activity, (b) hydroxyl radical scavenging activity, (c) ferric reducing antioxidant power assay, (d) inhibition rate of lipid peroxidation assay (TBARS). At least triplicate analyses were performed. Different letters above the columns denote significant differences ($p < 0.05$). DPPH: 2,2-Diphenyl-1-picrylhydrazyl radical, TBARS: thiobarbituric acid reactive substances.

3.3.3. Bioactive compounds formed during VJ fermentation

3.3.3.1. UPLC-QTOF-MS/MS characterization of fermented VJ

A total of 12, 12, and 14 compounds were tentatively identified from VJ, VJ + WiKim39, and VJ + WiKim0124, respectively, by their exact masses, MS/MS spectra, and molecular formulas. As shown in Table 3.3, the metabolites consisted of organic acids, phenols, sugars, and miscellaneous compounds. Among these, the components detected only in the LAB-fermented products were d-LA, ILA, and 3-PLA; these compounds were further confirmed quantitatively by comparison with standard solutions (Fig. 3.2C, 3.3, 3.4, 3.5 and Table 3.4). All the fermented VJs exhibited significantly higher concentrations than their respective non-fermented VJ. VJ + WiKim39 contained the highest levels of d-LA, ILA, and 3-PLA, at 3535.63, 222.68, and 2687.33 ng/mL, whereas VJ contained the lowest at 34.35, 24.18, and 23.18 ng/mL, respectively. The first identification step allowed the subsequent quantification of LAB-derived influencing factors and aimed to elucidate the expected impact of WiKim39 and WiKim0124 on the production of bioactive substances through VJ fermentation.

The leucine derivative metabolite, d-LA (2-hydroxyisocaproic acid), is produced during *Lactobacillus*-mediated fermentation and is also found in human tissues. Reportedly, d-LA exhibited anti-inflammatory effects in a murine *Candida* biofilm model (Nieminen, et al., 2014). Because D-LA can improve muscle recovery by increasing protein synthesis, it can be used as a food additive to promote muscle growth. In addition, D-LA is used as an

antibacterial agent and as a treatment for infected body cavities and sinuses. (Sakko, et al., 2012). ILA is a microbial tryptophan-derived indole compound, which acts as an antioxidant and free-radical scavenger (Suzuki, Kosaka, Shindo, Kawasumi, Kimoto-Nira, & Suzuki, 2013). ILA also promotes the inflammatory control process (Sakurai, Odamaki, & Xiao, 2019) and neuronal developmental processes (Wong, Tanaka, Kuhara, & Xiao, 2020). 3-PLA, a phenolic acid, is synthesized during phenylalanine metabolism in LAB. High levels of 3-PLA are produced during LAB-mediated fermentation; 3-PLA has broad antibacterial activity against bacteria and fungi, making it a promising naturally-occurring substance that can be used for extending the shelf life of food (Jung, Hwang, & Lee, 2019). Furthermore, 3-PLA is non-toxic to cells and animals, and the dietary supplementation of 3-PLA in animal models enhances its immunomodulatory effects (Rajanikar, Nataraj, Naithani, Ali, Panjagari, & Behare, 2021). Our LAB-fermented VJs were rich in these compounds, providing clues to their functional properties and potential relevance.

Table 3.3. Tentatively identified compounds from probiotic vegetable juice samples by UPLC-QTOF-MS/MS under negative ion mode.

Class	Tentative identification	RT (min)	Molecular Formula	Molecular Weight	Molecular ion [M-H] ⁻ (m/z)	Error (ppm)	VJ	VJ+ WiKim39	VJ+ WiKim0124
Organic acids	Citric acid	1.52	C ₆ H ₈ O ₇	192	191.02	0.263	●*	●	●
	3-O-Coumaroylquinic acid	14.09	C ₁₆ H ₁₈ O ₈	338.1	337.094	2.856	●	●	●
	D-Leucic acid ^a	12.31	C ₆ H ₁₂ O ₃	132.1	131.072	5.655	ND	●	●
	1,8-nonanedioic acid	23.55	C ₉ H ₁₆ O ₄	188.1	187.098	3.655	●	●	●
	Indole-3-lactic acid ^a	17.84	C ₁₁ H ₁₁ NO ₃	205.1	204.067	1.636	ND	●	●
	Malic acid	1.25	C ₄ H ₆ O ₅	134	133.015	2.128	●	ND	ND
Phenols	Caffeic acid	10.92	C ₉ H ₈ O ₄	180	179.036	1.978	●	ND	●
	5-Hydroxyquinoline	18.28	C ₉ H ₇ NO	145.1	144.046	4.951	●	●	●
	3-Phenyllactic acid ^a	15.12	C ₉ H ₁₀ O ₃	166.1	165.056	2.802	ND	●	●
	Salicylic acid	7.39	C ₇ H ₆ O ₃	138	137.024	0.054	●	●	●
	Neochlorogenic acid	7.77	C ₁₆ H ₁₈ O ₉	354.1	353.089	2.492	●	●	●
	Ferulic acid	17.69	C ₁₀ H ₁₀ O ₄	194.1	193.051	1.646	●	ND	●
Sugar	Sucrose	1.14	C ₁₂ H ₂₂ O ₁₁	342.1	341.109	2.319	●	●	●
	D-Tagatose	1.09	C ₆ H ₁₂ O ₆	180.1	179.057	2.029	●	●	●
Miscellaneous	9-(2,3-dihydroxypropoxy)-	23.29	C ₁₂ H ₂₂ O ₆	262.1	261.135	1.907	●	●	●

* Circles indicates presence of metabolites. ^a, The compound was further identified using the corresponding standard compound ND, not detected.

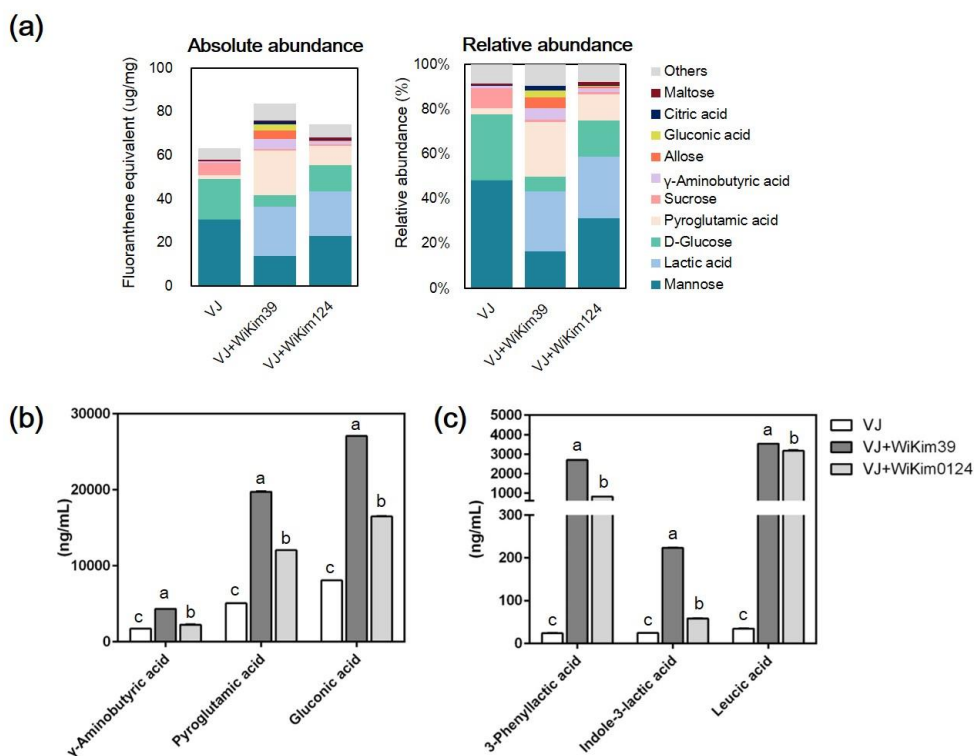
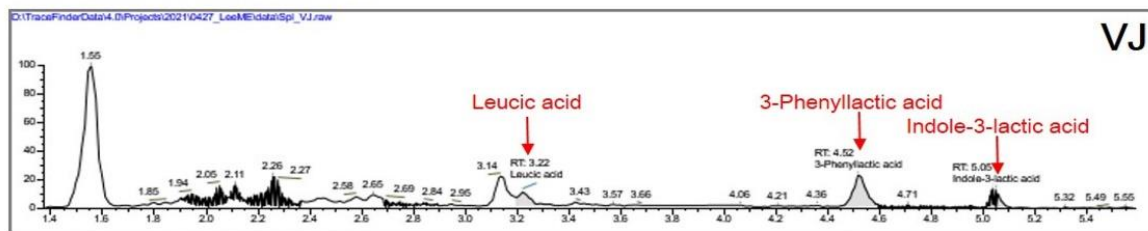


Fig. 3.2. Identification of metabolite profile in fermented or non-fermented vegetable juice. (a) GC-MS profile of the top 10, most abundant metabolites. (b,c) Quantification of significantly differentiated compounds from GC-MS or UPLC-QTOF-MS/MS using UPLC-QTOF-MS/MS. (Details of ion chromatograms are shown in Figures 3.3, 3.4, 3.5, 3.6, 3.7, and 3.8). GC-MS: gas chromatography-mass spectrometry, UPLC-QTOF-MS/MS: ultra-performance liquid chromatography with quadrupole time-of-flight tandem mass spectrometry. Different letters denote significant differences ($p < 0.05$, ANOVA, Tukey-HSD).

Total Ion Chromatogram



MS/MS

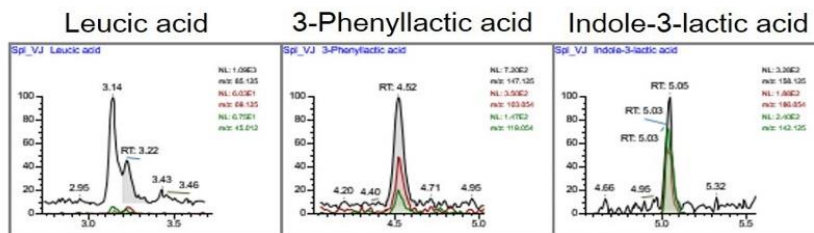
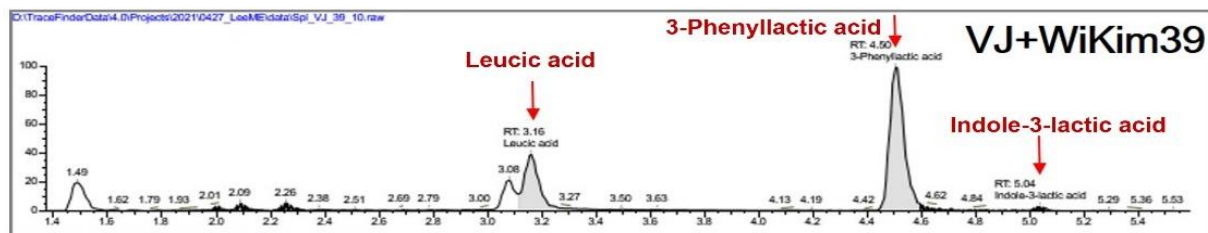


Fig. 3.3. Total Ion Chromatogram obtained using UPLC-QTOF-MS/MS in VJ. Quantification of significantly differentiated compounds from the UPLC-QTOF-MS/MS profile was performed using negative ion mode electrospray ionization mass spectrometry of the fermented VJ. Each peak represents leucic acid, 3-phenyllactic acid, and indole-3-lactic acid.

Total Ion Chromatogram



MS/MS

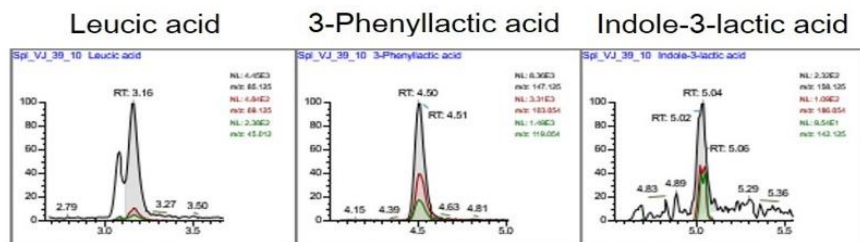
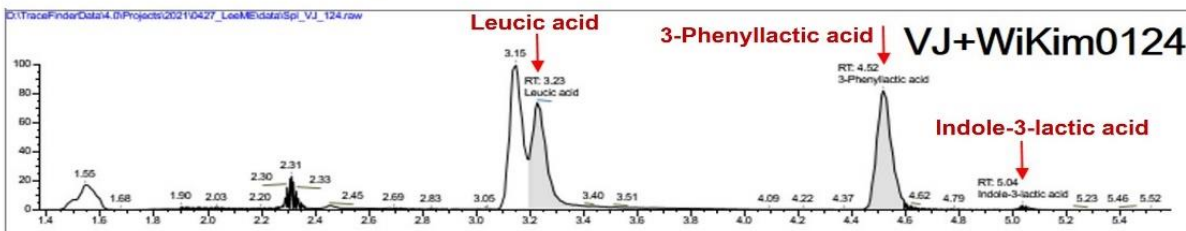


Fig. 3.4. Total Ion Chromatogram obtained using UPLC-QTOF-MS/MS in VJ+WiKim39. Quantification of significantly differentiated compounds from the UPLC-QTOF-MS/MS profile was performed using negative ion mode electrospray ionization mass spectrometry of the fermented VJ+WiKim39. Each peak represents leucic acid, 3-phenyllactic acid, and indole-3-lactic acid.

Total Ion Chromatogram



MS/MS

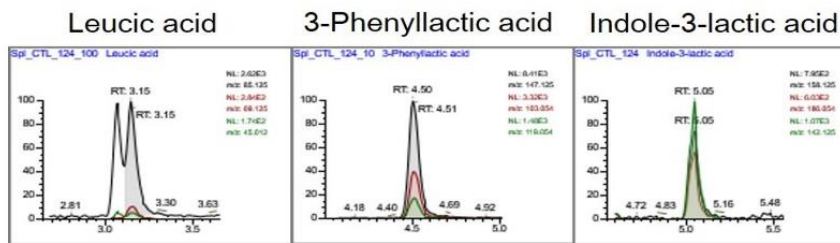
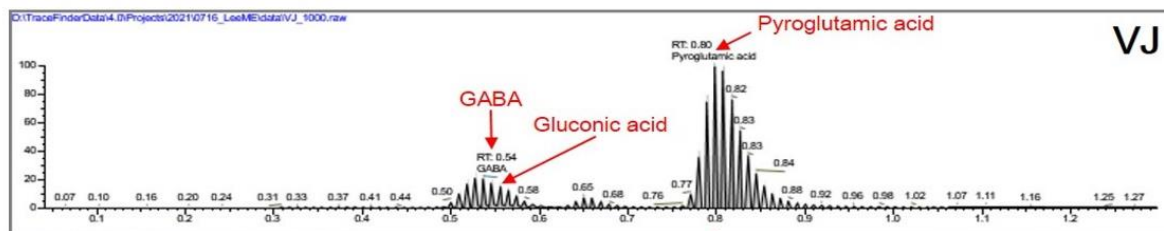


Fig. 3.5. Total Ion Chromatogram obtained using UPLC-QTOF-MS/MS in VJ+WiKim0124. Quantification of significantly differentiated compounds from the UPLC-QTOF-MS/MS profile was performed using negative ion mode electrospray ionization mass spectrometry of the fermented VJ+WiKim0124. Each peak represents leucic acid, 3-phenyllactic acid, and indole-3-lactic acid.

Total Ion Chromatogram



MS/MS

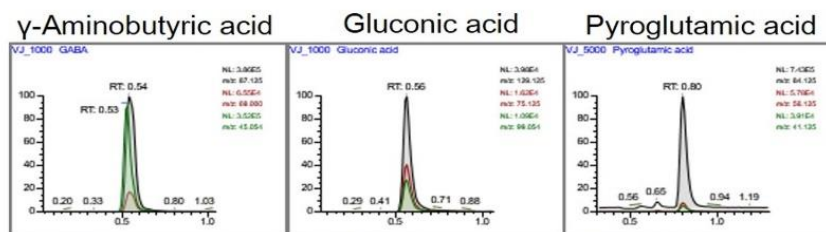
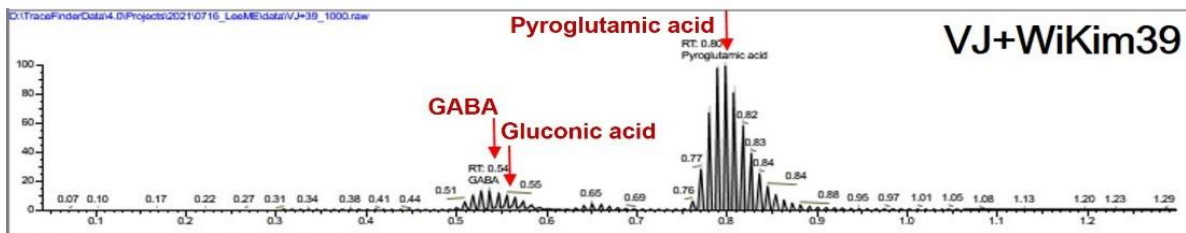


Fig. 3.6. Total Ion Chromatogram obtained by UPLC-QTOF-MS/MS in VJ. Quantification of significantly differentiated compounds from the UPLC-QTOF-MS/MS profile was performed using negative ion mode electrospray ionization mass spectrometry of the fermented VJ. Each peak represents γ -aminobutyric acid, gluconic acid, and pyroglutamic acid.

Total Ion Chromatogram



MS/MS

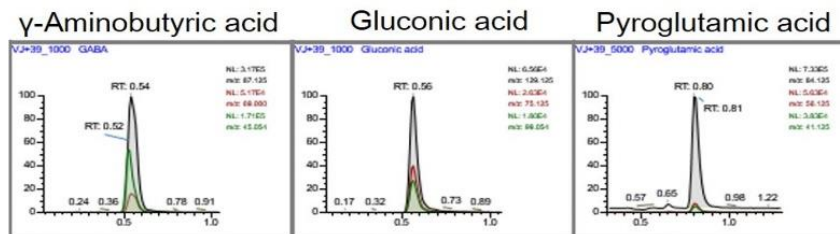
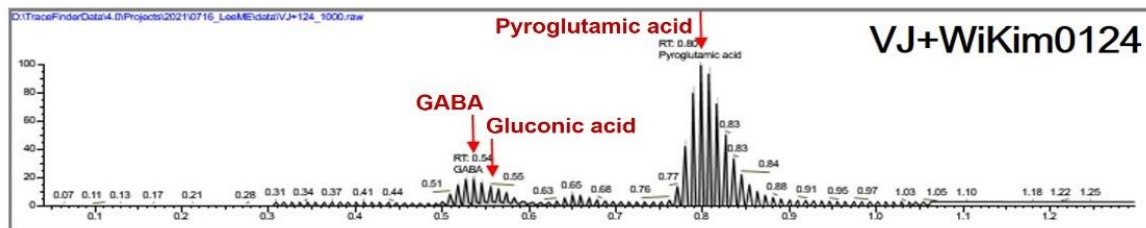


Fig. 3.7. Total Ion Chromatogram obtained by UPLC-QTOF-MS/MS in VJ+Wikim39. Quantification of significantly differentiated compounds from the UPLC-QTOF-MS/MS profile was performed using negative ion mode electrospray ionization mass spectrometry of the fermented VJ. Each peak represents γ -aminobutyric acid, gluconic acid, and pyroglutamic acid.

Total Ion Chromatogram



MS/MS

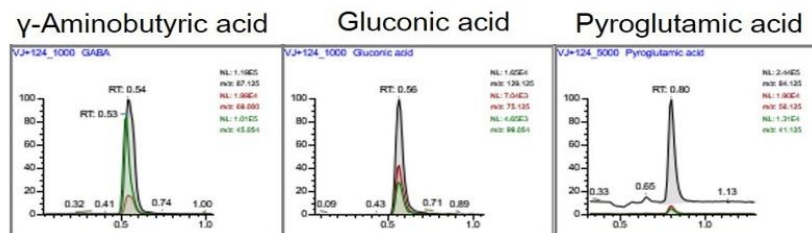


Fig. 3.8. Total Ion Chromatogram obtained by UPLC-QTOF-MS/MS in VJ+Wikim0124. Quantification of significantly differentiated compounds from the UPLC-QTOF-MS/MS profile was performed using negative ion mode electrospray ionization mass spectrometry of the fermented VJ. Each peak represents γ -aminobutyric acid, gluconic acid, and pyroglutamic acid.

Table 3.4. Quantitative characterization of significant bioactive compounds in VJ samples by UPLC-QTOF-MS/MS.

Compound name	RT (min)	Ionization (ESI-/ESI+)	Molecular ion (m/z)	MSMS products ions (m/z)	Collision energy (V)	(ng/mL)		
						VJ	VJ+ WiKim39	VJ+ WiKim0124
D-Leucic acid	3.01	[M-H]-	131	45.01	13.76	34.18 ± 0.25	3532.82 ± 3.98	3147.06 ± 4.16
				69.13	20.42			
				85.13	12.25			
Indole-3-lactic acid	3.95	[M-H]-	204	142.13	18.48	24.59 ± 0.58	226.34 ± 5.18	59.19 ± 1.15
				158.13	15.15			
				186.05	13.47			
3-Phenyllactic acid	4.26	[M-H]-	165	103.05	15.70	23.59 ± 0.58	2693.67 ± 8.96	819.57 ± 0.62
				119.05	16.79			
				147.13	11.23			
γ -Aminobutyric acid	0.54	[M+H]+	104.09	45.05	21.01	1728.70 ± 13.90	4334.11 ± 16.33	2245.83 ± 56.45
				69.00	15.49			
				87.13	10.52			
Gluconic acid	0.56	[M-H]-	195	75.13	17.76	8080.95 ± 34.90	27073.61 ± 18.27	16500.66 ± 57.78
				99.05	14.14			
				129.13	12.20			
Pyroglutamic acid	0.8	[M+H]+	130.04	41.13	21.81	5071.72 ± 12.39	19741.34 ± 65.51	12061.11 ± 11.83
				56.13	24.12			
				84.13	13.00			

3.3.3.2. GC-MS characterization of fermented VJ

A total of 29, 31, and 31 volatile constituents were tentatively identified from VJ, VJ + WiKim39, and VJ + WiKim0124, respectively, through GC-MS. The compounds were categorized as amino acids, fatty acids, organic acids, sugars, and miscellaneous (Table 3.5). To determine differences in the composition of volatiles between LAB-fermented and non-fermented VJ products, the 10 most abundant volatiles in the samples (Fig. 3.2a), sugars (12.42–26.27%), organic acids (0.61–13.33%), and amino acids (1.08–12.27%) were dominant in the total proportion. Sugars (mannose, d-glucose, and sucrose) showed the highest abundance ratio in the VJ; on the other hand, organic acids and amino acids were increased in fermented VJ. The reduction in sugars during fermentation was a result of bioconversion to organic acids and the use of LAB strains for propagation (Ye, Huang, Terefe, & Augustin, 2019). In particular, VJ + WiKim39 significantly reduced the absolute amount of sugar while increasing the content of organic acids and amino acids. In these data, pyroglutamic acid (PGA), γ -aminobutyric acid (GABA), and gluconic acid (GA) were significantly increased during LAB fermentation. These compounds were quantitatively confirmed using standard solutions (Fig. 3.2b, 3.6, 3.7, 3.8 and Table 3.4). VJ + WiKim39 contained the highest levels of GABA, PGA, and GA, while VJ contained the lowest. An obvious difference in trend was observed between VJ and fermented VJ.

PGA (oxoproline) and GABA are widely recognized as important

biomarkers for diseases and effects of drugs (Eckstein, Ammerman, Reveles, & Ackermann, 2008). PGA is a glutamic acid derivative lacking a water molecule; it has been shown to have pharmacological properties for the regulation of amino acid transport and to accelerate the removal of potentially harmful amino acids (Mucchetti, Locci, Massara, Vitale, & Neviani, 2002) . Thus, PGA may serve as a therapeutic target in glutamate cytotoxicity, which is toxic to the brain at very low concentrations and leads to ischemia or traumatic brain injury (Hawkins, Simpson, Mokashi, & Vina, 2006). GABA is present in many vegetables and fruit. This amino acid has therapeutic effects on autoimmune diseases, including neurodegenerative diseases (Bhat, et al., 2010). Moreover, GABA reduces blood pressure (Inoue, et al., 2003), has neuroprotective effects, modulates inflammation (Lima, Louzada, De Mello, & Ferreira, 2003) and has antioxidant activity (Wang, Luo, Huang, Yang, Gao, & Du, 2014). Some LAB possess mechanisms to produce GABA, a bioactive compound with significant physiological activity. GABA production is primarily mediated by the glutamate decarboxylase (GAD) system, in which lactic acid bacteria convert glutamate into GABA using GAD, with carbon dioxide (CO₂) as a byproduct of this process (Pannerchelvan et al., 2023). In this study, pyroglutamic acid, identified as one of the key metabolites, is not directly converted into GABA but has been reported to contribute indirectly to GABA production via its conversion to glutamate (Werf, Orłowski, & Meister, 1971). Based on this, it is presumed that GABA could have been

generated in the fermented vegetable beverage.

GA and its salts are produced by the oxidation of the first carbon of β -D-glucose to a carbonyl group by chemical or enzymatic transformation. GA and its salts have a high ability to form water-soluble complexes with divalent or trivalent metal ions, making suitable for various pharmaceutical, food, and other industrial applications (Rico-Rodriguez, Villamiel, Ruiz-Aceituno, Serrato, & Montilla, 2020). GA and its derivatives could potentially be effective as intestinal regulators or inhibitors of intestinal decay in both animals and humans. Research in this area has focused on the antioxidant properties of GA derivatives (Canete-Rodriguez, Santos-Duenas, Jimenez-Hornero, Ehrenreich, Liebl, & Garcia-Garcia, 2016).

Table 3.5. Tentatively identified compounds from probiotic vegetable juice samples by GC-MS.

Class	Tentative identification	RT (min)	Molecular Formula	Molecular Weight	Fluoranthene equivalent ug/mg		
					VJ	VJ+ WiKim39	VJ+ WiKim0124
Amino acids	Alanine_2TMS	17.37	C ₃ H ₇ NO ₂	116	0.013	0.134	0.196
	Valine_2TMS	23.17	C ₅ H ₁₁ NO ₂	142	0.021	0.083	0.121
	Glycine_3TMS	23.38	C ₂ H ₅ NO ₂	174	0.096	0.655	0.175
	Pyroglutamic acid_2TMS ^a	29.09	C ₅ H ₇ NO ₃	156	1.558	20.438	8.650
	γ-Aminobutyric acid_3TMS ^a	29.30	C ₄ H ₉ NO ₂	174	0.592	4.362	1.300
	Proline_2TMS	39.74	C ₅ H ₉ NO ₂	217	0.004	0.007	0.246
	Serine_2TMS	43.38	C ₃ H ₇ NO ₃	103	ND	0.341	0.092
Fatty acids	Propanoic acid_1TMS	16.52	C ₃ H ₆ O ₂	147	0.017	0.469	0.004
	Stearic acid_1TMS	45.44	C ₁₈ H ₃₆ O ₂	319	0.338	0.421	0.063
	Palmitic acid_1TMS	51.79	C ₁₆ H ₃₂ O ₂	217	0.692	0.445	0.071
	Oleic acid_1TMS	55.63	C ₁₈ H ₃₄ O ₂	117	0.063	0.072	0.013

Organic acids	Lactic acid_2TMS	16.00	C ₃ H ₆ O ₃	147	0.071	22.645	20.433
	Malic acid_3TMS	22.23	C ₄ H ₆ O ₅	174	0.963	ND	ND
	Glyceric acid_3TMS	23.94	C ₃ H ₆ O ₄	147	0.033	0.062	0.071
	Fumaric acid_2TMS	24.57	C ₄ H ₄ O ₄	245	0.021	0.121	0.033
	Citric acid_4TMS	28.09	C ₆ H ₈ O ₇	147	0.058	1.679	0.342
	Gluconic acid_6TMS	48.50	C ₆ H ₁₂ O ₇	147	0.071	2.562	0.304
	Glycolic acid_2TMS	42.96	C ₂ H ₄ O ₃	103	0.029	0.403	0.092
	Succinic acid_2TMS	50.60	C ₄ H ₆ O ₄	117	0.054	0.821	0.225
Sugar	Fructose_5TMS	22.01	C ₆ H ₁₂ O ₆	116	0.029	0.410	0.100
	Arabinose_4TMS	33.32	C ₅ H ₁₀ O ₅	103	0.013	0.114	0.042
	Inositol_6TMS	37.80	C ₆ H ₁₂ O ₆	292	0.017	0.155	0.029
	Maltose_8TMS	40.56	C ₁₂ H ₂₂ O ₁₁	147	0.529	0.138	0.921
	Mannose_5TMS	44.90	C ₆ H ₁₂ O ₆	205	30.417	13.617	23.067
	Myoinositol_6TMS	46.80	C ₆ H ₁₂ O ₆	217	0.225	0.800	0.413
	D-Glucose_5TMS	47.81	C ₆ H ₁₂ O ₆	204	18.671	5.559	12.104
	Fructofuranose_5TMS	49.58	C ₆ H ₁₂ O ₆	217	ND	0.162	0.017

	Allose_6TMS	53.25	C ₆ H ₁₂ O ₆	319	0.088	4.045	0.342
	Mannitol_6TMS	56.29	C ₆ H ₁₄ O ₆	117	ND	0.579	0.017
	Sucrose_8TMS	63.71	C ₁₂ H ₂₂ O ₁₁	361	5.746	0.776	0.7179
Miscellaneous	Ribonic acid_5TMS	20.76	C ₅ H ₁₀ O ₆	144	0.013	0.183	0.025
	Aminoethanol_3TMS	23.58	C ₂ H ₇ NO	147	0.133	0.645	0.229

^a, The compound was further identified using the corresponding standard compound. ND, not detected.

3.3.3.3. Comparative analysis of fermented VJ metabolites and their antioxidant properties

To intuitively represent the difference between non-fermented and fermented VJs, a heat map (Fig. 3.9) was produced, along with hierarchical clusters based on the mean values of component concentrations from LC-QTOF-MS/MS and GC-MS. For the columns and rows, the clustering method was used based on the mean. The heat map shows the changes in the relative chemical composition of each type, showing differences that could be related to different LAB strains. Two clusters were observed in rows and columns, emphasized by hierarchical clustering. According to this analysis, VJ and VJ + WiKim0124 displayed similar features, with a relatively high amount of sugars. The overall sugar content was high in VJ, and only the mannose content was high in VJ + WiKim0124. By contrast, in VJ + WiKim39, the content of metabolites, other than sugars, was high. This cluster demonstrated a significant difference in crucial metabolites between VJ + WiKim39 and other samples. The clusters shown in the row represent the distribution patterns among the metabolites. In the fermented VJ samples, the sugar content decreased and the amount of organic acids and amino acids increased. Figure 3.10 compares the production of key metabolites by inoculating VJ with other *Lactobacillaceae* strains, demonstrating that WiKim39 produced significantly higher amounts. This highlights WiKim39's exceptional metabolite production capability among *Lactobacillaceae* strains isolated from kimchi. Studies have found a positive

correlation between antioxidant capacity and polyphenol compounds in plant-based foods, such as fruits and vegetables (Ofosu, et al., 2021). However, in this study, the variety and content of individual metabolites contributed significantly to differentiating the fermented VJ beverages. In addition to the phenolic acids in the fermented VJs, organic acids, and amino acids may correlate with antioxidant activity.

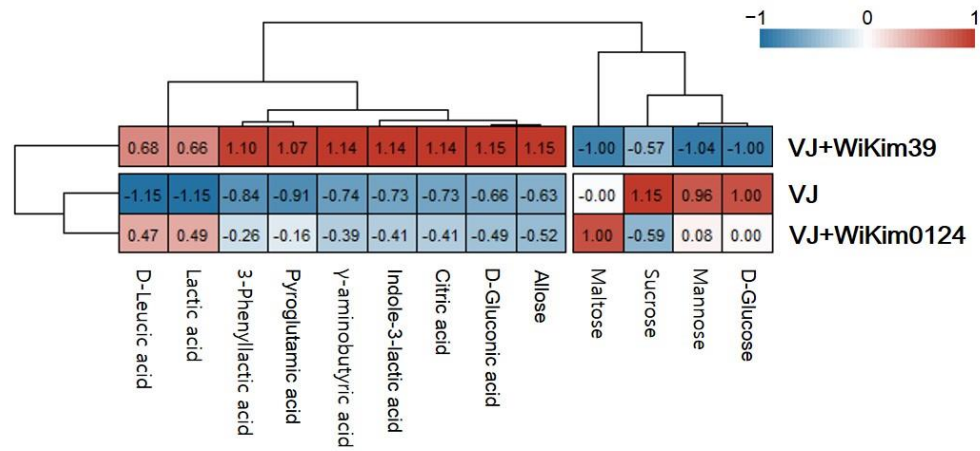


Fig. 3.9. Heatmap. Distribution and concentration of metabolites among samples. Red boxes indicate higher concentrations, and blue boxes indicate lower concentrations. The numbers within the boxes represent the relative abundance values of the data.

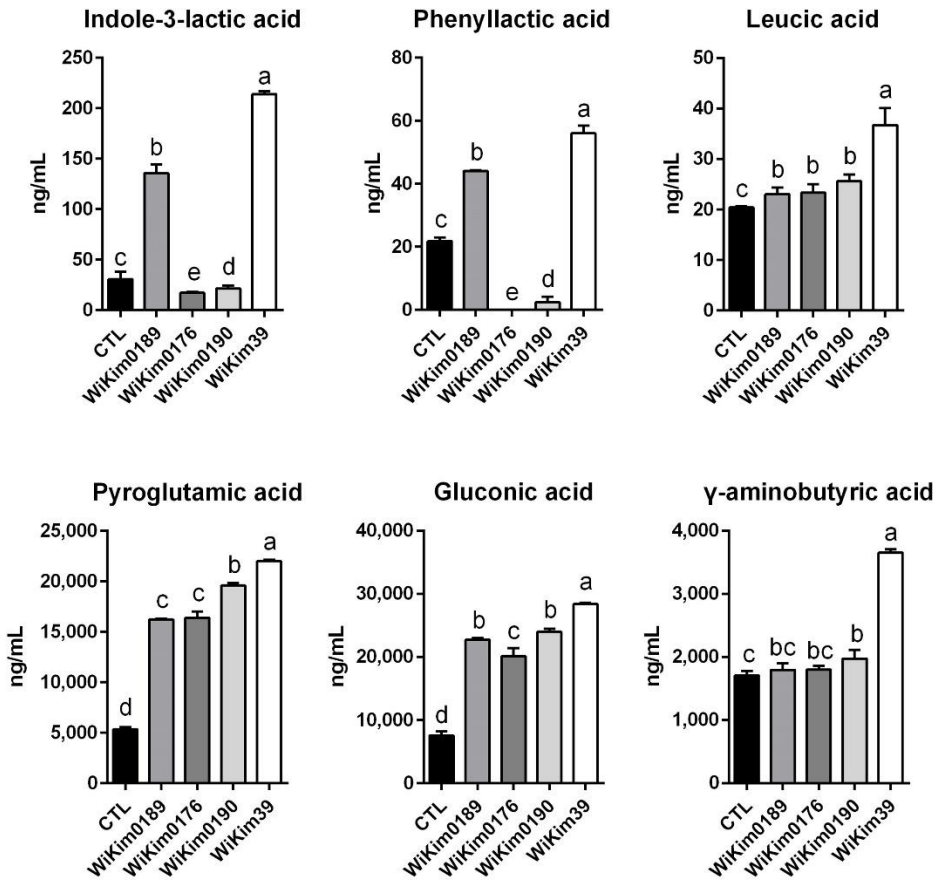


Fig. 3.10. The production of key metabolites in VJ inoculated with other *Lactobacillaceae* strains. Quantification of six significantly differentiated compounds from VJ fermentation was conducted. The analysis was performed using ultra-performance liquid chromatography with quadrupole time-of-flight tandem mass spectrometry. Different letters denote significant difference. CTL: non-fermented VJ; WiKim0189: *Lactiplantibacillus plantarum* WiKim0189; WiKim0176: *Latilactobacillus sakei* WiKim0176; WiKim0190: *Latilactobacillus sakei* WiKim0190; WiKim39: *Companilactobacillus allii* WiKim39 ($p < 0.05$, ANOVA, Tukey-HSD).

3.4. Conclusions

To verify the health-promoting effects of LAB-fermented VJ, metabolites generated through LAB fermentation were analyzed to establish the basis for a functional drink. We profiled VJ, VJ + WiKim39, and VJ + WiKim0124 using LC-QTOF-MS/MS and GC-MS and investigated the correlation between antioxidant capacity and the metabolites in fermented and non-fermented VJs. Significant metabolite changes were found in the LAB-fermented VJs and a significant positive correlation between compounds and their antioxidant capacities was observed. Based on these results, six functional active ingredients were identified, including three organic acids, one phenol, and two amino acids. More active substances were detected in VJ + WiKim39 than in VJ + WiKim0124. The results demonstrated a positive effect of LAB fermentation on antioxidant activities. Our results are promising and suggest that lactic acid bacteria *C. allii* WiKim39 and *L. lactis* WiKim0124 isolated from kimchi are promising for the development of probiotic beverages; thus, they could be used as functional starter cultures to increase the antioxidant activity of plant-based foods during fermentation. Moreover, further studies on phenolic compounds and flavonoid content variation during the VJ fermentation process will be necessary in the future.

3.5. References

- Bhat, R., Axtell, R., Mitra, A., Miranda, M., Lock, C., Tsien, R. W., & Steinman, L. (2010). Inhibitory role for GABA in autoimmune inflammation. *Proc Natl Acad Sci U S A*, *107*(6), 2580-2585.
- Canete-Rodriguez, A. M., Santos-Duenas, I. M., Jimenez-Hornero, J. E., Ehrenreich, A., Liebl, W., & Garcia-Garcia, I. (2016). Gluconic acid: properties, production methods and applications—an excellent opportunity for agro-industrial by-products and waste biovalorization. *Process Biochemistry*, *51*(12), 1891-1903.
- Carrillo, C., Wilches-Pérez, D., Hallmann, E., Kazimierczak, R., & Rembiałkowska, E. (2019). Organic versus conventional beetroot. Bioactive compounds and antioxidant properties. *Lwt*, *116*, 108552.
- Choi, I. S., Ko, S. H., Lee, M. E., Kim, H. M., Yang, J. E., Jeong, S.-G., Lee, K. H., Chang, J. Y., Kim, J.-C., & Park, H. W. (2021). Production, Characterization, and Antioxidant Activities of an Exopolysaccharide Extracted from Spent Media Wastewater after *Leuconostoc mesenteroides* WiKim32 Fermentation. *ACS omega*, *6*(12), 8171-8178.
- de Souza, S. A., da Silva, T. M. G., da Silva, E. M. S., Camara, C. A., & Silva, T. M. S. (2018). Characterisation of phenolic compounds by

- UPLC-QTOF-MS/MS of geopropolis from the stingless bee *Melipona subnitida* (jandaira). *Phytochem Anal*, 29(6), 549-558.
- Dias, C. O., Scariot, M. C., Amboni, R. D. d. M. C., & Arisi, A. C. M. (2020). Application of propidium monoazide coupled with quantitative PCR to evaluate cell viability of *Bifidobacterium animalis* subsp. *lactis* in a non-dairy probiotic beverage. *Annals of Microbiology*, 70(1), 1-7.
- Eckstein, J. A., Ammerman, G. M., Reveles, J. M., & Ackermann, B. L. (2008). Analysis of glutamine, glutamate, pyroglutamate, and GABA in cerebrospinal fluid using ion pairing HPLC with positive electrospray LC/MS/MS. *J Neurosci Methods*, 171(2), 190-196.
- Ghani, M. A., Barril, C., Bedgood, D. R., Jr., & Prenzler, P. D. (2017). Measurement of antioxidant activity with the thiobarbituric acid reactive substances assay. *Food Chem*, 230, 195-207.
- Hawkins, R. A., Simpson, I. A., Mokashi, A., & Vina, J. R. (2006). Pyroglutamate stimulates Na⁺-dependent glutamate transport across the blood-brain barrier. *FEBS Lett*, 580(18), 4382-4386.
- Inoue, K., Shirai, T., Ochiai, H., Kasao, M., Hayakawa, K., Kimura, M., & Sansawa, H. (2003). Blood-pressure-lowering effect of a novel fermented milk containing gamma-aminobutyric acid (GABA) in mild hypertensives. *Eur J Clin Nutr*, 57(3), 490-495.
- Jeff-Agboola, Y., & Oguntuase, O. (2006). Effect of *Bacillus sphaericus* on proximate composition of soybean (*Glycine max*) for the production

of soy iru. *Pakistan Journal of Nutrition*, 5(6), 606-607.

Jung, S., Hwang, H., & Lee, J.-H. (2019). Effect of lactic acid bacteria on phenyllactic acid production in kimchi. *Food Control*, 106, 106701.

Kusznierewicz, B., Smiechowska, A., Bartoszek, A., & Namiesnik, J. (2008). The effect of heating and fermenting on antioxidant properties of white cabbage. *Food Chem*, 108(3), 853-861.

Kwaw, E., Ma, Y., Tchabo, W., Apaliya, M. T., Wu, M., Sackey, A. S., Xiao, L., & Tahir, H. E. (2018). Effect of lactobacillus strains on phenolic profile, color attributes and antioxidant activities of lactic-acid-fermented mulberry juice. *Food Chem*, 250, 148-154.

Landete, J. M., Curiel, J. A., Rodríguez, H., de las Rivas, B., & Muñoz, R. (2014). Aryl glycosidases from *Lactobacillus plantarum* increase antioxidant activity of phenolic compounds. *Journal of Functional Foods*, 7, 322-329.

Latté, K. P., Appel, K.-E., & Lampen, A. (2011). Health benefits and possible risks of broccoli—An overview. *Food and Chemical Toxicology*, 49(12), 3287-3309.

Lee, M., Song, J. H., Jung, M. Y., Lee, S. H., & Chang, J. Y. (2017). Large-scale targeted metagenomics analysis of bacterial ecological changes in 88 kimchi samples during fermentation. *Food Microbiol*, 66, 173-183.

Lee, M., Song, J. H., Lee, S. H., Jung, M. Y., & Chang, J. Y. (2018). Effect of seasonal production on bacterial communities in Korean industrial

kimchi fermentation. *Food Control*, 91, 381-389.

Lee, M. E., Jang, J. Y., Lee, J. H., Park, H. W., Choi, H. J., & Kim, T. W.

(2015). Starter cultures for kimchi fermentation. *J Microbiol Biotechnol*, 25(5), 559-568.

Leung, R., Venus, C., Zeng, T., & Tsopmo, A. (2018). Structure-function

relationships of hydroxyl radical scavenging and chromium-VI reducing cysteine-tripeptides derived from rye secalin. *Food Chem*, 254, 165-169.

Li, T., Jiang, T., Liu, N., Wu, C., Xu, H., & Lei, H. (2021).

Biotransformation of phenolic profiles and improvement of antioxidant capacities in jujube juice by select lactic acid bacteria. *Food Chem*, 339, 127859.

Li, Z., Teng, J., Lyu, Y., Hu, X., Zhao, Y., & Wang, M. (2019). Enhanced

antioxidant activity for apple juice fermented with *Lactobacillus plantarum* ATCC14917. *Molecules*, 24(1), 51.

Lima, A. C. P., Louzada, P. R., De Mello, F. G., & Ferreira, S. T. (2003).

Neuroprotection against A β and glutamate toxicity by melatonin: Are GABA receptors involved? *Neurotoxicity research*, 5(5), 323-327.

Liu, D., Guo, Y., Wu, P., Wang, Y., Kwaku Golly, M., & Ma, H. (2020). The

necessity of walnut proteolysis based on evaluation after in vitro simulated digestion: ACE inhibition and DPPH radical-scavenging activities. *Food Chem*, 311, 125960.

- Liu, S., Yu, Q., Huang, H., Hou, K., Dong, R., Chen, Y., Xie, J., Nie, S., & Xie, M. (2020). The effect of bound polyphenols on the fermentation and antioxidant properties of carrot dietary fiber in vivo and in vitro. *Food & function*, *11*(1), 748-758.
- Manga, J. A. M., Zangué, S. C. D., Tatsadjeu, L. N., Zargar, M., Albert, E., & Bayat, M. (2019). Producing probiotic beverage based on raffia sap fermented by *Lactobacillus fermentum* and *Bifidobacterium bifidum*. *Res. on Crops*, *20*, 629-634.
- Mucchetti, G., Locci, F., Massara, P., Vitale, R., & Neviani, E. (2002). Production of pyroglutamic acid by thermophilic lactic acid bacteria in hard-cooked mini-cheeses. *J Dairy Sci*, *85*(10), 2489-2496.
- Nguyen, B. T., Bujna, E., Fekete, N., Tran, A. T. M., Rezessy-Szabo, J. M., Prasad, R., & Nguyen, Q. D. (2019). Probiotic Beverage From Pineapple Juice Fermented With *Lactobacillus* and *Bifidobacterium* Strains. *Front Nutr*, *6*, 54.
- Nieminen, M. T., Hernandez, M., Novak-Frazer, L., Kuula, H., Ramage, G., Bowyer, P., Warn, P., Sorsa, T., & Rautemaa, R. (2014). DL-2-hydroxyisocaproic acid attenuates inflammatory responses in a murine *Candida albicans* biofilm model. *Clin Vaccine Immunol*, *21*(9), 1240-1245.
- Oforu, F. K., Elahi, F., Daliri, E. B., Tyagi, A., Chen, X. Q., Chelliah, R., Kim, J. H., Han, S. I., & Oh, D. H. (2021). UHPLC-ESI-QTOF-MS/MS characterization, antioxidant and antidiabetic properties of

sorghum grains. *Food Chem*, 337, 127788.

Ogodo, A. C., Ugbogu, O. C., Onyeagba, R. A., & Okereke, H. C. (2018).

In-vitro starch and protein digestibility and proximate composition of soybean flour fermented with lactic acid bacteria (LAB) consortia. *Agriculture and Natural Resources*, 52(5), 503-509.

Olukomaiya, O. O., Adiamo, O. Q., Fernando, W. C., Mereddy, R., Li, X., &

Sultanbawa, Y. (2020). Effect of solid-state fermentation on proximate composition, anti-nutritional factor, microbiological and functional properties of lupin flour. *Food chemistry*, 315, 126238.

Pannerchelvan, S., Rios-Solis, L., Wong, F. W. F., Zaidan, U. H., Wasoh, H.,

Mohamed, M. S., & Halim, M. (2023). Strategies for improvement of gamma-aminobutyric acid (GABA) biosynthesis via lactic acid bacteria (LAB) fermentation. *Food & Function*, 14(9), 3929-3948.

Rajanikar, R., Nataraj, B. H., Naithani, H., Ali, S. A., Panjagari, N. R., &

Behare, P. V. (2021). Phenyllactic Acid: A Green Compound for Food Biopreservation. *Food Control*, 108184.

Rico-Rodriguez, F., Villamiel, M., Ruiz-Aceituno, L., Serrato, J. C., &

Montilla, A. (2020). Effect of the lactose source on the ultrasound-assisted enzymatic production of galactooligosaccharides and gluconic acid. *Ultrason Sonochem*, 67, 104945.

Sakko, M., Tjäderhane, L., Sorsa, T., Hietala, P., Järvinen, A., Bowyer, P., &

Rautemaa, R. (2012). 2-Hydroxyisocaproic acid (HICA): a new potential topical antibacterial agent. *International journal of*

antimicrobial agents, 39(6), 539-540.

- Sakurai, T., Odamaki, T., & Xiao, J. Z. (2019). Production of Indole-3-Lactic Acid by Bifidobacterium Strains Isolated from Human Infants. *Microorganisms*, 7(9).
- Soares, J. C., Rosalen, P. L., Lazarini, J. G., Massarioli, A. P., da Silva, C. F., Nani, B. D., Franchin, M., & de Alencar, S. M. (2019). Comprehensive characterization of bioactive phenols from new Brazilian superfruits by LC-ESI-QTOF-MS, and their ROS and RNS scavenging effects and anti-inflammatory activity. *Food Chem*, 281, 178-188.
- Surveswaran, S., Cai, Y.-Z., Corke, H., & Sun, M. (2007). Systematic evaluation of natural phenolic antioxidants from 133 Indian medicinal plants. *Food chemistry*, 102(3), 938-953.
- Suzuki, Y., Kosaka, M., Shindo, K., Kawasumi, T., Kimoto-Nira, H., & Suzuki, C. (2013). Identification of antioxidants produced by *Lactobacillus plantarum*. *Bioscience, biotechnology, and biochemistry*, 121006.
- Tohidi, B., Rahimmalek, M., & Arzani, A. (2017). Essential oil composition, total phenolic, flavonoid contents, and antioxidant activity of *Thymus* species collected from different regions of Iran. *Food Chem*, 220, 153-161.
- Wang, Y., Luo, Z., Huang, X., Yang, K., Gao, S., & Du, R. (2014). Effect of exogenous γ -aminobutyric acid (GABA) treatment on chilling injury

and antioxidant capacity in banana peel. *Scientia Horticulturae*, 168, 132-137.

Werf, P. V. D., Orłowski, M., & Meister, A. (1971). Enzymatic conversion of 5-oxo-L-proline (L-pyrrolidone carboxylate) to L-glutamate coupled with cleavage of adenosine triphosphate to adenosine diphosphate, a reaction in the γ -glutamyl cycle. *Proceedings of the National Academy of Sciences*, 68(12), 2982-2985.

Wong, C. B., Tanaka, A., Kuhara, T., & Xiao, J. Z. (2020). Potential Effects of Indole-3-Lactic Acid, a Metabolite of Human Bifidobacteria, on NGF-induced Neurite Outgrowth in PC12 Cells. *Microorganisms*, 8(3).

Ye, J.-H., Huang, L.-Y., Terefe, N. S., & Augustin, M. A. (2019). Fermentation-based biotransformation of glucosinolates, phenolics and sugars in retorted broccoli puree by lactic acid bacteria. *Food chemistry*, 286, 616-623.

Yu, L. L., Zhou, K. K., & Parry, J. (2005). Antioxidant properties of cold-pressed black caraway, carrot, cranberry, and hemp seed oils. *Food chemistry*, 91(4), 723-729.

This chapter comprises articles, published in *Food and function* with minor modification as a partial fulfillment of Moeun Lee's Ph.D. program

Chapter 4.

Anti-obesity effect of vegetable juice fermented with lactic acid bacteria isolated from kimchi in C57BL/6J mice and human mesenchymal stem cells

Abstract

Strategies are being developed for the treatment and prevention of obesity based on the use of probiotics. However, little is known about the association between LAB and the effects of food matrices. This study aimed to investigate the effect of fermented vegetable juice (VJ) obtained from a blend of four crops (*Brassica oleracea* var. *capitata*, *B. oleracea* var. *italica*, *Daucus carota* L., and *Beta vulgaris*) on adipogenesis along with the identification of active compounds. Two lactic acid bacteria (LAB) (*Companilactobacillus allii* WiKim39 and *Lactococcus lactis* WiKim0124), isolated from kimchi, were used to ferment the VJ and their effectiveness was evaluated in differentiated human mesenchymal stem cells and obese mice. *In vitro* antibody array analysis was done to understand signaling proteins in adipogenesis. Gene Ontology enrichment analysis showed that differentially expressed proteins are related to biological processes including immunological processes. These were effectively regulated by LAB and fermented VJ. Supplementation of fermented VJ reduced the weight gain, blood biochemical indicators, and liver fat accumulation in mice. Oil Red O staining indicated that the fermentation metabolites of VJ (indole-3-lactic acid, leucic acid, and phenyllactic acid) had an inhibitory effect on lipid accumulation *in vitro*. Therefore, it can be concluded that LAB-fermented

VJ and its metabolites have the potential to counter obesity, and thus can be therapeutically effective.

Keywords: *Companilactobacillus allii* WiKim39, *Lactococcus lactis*

WiKim0124, kimchi starter, antiobesity, human mesenchymal stem cells

4.1. Introduction

Many probiotic lactic acid bacteria (LAB) are reported to alleviate obesity and obesity-associated metabolic disorders. The proposed mechanisms of action include modulation of adipokines and immunometabolic parameters (Fabersani et al., 2017; Fabersani et al., 2019), increased expression of fatty acid oxidation genes, reduced lipid accumulation, altered serum profile, and changes in the gut microbiome (Dahiya et al., 2017). Paraprobiotics are known non-viable microorganisms or bacterial-free extracts that promote health by exhibiting bioactivities (Cuevas-González, Liceaga, & Aguilar-Toalá, 2020). Paraprobiotics include peptides, peptidoglycan-derived muropeptides, exopolysaccharides, cell surface-layer proteins, cell-secreted proteins, bacteriocins, and organic acids. The health-promoting effects of paraprobiotics include improved immune response, reduction in host inflammation-induced weight gain, and alleviation of hyperlipidemia (Kim, Lee, Han, Seo, & Kim, 2021).

Kimchi, prepared from vegetables seasoned with spices, is a well-known fermented food in Korea (Lee, Song, Shim, & Chang, 2020). Several studies have been conducted on the health benefits of the bioactive metabolites of kimchi. LABs, isolated from kimchi, have been reported to exhibit beneficial properties like immunomodulation, antiobesity, antidiabetic, and

anti-cancer (Lee et al., 2015). Moreover, exopolysaccharides synthesized by kimchi LAB show antioxidant activities (Choi et al., 2021). In addition, recently, we developed LAB fermented vegetable juices (VJ) from four local crops (cabbage (*Brassica oleracea* var. *capitata*), broccoli (*B. oleracea* var. *italica*), carrots (*Daucus carota* L.), and beetroot (*Beta vulgaris*)), preserved from a year prior, on the Jeju island, which had a negative impacting rural industries. LAB fermentation improved the quality of vegetable juices by enhancing the nutritional quality and functional properties. VJ fermented with *Companilactobacillus allii* WiKim39 and *Lactococcus lactis* WiKim0124, isolated from kimchi, exhibited immunomodulatory functions (Yun, Lee, Song, Choi, & Chang, 2022) and, improved the antioxidant properties. These health benefits are mainly due to the enhanced production of functional bioactive compounds such as phenolics (3-phenyllactic acid) and other organic acids (D-leucic and indole-3-lactic acids) (Lee et al., 2021a).

Obesity, a global epidemic, influences more than 700 million people (Li et al., 2021). It is associated with cardiovascular complications, diabetes, hypertension, and cancer (Gil-Rodríguez & Beresford, 2019). Probiotics have beneficial effects against obesity-related metabolic complications, including distorted lipid profiles and improve immune modulation (Tang, Kong, Shan, Lu, & Lu, 2021). Some studies have demonstrated that the supplementation of prebiotics, which stimulates the growth and development of symbiotic microorganisms, is more effective in improving

human health than the probiotics (Ejtahed et al., 2019). Fermented foods and beverages, based on vegetable matrices, are widely reported for their health-promoting properties. However, these approaches and health claims lack scientific evidence due to the absence of relevant data (Al Kassaa, Hamze, Hober, Chihib, & Drider, 2014).

The present study aimed to (i) investigate the effect of fermented VJ on adipogenesis and cellular adipokine profile in mature human adipose-derived mesenchymal stem cells, (ii) exploring the antiobesity potential and its mechanism of action in high-fat diet-induced obese mice, and (iii) identify the active substances in LAB (*C. allii* WiKim39 and *L. lactis* WiKim0124) fermentation metabolites.

4.2. Material and Methods

4.2.1. Bacterial strains

Companilactobacillus allii WiKim39 (GenBank ID: NR_159087.1) and *L. lactis* WiKim0124 (GenBank ID: MZ424472.1), isolated from kimchi, were utilized in this study. The LAB strains were cryopreserved in De Man, Rogosa, and Sharpe (MRS) broth, containing 15% (v/v) glycerol, at -80 °C. Ahead of the experiment, the stock cultures were revived in MRS broth at 30 °C for 24 h. The bacterial cells were harvested via centrifugation (6000 × g, 10 min, 4 °C) and washed twice with phosphate buffered saline (PBS).

4.2.2. Preparation and fermentation of VJ

VJ was prepared as described in a previous study ¹⁰. Briefly, from the harvested crops of the Jeju island (Korea) in 2020, a mixture was prepared to contain 12% cabbage (*B. oleracea* var. capitata), 12% broccoli (*B. oleracea* var. italica), 12% carrots (*D. carota* L.), and 10% beetroot (*B. vulgaris*), and 54% purified water. The vegetable mixture was extracted with hot water (107 °C for 2 h) and °Brix of VJ samples was adjusted with food-grade glucose for optimal growth conditions. A total of 10⁷ colony forming units (CFU)/mL of each strain (WiKim39 or WiKim0124) were inoculated

into the VJ to initiate fermentation (30 °C for 48 h). For *in vitro* experiments, the fermented VJs were subjected to 95 °C for 10 min to eliminate the bacterial strains. This suspension was freeze-dried and stored at -80 °C. Non-fermented VJ was used as a control.

4.2.3. Cell culture and adipogenic differentiation

Human adipose-derived mesenchymal stem cells (hMSCs) were obtained from the American Type Culture Collection (PCS-500-011) and cultured at 37 °C and 5% CO₂ in basal medium, prepared using the MesenCult proliferation kit (StemCell Technologies, Vancouver, Canada). To assess adipogenic differentiation, cells were harvested at passage three and cultured in MesenCult medium supplemented with the Adipogenic Differentiation Kit (StemCell Technologies, Vancouver, Canada) at a density of 1.5×10^4 cells/mL in 6-well plates, according to the manufacturer's instructions. The medium was changed every 2 d for 21 d. Adipogenesis differentiation was evaluated by Oil Red O staining as previously described (Deng et al., 2020). Briefly, cells were fixed in 10% formaldehyde in PBS, washed with PBS, stained with Oil Red O solution (Sigma-Aldrich, St. Louis, MO, USA) for 10 min, and repeatedly rinsed with distilled water. Lipid droplets were extracted by incubating with 100% isopropanol for 15 min. The optical density (OD) of the solution was measured at 500 nm. D-leucic acid (LA), indole-3-lactic acid (ILA), and 3-phenyllactic acid (PLA) standards were obtained from Sigma Aldrich (St. Louis, MO, USA).

4.2.4 *In vitro* cytotoxicity test

Bacterial cells were harvested, suspended in PBS, sonicated, and centrifuged as previously described (Lee et al., 2018). Supernatants of bacterial cell extracts were filter-sterilized (0.45 μm), lyophilized, and used to perform the anti-adipogenesis assay in hMSCs. To evaluate the cytotoxicity assay, 10^4 cells/well were plated in a 96-well plate and incubated for 48 h in a medium containing LAB lysates (concentration range of 0.5 to 5 mg/mL) and fermented or non-fermented VJ samples (concentration range of 5 to 100 mg/mL). For estimation of the active substances in fermented VJs, LA, ILA, and PLA were treated at concentration ranges of 0.63 to 40 mM. Cell viability was measured using 2,3-bis[2-methoxy-4-nitro-5-sulphophenyl]-2H-tetrazolium-5-carboxanilide disodium salt (XTT) assay, as described previously (Kamiloglu, Sari, Ozdal, & Capanoglu, 2020).

4.2.5. Antibody array analysis

Fully matured hMSCs were collected and lysed. The lysates were centrifuged for 20 min at $15,000 \times g$, and supernatants were collected for the experiment. Protein concentration was estimated using the Bradford assay (Bradford, 1976). For multiple protein detection, human obesity antibody array membrane (ab169819, Abcam, Cambridge, UK) was used according to the manufacturer's protocol. Briefly, the provided blocking buffer was added

to the array membranes for 30 min. The membranes were then incubated with 1 mg of cell lysates/array membrane, followed by the addition of a biotinylated detection antibody. The membranes were incubated on a rocker with horseradish peroxidase-conjugated streptavidin (1: 100). Spots on the array membranes were scanned and quantified by densitometry (Chemidoc, Bio-Rad, Hercules, CA, USA).

4.2.6. Bioinformatic analysis

Proteins with a \log_2 fold change of $\geq |1|$ in the adipogenic differentiation group (CON) versus the pre-adipocytic group (NOR) were assigned as differentially expressed proteins (DEPs). Specific information on all proteins was obtained from the UniProt database (<https://www.uniprot.org/>). To evaluate functional enrichment, DEPs were searched against the Gene Ontology (GO) (<http://geneontology.org/>) database. Characteristics of DEPs were examined by GO enrichment analysis using the Biological Networks Gene Ontology (BiNGO) plug-in of Cytoscape (Maere, Heymans, & Kuiper, 2005). Fisher's exact test was used to determine the significance of GO term enrichment for multiple testing and the resulting p-value was adjusted with the false discovery rate (FDR) (cutoff < 0.01). Hierarchical clustering heatmap analysis of DEPs was generated with the "pheatmap" package in R (v3.3.2; <https://www.r-project.org/>).

4.2.7. Animals

National Academy of Science of the National Institutes of Health (NIH) guidelines for “Guide for the Care and Use of Laboratory Animals” were observed for animal experiments. The animal care and protocols were reviewed and approved by the World Institute of Kimchi’s Institutional Animal Care and Use Committee (WIKIM IACUC 202033). Six-week-old male C57BL/6J mice were obtained from Orient Bio (Seongnam, Korea). Mice were kept in ventilated polysulfone cages (200W×318D×145H (mm), four mice per cage) in a temperature and humidity-controlled facility with distilled water and food *ad libitum*. After 1 week, 56 mice were randomly distributed into seven groups (n = 8 per group) as follows: i) normal control (NOR); mice received a standard pellet feed (Research Diet Inc., D10001, 10 kcal% fat) with distilled water, ii) obesity-induced group (HFD); received a high-fat diet (Research Diet Inc., D12492, 60 kcal% fat) with distilled water, iii) HFD with *C. allii* WiKim39 (WiKim39), iv) HFD with *L. lactis* WiKim0124 (WiKim0124), v) HFD with non-fermented VJ (VJ), vi) HFD with *C. allii* WiKim39-fermented VJ (VJ + WiKim39), and vii) HFD with *L. lactis* WiKim0124-fermented VJ (VJ + WiKim0124). Food intake and body weight were recorded weekly. All experimental groups were orally administered 10 mL kg⁻¹ of body weight every second day for 8 w. At the end of the experiment, serum and tissue were collected and samples were stored at -80 °C until further use.

4.2.8. Dietary dosage information

Companilactobacillus allii WiKim39 and *L. lactis* WiKim0124 live cells were lyophilized after mass culture. The LAB powder was rehydrated in sterilized distilled water for 1 h at room temperature to a total dose of 1×10^9 CFU $200 \mu\text{L}^{-1} \text{d}^{-1}$ before oral gavage. The VJ treated groups (VJ, VJ + WiKim39, VJ + WiKim0124) received a daily dose of 250 mg kg^{-1} body weight. The VJ treatment group dose was calculated according to the human equivalent dose as follows: 250 mg kg^{-1} was estimated to be approximately 1600 mg per 60 kg adult person a day, equal to the consumption of 20 mL VJ when considering the freeze-dried yield.

4.2.9. Histological analysis

Liver and epididymal fat tissues were fixed in 10% neutral buffered formalin and histology was performed as described previously (Yun et al., 2022). Tissues stained with hematoxylin and eosin (H&E) were examined under an optical microscope (magnification, 20 \times ; Olympus, Japan).

4.2.10. Plasma biochemical indicators

Plasma triglycerides (TG), total cholesterol (T-CHO), glucose, aspartate aminotransferase (AST), alanine aminotransferase (ALT), and alkaline phosphatase (ALP) levels were determined using a FUJI DRI-CHEM 7000 (Fujifilm, Tokyo, Japan), following the manufacturer's instructions. The concentration of leptin was measured using the Bio-Plex

Pro Mouse Diabetes-Plex Assay (Bio-Rad, USA).

4.2.11. Quantitative reverse transcription-polymerase chain reaction (qRT-PCR)

Epididymal fat tissue (0.1 g) was homogenized with a bead-beating grinder and lysis system (cycle 2, FastPrep-24; MPBIO, Seoul, Korea). RNA was extracted using the RNeasy kit (Qiagen, Valencia, CA, USA). Approximately 10 ng of RNA was used for qRT-PCR amplification with a QuantiFast SYBR Green RT-PCR Kit (Qiagen, Valencia, CA, USA). The reaction conditions were as follows: reverse transcription at 50 °C for 10 min, activation step at 95 °C for 5 min, denaturation at 95 °C for 10 s, and annealing and extension at 60 °C for 30 s for 35 cycles. The result was normalized to that of beta-actin.

4.2.12. Statistical analysis

The statistical significance was analyzed using Tukey's honest significant difference (HSD) test performed with the "*agricolae*" package of R for group comparisons. Results with $p < 0.05$ were considered statistically significant. All experiments were performed in triplicate, and results were expressed as mean \pm standard deviation (SD).

4.3. Results

4.3.1. Effects of LAB fermented VJ on the differentiated hMSCs and adipogenic proteins

To investigate the effect of LAB on cell viability, hMSC preadipocytes were incubated with varying concentrations of LAB lysates and fermented VJ products. Treatment with 2 mg/mL of LAB lysate and 20 mg/mL of VJ did not cause any cytotoxicity (Fig. 4.1a, c). To investigate the anti-adipogenic effect, lipid accumulation was measured using the Oil-Red O staining assay. The treatment group showed reduced lipid accumulation in hMSCs indicating the maximum effectiveness of *C. allii* WiKim39 lysates, followed by a subsequent reduction in the effectiveness after treatment with *L. lactis* WiKim0124 lysates, *C. allii* WiKim39 fermented VJ, *L. lactis* WiKim124 fermented VJ, and non-fermented samples (Fig. 4.1b and d). Based on this result, further treatments were administered at these concentrations to investigate the anti-adipogenic mechanism of LAB-fermented VJ. Antibody array analysis was performed on fully matured hMSCs to simultaneously identify 62 proteins related to adipogenesis. We selected 38 DEPs with \log_2 fold changes $\geq |1|$ between the differentiated hMSCs and experimental groups. The array map and profile are shown in Figure 4.2-4.3. The heat map of the DEPs and cluster analysis are shown in

Fig. 4.4. The expression of each DEP was clustered according to the experimental groups, indicating that DEPs had distinctly different expression patterns. We found that most proteins were upregulated compared to that in NOR and downregulated compared to that CON in the LAB and LAB-fermented VJ treatment groups. *C. allii* WiKim39 and *C. allii* WiKim39 fermented VJs were able to suppress the expression of most proteins.

Bioinformatic analysis was done to elucidate the change in the DEPs. For GO enrichment analysis, the DEPs of the treatment groups were compared to the CON (Fig. 4.5). GO enrichment analysis indicated molecular function (MF) and biological process (BP); LAB or LAB-fermented VJ groups were associated with the activation of inflammatory response pathways such as cytokine activity, chemokine activity, immune system process, and positive response to a stimulus. BP related to the immune and stimulation regulation were significantly enriched in VJ+WiKim39 and WiKim39 compared to the HFD group. In contrast, they showed mild enrichment in the VJ group compared to the others.

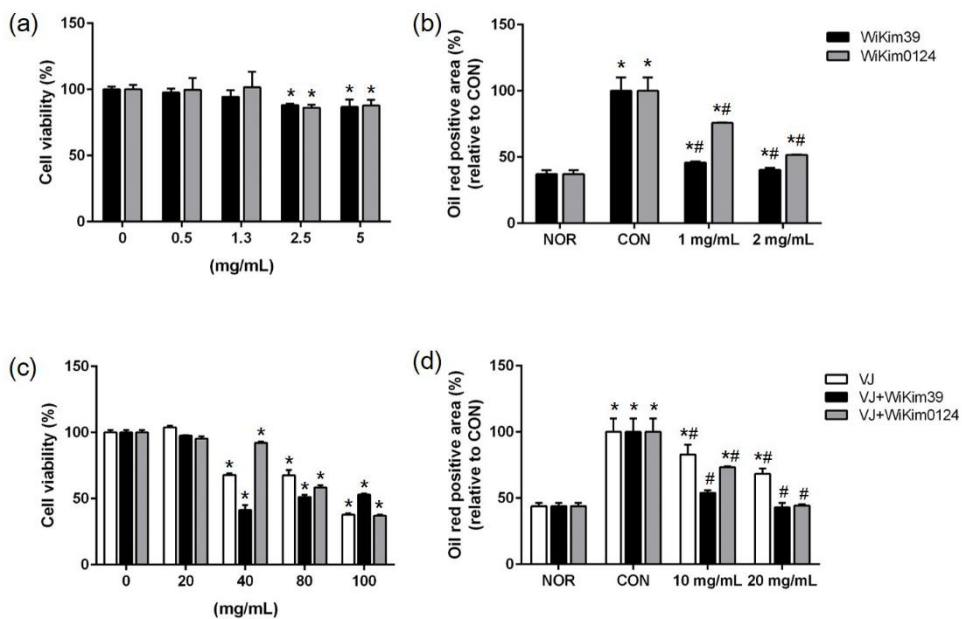


Fig. 4.1. Effect of LAB and LAB fermented VJ on cell viability (a, c) and adipogenic differentiation (b, d). * $p < 0.05$ indicates statistically significant differences between NOR and experimental groups, and # $p < 0.05$ indicates statistically significant differences between CON and experimental groups. Values are expressed as the mean \pm SD (n = 3).

	A	B	C	D	E	F	G	H	I	K	K	L	M	N
1	POS	POS	NEG	NEG	4-1BB	ACE-2	Acrrp30	Adipsin	AgRP	Ang-2	Angiopoietin-1	ANGPTL4	CRP	ENA-78
2	POS	POS	NEG	NEG	4-1BB	ACE-2	Acrrp30	Adipsin	AgRP	Ang-2	Angiopoietin-1	ANGPTL4	CRP	ENA-78
3	Fas	FGF-6	Growth Hormone	HCC-4	IFN- γ	IGFBP-1	IGFBP-2	IGFBP-3	IGF-1	IGF-1 SR	IL-1 R4/ST2	IL-1 sRI	IL-10	IL-11
4	Fas	FGF-6	Growth Hormone	HCC-4	IFN- γ	IGFBP-1	IGFBP-2	IGFBP-3	IGF-1	IGF-1 SR	IL-1 R4/ST2	IL-1 sRI	IL-10	IL-11
5	IL-12	IL-1 α	IL-1 β	IL-6	IL-6 sR	IL-8	Insulin	IP-10	Leptin R	Leptin	LIF	Lymphotactin	MCP-1	MCP-3
6	IL-12	IL-1 α	IL-1 β	IL-6	IL-6 sR	IL-8	Insulin	IP-10	Leptin R	Leptin	LIF	Lymphotactin	MCP-1	MCP-3
7	MCSF	MIF	MIP-1 β	MSP α	OPG	OSM	PAI-1	PARC	PDGF-AA	PDGF-AB	PDGF-BB	RANTES	Resistin	Serum Amyloid A
8	MCSF	MIF	MIP-1 β	MSP α	OPG	OSM	PAI-1	PARC	PDGF-AA	PDGF-AB	PDGF-BB	RANTES	Resistin	Serum Amyloid A
9	SDF-1	sTNF RII	sTNT RI	TECK	TGF- β	TIMP-1	TIMP-2	TNF- α	VEGF	XEDAR	BLANK	BLANK	BLANK	POS
10	SDF-1	sTNF RII	sTNT RI	TECK	TGF- β	TIMP-1	TIMP-2	TNF- α	VEGF	XEDAR	BLANK	BLANK	BLANK	POS

POS: Positive control, NEG: Negative control, BLANK: No antibody

Fig. 4.2. Identification of differentially expressed proteins (DEPs) in human mesenchymal stem cells treated with WiKim39 and WiKim0124 fermented vegetable juices using antibody array. Array map used in the panel.

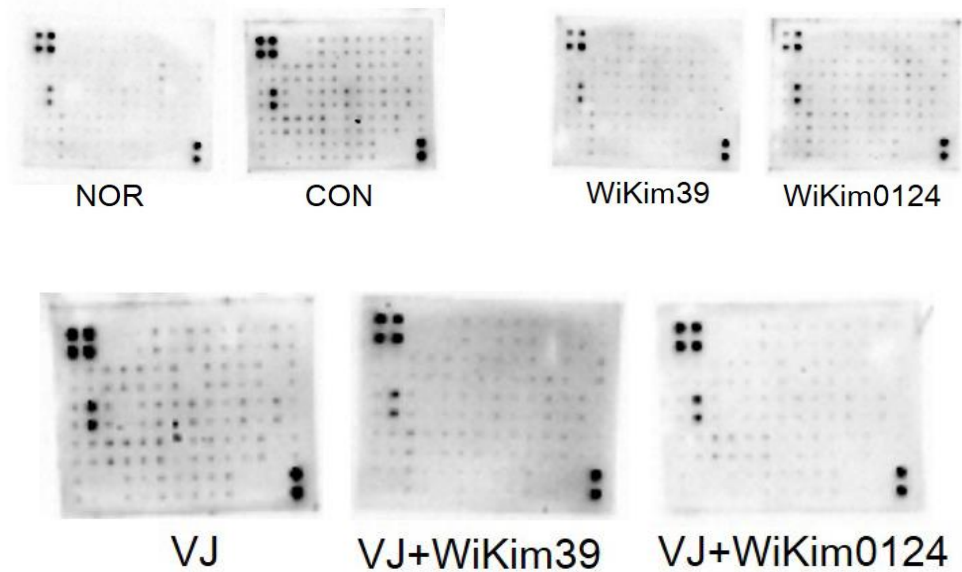


Fig. 4.3. Identification of differentially expressed proteins (DEPs) in human mesenchymal stem cells treated with WiKim39 and WiKim0124 fermented vegetable juices using antibody array. Human antibody array panel used in this study (Raw image files). The signal intensity of the arrays was analyzed using a densitometer. The relative fold change of proteins was calculated after normalization to the positive control (n = 2). 4-1BB, tumor necrosis factor receptor superfamily; ACE-2,

Angiotensin-converting enzyme 2; Acrp30, adiponectin; Adipsin, complement factor D; AgRP, agouti related neuropeptide; Ang-2, angiopoietin 2; Angiopoietin-1, angiopoietin 1; ANGPTL4, angiopoietin like 4; CRP, C-reactive protein; ENA-78, C-X-C motif chemokine ligand 5; Fas, fatty acid synthase; FGF-6, fibroblast growth factor 6; Growth hormone, growth hormone; HCC-4, C-C motif chemokine ligand 16; IFN- γ , interferon gamma; IGFBP-1, insulin-like growth factor-binding protein-1; IGFBP-2, insulin-like growth factor binding protein 2; IGFBP-3, insulin-like growth factor binding protein 3; IGF-1, insulin-like growth factor 1; IGF-1R, insulin-like growth factor-I receptor; IGF-1 SR, interleukin 1 receptor-like 4; IL-1 sR1, interleukin 1 soluble receptor 1; IL-10, interleukin 10; IL-11, interleukin 11; IL-12, interleukin 12; IL-1 α , interleukin 1 alpha; IL-1 β , interleukin 1 beta; IL-6, interleukin 6; IL-6 sR, interleukin 6 soluble receptor; IL-8, interleukin 8; Insulin, insulin; IP-10, C-X-C motif chemokine ligand 10; Leptin R, Leptin receptor; Leptin, leptin; LIF, leukemia inhibitory factor; Lymphotoxin, lymphotoxin; MCP-1, monocyte chemoattractant protein-1; MCP-3, monocyte chemoattractant protein-3; MCSF, macrophage colony-stimulating factor; MIF, macrophage migration inhibitory factor; MIF-1 β , macrophage migration inhibitory factor 1 beta; MSP α , macrophage stimulating protein alpha; OPG, osteoprotegerin; OSM, oncostatin M; PAI-1, plasminogen activator inhibitor-1; PARC, pulmonary and activation-regulated chemokine; PDGF-AA, platelet-derived growth factor; PDGF-AB, platelet-derived growth factor; PDGF-BB, platelet-derived

growth factor; RANTES, regulated upon activation, normal T cell expressed and presumably secreted; Resistin, resistin; Serum amyloid A, serum amyloid A; SDF-1, stromal cell-derived factor 1; sTNF-R1, soluble tumor necrosis factor receptor type 1; sTNF-R2, soluble tumor necrosis factor receptor 2; TGF- β , transforming growth factor beta 1; TIMP1, tissue inhibitor matrix metalloproteinase 1; TIMP2, tissue inhibitor matrix metalloproteinase 2; TNF- α , tumor necrosis factor alpha; VEGF-A, vascular endothelial growth factor A; XEDAR, X-linked ectodermal dysplasia receptor.

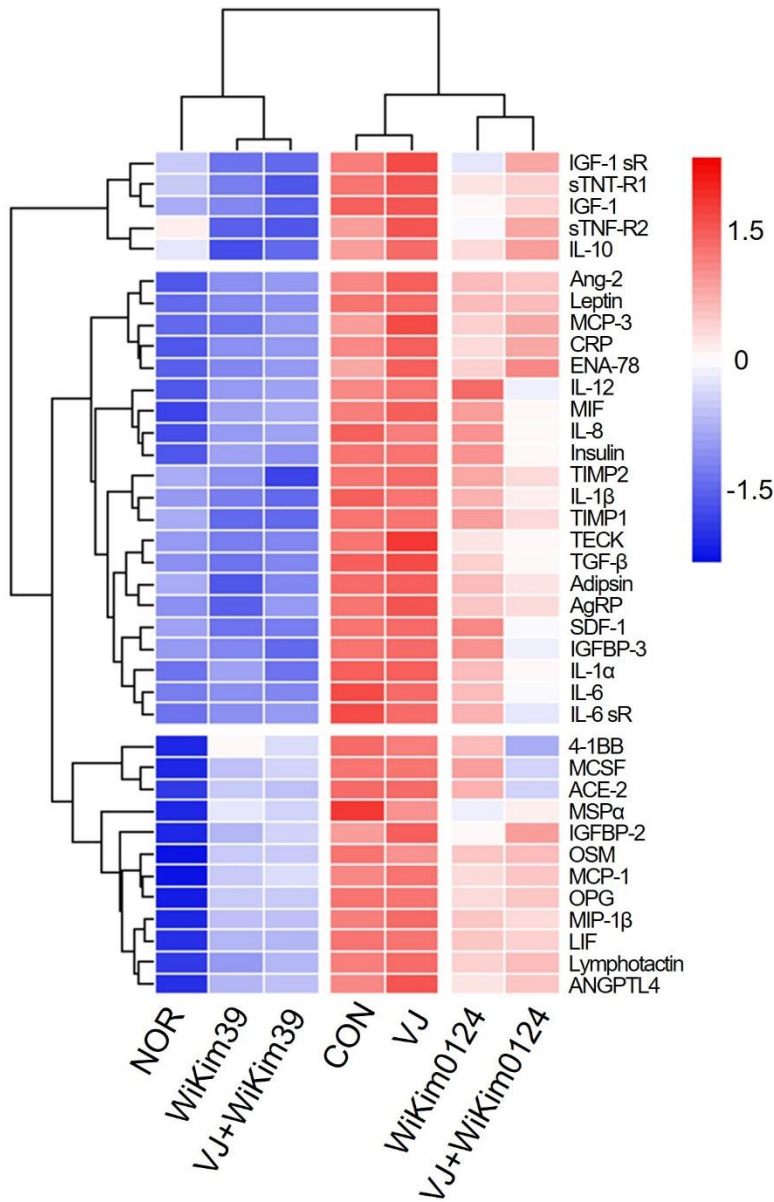


Fig. 4.4. Analysis of the antibody array. Hierarchical cluster analysis of differentially expressed proteins (DEPs). A total of 38 proteins are visualized on the heat map. Different colors represent the relative abundance of proteins, where red represents a higher intensity and blue represents a lower intensity.

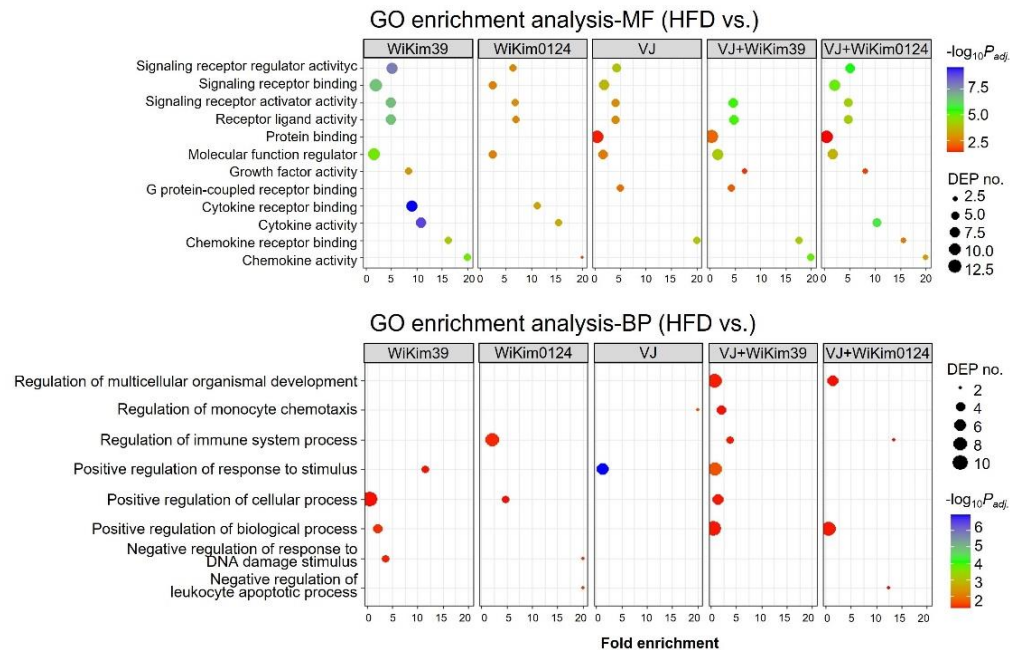


Fig. 4.5. Analysis of the antibody array. Scatter plots of enriched GO pathways relevant to biological processes and molecular function. GO classification of DEPs from the control (CON) vs. experimental groups. GO, Gene Ontology; MF, molecular function; BP, biological process.

4.3.2. Effects of LAB and LAB fermented VJs administration on body weight, plasma lipid profile, and adipocyte size in mice

To investigate the inhibitory effect of LAB and fermented VJ on lipid accumulation, an HFD-induced obesity mouse model was established, as described previously. As shown in Figure 4.6 and Table 4.1, i) all the treatments resulted in a reduction in the body (Fig. 4.6a), liver, spleen, and white adipose tissue weight gain (Table 4.1). Throughout the experiment for 8w, the weights increased in the HFD mouse group and the weight gain was kept in check by the treatments. However, no significant differences were observed amongst the treatments on the extent of weight gain. The same trend was observed for TG and TCHO (Fig. 4.6b-d), ii) In the LAB treatment group, the H&E staining results indicated that epididymal adipose and liver tissue and the adipocyte area looked similar to the NOR group (Fig. 4.7a-c), and iii) in glucose, the main differences appeared in fermented VJ treatment group (Fig. 4.7d), iv). For all the treatments, the insulin values were equivalent to NOR values (Fig. 4.7e) and reduced leptin level during treatment (Fig. 4.7f). Consistent with these results, an increase in the levels of plasma AST, ALT, ALP, liver-free fatty acids (FFA), TG, and TCHO were observed (Fig. 4.8-4.9). LAB and fermented VJ administration effectively ameliorated plasma lipid index and hepatic lipid accumulation. This result was like the NOR group but not the VJ-fed group. Plasma ALP, plasma FFA, hepatic TG, and hepatic TCHO showed the lowest levels in the fermented VJ-supplemented groups.

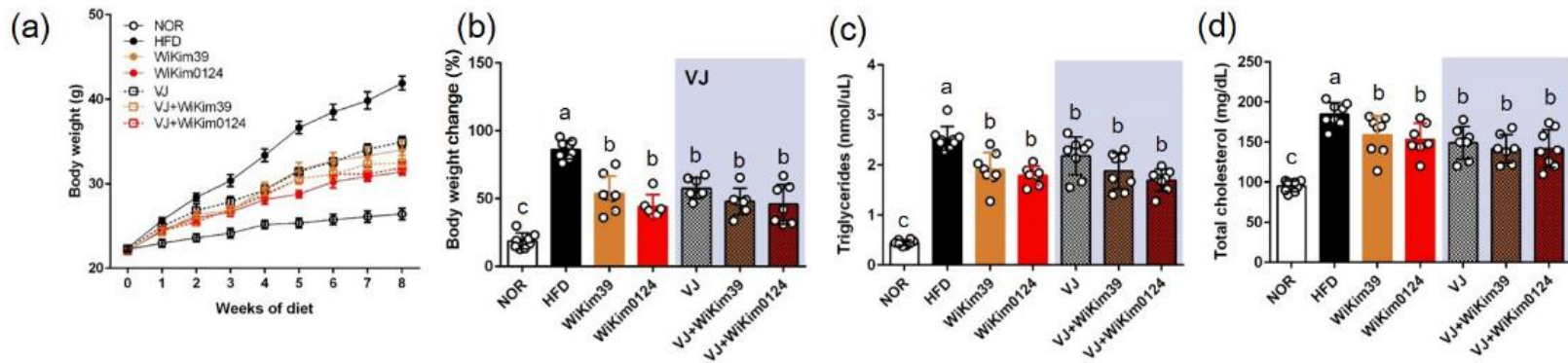


Fig. 4.6. Effects of WiKim39 and WiKim0124 fermented vegetable juice on high-fat diet-induced obese mice. (a) body weight, (b) change in body weight over the experiment duration (8 w) $[(\text{Weight at 8w} - \text{Weight at 0w}) * 100] - 100$, (c) plasma triglycerides, (d) total plasma cholesterol. Different letters denote significant differences ($p < 0.05$, ANOVA, Tukey's HSD). Values are expressed as mean \pm SD.

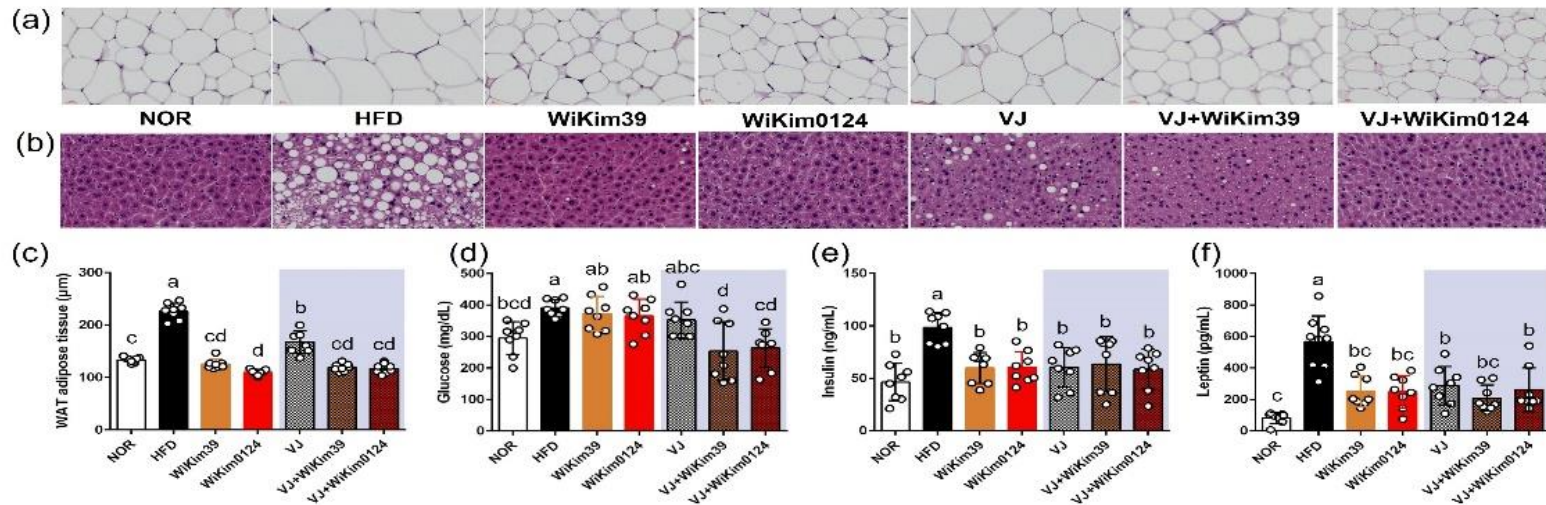


Fig. 4.7. Effects of WiKim39 and WiKim0124 fermented vegetable juice on high-fat diet-induced obese mice. (a) H&E staining of epididymal adipose tissue (white adipose tissue) sections (40 ×), (b) H&E staining of liver tissue sections (40×), (c) average white adipose tissue adipocyte area (quantified under microscope, n = 10), (d) plasma glucose, (e) plasma insulin, and (f) plasma leptin. Different letters denote significant differences ($p < 0.05$, ANOVA, Tukey's HSD). Values are expressed as mean \pm SD; H&E is hematoxylin and eosin stain.

Table 4.1. Organ and adipose tissue weights in mice fed with high-fat diet and LAB-fermented VJs for 8 weeks.

(g)	NOR	HFD	WiKim39	WiKim0124	VJ	VJ+ WiKim39	VJ+ WiKim0124
Liver	1.12±0.06 ^b	1.44±0.12 ^a	1.05±0.05 ^b	0.92±0.02 ^b	1.09±0.07 ^b	1.08±0.07 ^b	1.05±0.07 ^b
Spleen	0.06±0.01 ^b	0.09±0.00 ^a	0.08±0.01 ^a	0.08±0.00 ^a	0.09±0.01 ^a	0.07±0.01 ^a	0.08±0.01 ^a
Epididymal fat	0.52±0.03 ^c	2.99±0.06 ^a	2.13±0.23 ^b	1.95±0.26 ^b	2.28±0.12 ^b	1.92±0.13 ^b	1.89±0.17 ^b
Visceral fat	0.44±0.02 ^c	2.88±0.21 ^a	1.38±0.18 ^b	1.22±0.18 ^b	1.63±0.14 ^b	1.33±0.15 ^b	1.25±0.13 ^b

Values are given as mean ± standard deviation (n = 8). Different superscripts in the same row are significantly different ($p < 0.05$, ANOVA, Tukey-HSD).

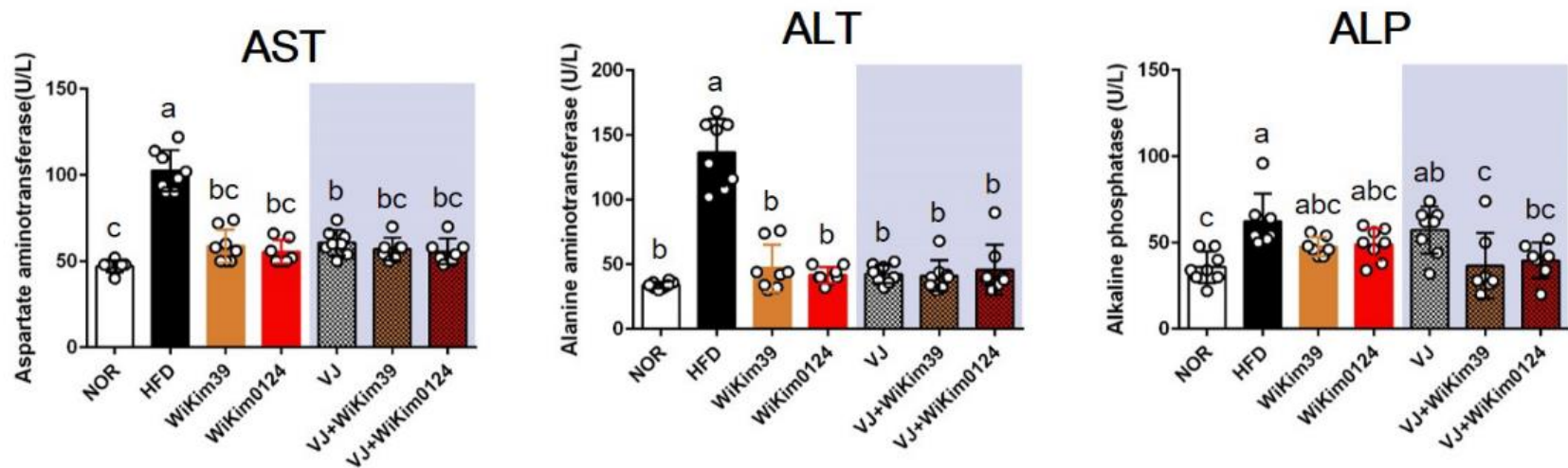


Fig. 4.8. Effects of WiKim39 and WiKim0124 fermented vegetable juice administration in high-fat diet-induced obese mice. Plasma AST (aspartate aminotransferase), plasma ALT alanine aminotransferase), plasma ALP (alkaline phosphatase). Different letters denote significant differences ($p < 0.05$, ANOVA, Tukey's HSD). Values are expressed as the mean \pm SD.

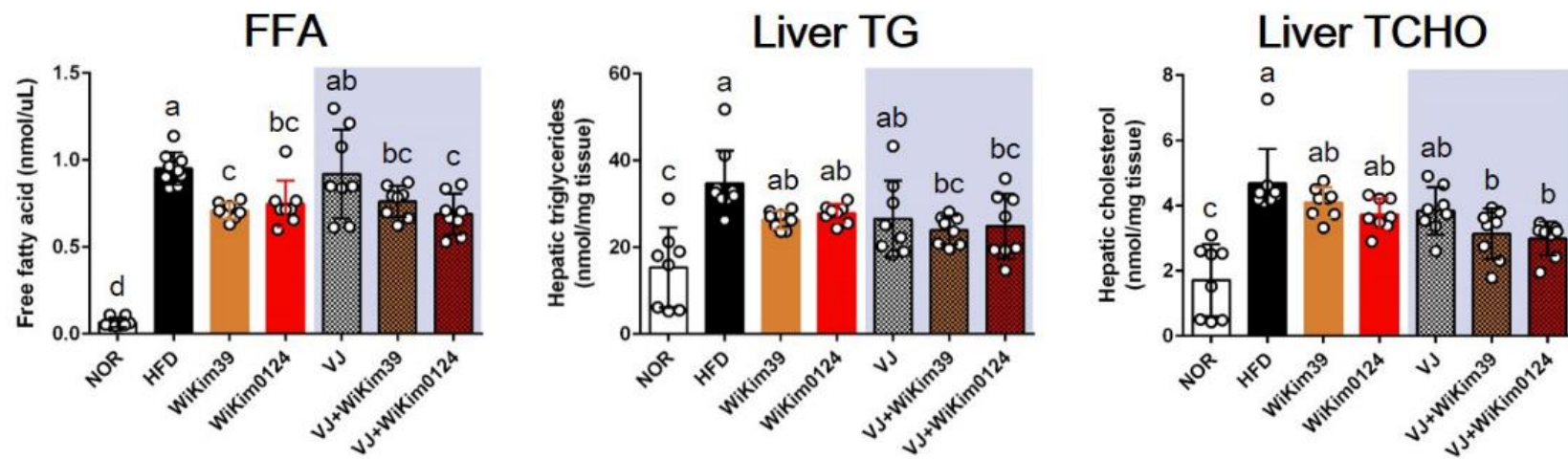


Fig. 4.9. Effects of WiKim39 and WiKim0124 fermented vegetable juice administration in high-fat diet-induced obese mice. plasma FFA (free fatty acids), hepatic triglycerides (TG), hepatic total cholesterol (TCHO) were measured. Different letters denote significant differences ($p < 0.05$, ANOVA, Tukey's HSD). Values are expressed as the mean \pm SD.

4.3.3. Expression of adipogenic transcription factors and related genes

To elucidate the mechanism of the antiobesity effect of LAB and LAB fermented VJ in obesity induced in mice by a high-fat diet, the expression of transcription factors and the related genes involved in adipogenesis inhibition in epididymal white adipose tissue (Fig. 4.10) was measured using qRT-PCR. As expected, the mRNA expression of sterol regulatory element binding protein-1c (*SREBP-1c*), CCAAT/enhancer-binding protein- α (*C/EBP- α*), proliferator-activated receptor γ (*PPAR- γ*), fatty-acid-binding protein 4 (*FABP4*), and fatty acid synthetase (*FAS*) were significantly increased in HFD compared to NOR. However, dietary administration of LAB and LAB-fermented VJ significantly reduced the expression of adipogenesis regulators. Most of these genes were downregulated in the LAB-administered group compared to the fermented VJ groups. Additionally, the activities of the key lipolytic enzymes, i.e., adipose triglyceride lipase (*ATGL*) and hormone-sensitive lipase (*HSL*), were increased in all the treatments except VJ. VJ did not show a significant difference compared to HFD. LAB-fermented VJ showed an increased level of *ATGL*. VJ+WiKim39 and VJ+WiKim0124 showed efficacy like LAB alone treatment. Therefore, the results indicate that fermented VJ reduced adipogenesis by regulating adipogenic genes, regulators, and lipolytic enzymes, though only VJ treatment was not as effective as fermented VJ treatment.

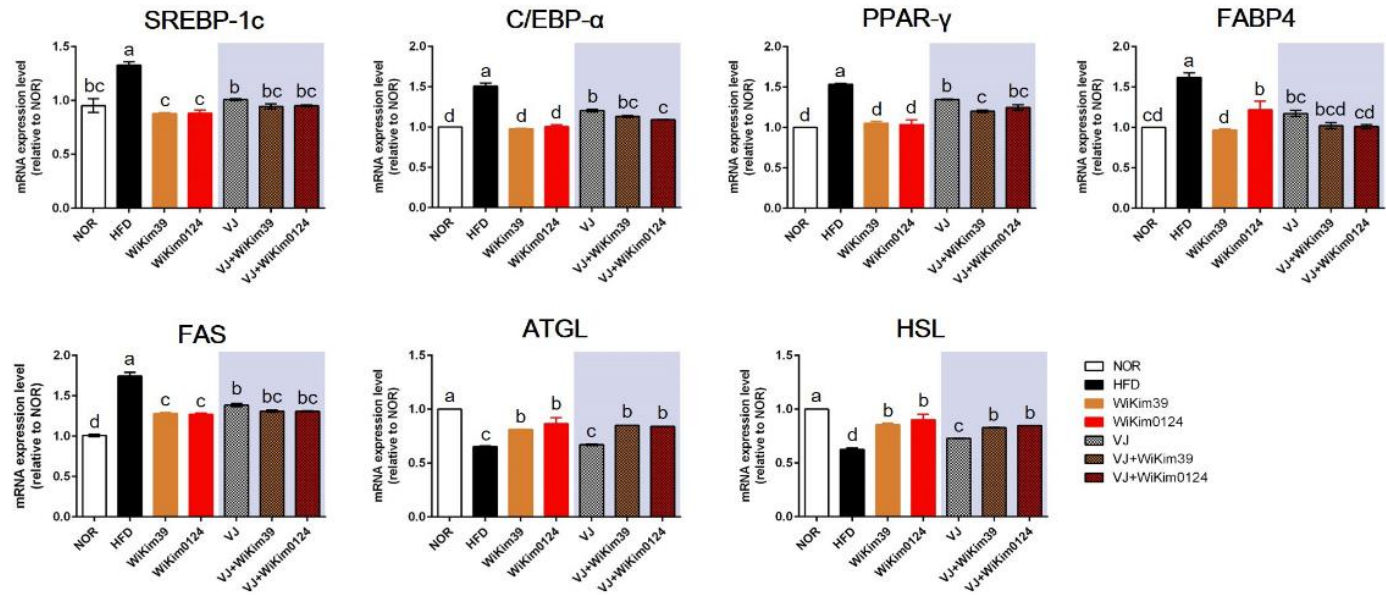


Fig. 4.10. Effects of WiKim39 and WiKim0124 fermented vegetable juices on the expression of genes related to lipid metabolism in the epididymal adipose tissues of high-fat diet-induced obese mice. The mRNA expression of *SREBP-1c*, *C/EBP-α*, *PPAR-γ*, *FABP4*, *FAS*, *ATGL*, and *HSL* measured using quantitative real-time polymerase chain reaction. Different letters denote significant differences ($p < 0.05$, ANOVA, Tukey's HSD). Values were expressed as the mean \pm SD ($n = 3$).

4.3.4. Inhibition of intracellular lipid accumulation of LAB fermented VJ metabolites in hMSCs

To explore functional bioactive ingredients in fermented VJs, we examined the effects of LA, ILA, and PLA on adipogenic differentiated hMSCs. No significant cytotoxicity was observed until 20 mM concentrations of the three compounds. Matured hMSCs were treated with varying concentrations of LA, ILA, and PLA. The lipid droplet accumulation reduced significantly within the cells of all the treatment groups compared to the untreated and differentiated cells. The inhibitory effect was concentration-dependent (Fig. 4.11). A noticeably higher effect was observed in ILA compared to PLA or LA.

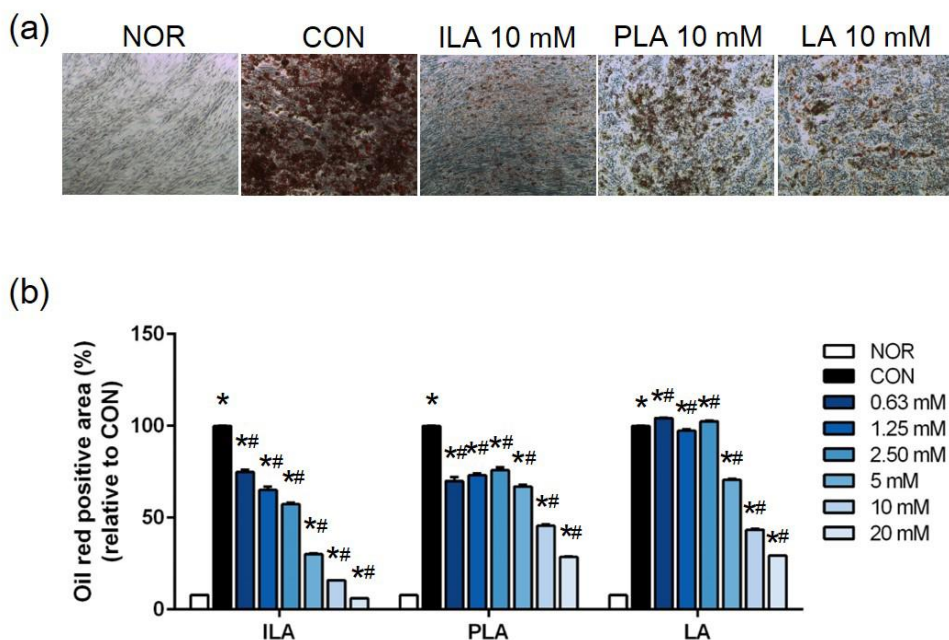


Fig. 4.11. Effects of potential anti-adipogenic agents present in vegetable juice fermented products on human mesenchymal stem cells. (a) Microscopy after Oil Red O staining and (b) quantified by absorbance at 517 nm. NOR, undifferentiated hMSCs; CON, adipogenic differentiated; 0.63 mM–20 mM, differentiated adipocytes with each single compound according to concentration (ILA: indole-3-lactic acid, PLA: phenyllactic acid, LA: leucic acid). * $p < 0.05$ indicates statistically significant differences between NOR and experimental groups, and # $p < 0.05$ indicates statistically significant differences between CON and experimental groups. Values are expressed as the mean \pm SD (n = 3).

4.4. Discussion

Adipokines are grouped into a diverse group of proteins that play roles in blood pressure, lipid metabolism, appetite and energy balance, insulin sensitivity, immunity, and inflammation (Aguilar-Valles, Inoue, Rummel, & Luheshi, 2015). Adipokines released from adipose tissue induce systemic inflammation and this pathway can be a therapeutic target for metabolic diseases (Rocha & Libby, 2009). Our previous study revealed that LAB fermented VJ has anti-inflammatory potential (Yun et al., 2022). Consistent with those results, in the current study, treatment of VJ fortified with functional LAB derived from kimchi alleviated lipid accumulation in adipocyte-differentiated hMSCs through cytokine modulation. Antibody array results under LAB lysate and LAB fermented VJ treatment indicated that the majority of DEPs were associated with immunomodulatory response categories. With MF and BP functional groups, GO enrichment analysis further showed that DEPs mainly participated in signaling receptor regulation activity, receptor ligand activity, and G protein-coupled receptor binding in response to negative regulation of DNA damage stimulus and negative regulation of the leukocyte apoptotic process. G protein-coupled receptors induce activation of the mitogen-activated protein kinases (MAPKs) (Lopez-Illasaca, Crespo, Pellici, Gutkind, & Wetzker, 1997).

MAPKs such as extracellular signal-regulated kinase (ERK), p38, and Jun N-terminal kinase (JNK) are widely-recognized to regulate embryogenesis, cell differentiation, cell proliferation, and cell death. They are also known as enhancers of adipogenesis and lipid accumulation (Seo, Lee, Hwang, Kim, & Lee, 2015). This linkage of G protein-coupled receptors with MAPKs may have a synergistic effect on the regulated production of proinflammatory adipokines.

Considering these results, LAB and VJ fortified with LAB were further tested in HFD-induced obese mice. The daily dosage was determined as 10^9 CFU per day of LAB or 250 mg kg^{-1} body weight of VJ samples. LAB and LAB fermented VJs treatments substantially reduced body weight gain, decreased body fat mass, suppressed the plasma lipid concentration index through down-regulation of *SREBP-1c*, *C/EBP α* , *PPAR γ* , *FABP4*, and *FAS* adipogenic genes and up-regulation of *ATGL*, and *HSL* lipolytic genes. Free fatty acids were subsequently released and adipocyte size decreased. Probiotics and prebiotics are microbiome managing materials for improving host health. They can also impact health-promoting properties of foods through the production of functionally bioactive substances during fermentation (Sanders, Merenstein, Reid, Gibson, & Rastall, 2019). In this study, we demonstrated the effect of LAB in mice and cells delivered alone or in a food matrix under different treatment conditions. Inflammation control by surface proteins or cell wall components (exopolysaccharide or lipopolysaccharides) has been previously reported when bacteria were

administered into cells or mice (Chipashvili et al., 2021; Hamidi et al., 2022). However, the effects of food matrix are not discussed in-depth in food microbiology and nutritional and physiological science. LAB with appropriate food matrices can improve bacterial cell growth and extend potency. The development of symbiotic combinations is another approach to stimulate LAB growth and efficacy (Pimentel, da Costa, Barão, Rosset, & Magnani, 2021). The bioavailability of phenolic compounds can be enhanced by the metabolism of LAB in a food matrix, thus, increasing their functionality (Morais, Borges, dos Santos Lima, Martín-Belloso, & Magnani, 2019). In a previous study, we compared the VJ+WiKim39 and VJ+WiKim0124 metabolites to non-fermented VJ and profiled them using ultra-performance liquid chromatography quadrupole time-of-flight tandem mass spectrometry (UPLC-QTOF-MS/MS). Some valid metabolites/molecules such as organic acids, phenols, and amino acids were identified. LA, ILA, and PLA exhibited the most significant antioxidant potential (Lee et al., 2021a). We hypothesized that these molecules present in the VJ could exert a synergistic effect on anti-obesity efficacy through functional LAB fermentation. As expected, LA, ILA, and PLA inhibited lipid accumulation in adipogenic differentiated hMSCs and showed the highest efficacy in ILA treatment. ILA is an indole derived from tryptophan metabolism in the gut microbiota (Qayed, Michonneau, Socié, & Waller, 2021). They play critical roles in innate immunity, reducing inflammation, and scavenging free radicals. Indoles can also suppress insulin secretion and

appetite, and slow gastric emptying (Geng, Ni, Sun, Li, & Feng, 2022). LA (2-hydroxyisocaproic acid) and PLA are derived from L-leucine and L-phenylalanine, respectively. They are LAB-produced metabolites and are gaining interest because of their antimicrobial potential and other pharmacological properties (Rajanikar et al., 2021). Unlike other natural organic acids, PLA does not have a pronounced effect on food taste. Therefore, PLA is a promising natural additive to extend the shelf life of food (Xu, Sun, Si, & Guo, 2021). Immunomodulatory effects of PLA and LA have been implicated in the consumption of fermented foods (Maha et al., 2019; Peters et al., 2019). The contribution of immune cells to metabolic diseases has shifted focus to adipose tissue-associated cells. However, these potential causes affect other metabolic regulatory tissues and promote inflammation and obesity comorbidities (Liu & Nikolajczyk, 2019). VJ fermented with WiKim39 and WiKim0124 suppressed lipid accumulation and improved an anti-obesogenic effect. These results suggest that LAB-fermented VJ metabolites can be a source of functional bioactive substances. Since the functionality of fermented food is determined by the sum of all effective metabolites, the use of a starter can provide the functionality to the fermented foods (Lee, Jeon, Yoo, & Kim, 2021b). Future studies should focus on identifying these substances and mechanisms associated with obesity and should consider obesity-related inflammation.

4.5. Conclusions

VJ fermented with WiKim39 and WiKim0124 effectively ameliorated fat accumulation *in vitro* and *in vivo*. We propose ILA, PLA, and LA as potential bioactive compounds that exhibit inhibitory effects on lipid accumulation *in vitro*. These findings demonstrate that *C. allii* WiKim39 and *L. lactis* WiKim0124 isolated from kimchi can be used as functional starters for plant-based foods and lay the foundation for functional probiotic beverages to prevent obesity progression.

4.6. References

- Aguilar-Valles, A., Inoue, W., Rummel, C., & Luheshi, G. N. (2015). Obesity, adipokines and neuroinflammation. *Neuropharmacology*, *96*, 124-134.
- Al Kassaa, I., Hamze, M., Hober, D., Chihib, N.-E., & Drider, D. (2014). Identification of vaginal lactobacilli with potential probiotic properties isolated from women in North Lebanon. *Microbial ecology*, *67* (3), 722-734.
- Bradford, M. M. (1976). A rapid and sensitive method for the quantitation of microgram quantities of protein utilizing the principle of protein-dye binding. *Analytical biochemistry*, *72* (1-2), 248-254.
- Chipashvili, O., Utter, D. R., Bedree, J. K., Ma, Y., Schulte, F., Mascarin, G., Alayyoubi, Y., Chouhan, D., Hardt, M., & Bidlack, F. (2021). Episymbiotic Saccharibacteria suppresses gingival inflammation and bone loss in mice through host bacterial modulation. *Cell Host & Microbe*, *29* (11), 1649-1662. e1647.
- Choi, I. S., Ko, S. H., Lee, M. E., Kim, H. M., Yang, J. E., Jeong, S. G., Lee, K. H., Chang, J. Y., Kim, J. C., & Park, H. W. (2021). Production, Characterization, and Antioxidant Activities of an Exopolysaccharide Extracted from Spent Media Wastewater after

Leuconostoc mesenteroides WiKim32 Fermentation. *ACS Omega*, 6 (12), 8171-8178.

Cuevas-González, P., Liceaga, A., & Aguilar-Toalá, J. (2020). Postbiotics and paraprobiotics: From concepts to applications. *Food Research International*, 136, 109502.

Dahiya, D. K., Puniya, M., Shandilya, U. K., Dhewa, T., Kumar, N., Kumar, S., Puniya, A. K., & Shukla, P. (2017). Gut microbiota modulation and its relationship with obesity using prebiotic fibers and probiotics: a review. *Frontiers in microbiology*, 8, 563.

Deng, W., Chen, H., Su, H., Wu, X., Xie, Z., Wu, Y., & Shen, H. (2020). IL6 receptor facilitates adipogenesis differentiation of human mesenchymal stem cells through activating P38 pathway. *International journal of stem cells*, 13 (1), 142.

Ejtahed, H.-S., Angoorani, P., Soroush, A.-R., Atlasi, R., Hasani-Ranjbar, S., Mortazavian, A. M., & Larijani, B. (2019). Probiotics supplementation for the obesity management; A systematic review of animal studies and clinical trials. *Journal of Functional Foods*, 52, 228-242.

Fabersani, E., Abeijon-Mukdsi, M. C., Ross, R., Medina, R., Gonzalez, S., & Gauffin-Cano, P. (2017). Specific Strains of Lactic Acid Bacteria Differentially Modulate the Profile of Adipokines In Vitro. *Front Immunol*, 8, 266.

Fabersani, E., Russo, M., Marquez, A., Abeijón-Mukdsi, C., Medina, R., &

- Gauffin-Cano, P. (2019). Modulation of intestinal microbiota and immunometabolic parameters by caloric restriction and lactic acid bacteria. *Food Research International*, *124*, 188-199.
- Geng, J., Ni, Q., Sun, W., Li, L., & Feng, X. (2022). The links between gut microbiota and obesity and obesity related diseases. *Biomedicine & Pharmacotherapy*, *147*, 112678.
- Gil-Rodríguez, A. M., & Beresford, T. P. (2019). Lipase inhibitory activity of skim milk fermented with different strains of lactic acid bacteria. *Journal of Functional Foods*, *60*, 103413.
- Hamidi, M., Okoro, O. V., Ianiri, G., Jafari, H., Rashidi, K., Ghasemi, S., Castoria, R., Palmieri, D., Delattre, C., & Pierre, G. (2022). Exopolysaccharide from the yeast *Papiliotrema terrestris* PT22AV for skin wound healing. *Journal of Advanced Research*.
- Ho, J. N., Jang, J. Y., Yoon, H. G., Kim, Y., Kim, S., Jun, W., & Lee, J. (2012). Anti-obesity effect of a standardised ethanol extract from *Curcuma longa* L. fermented with *Aspergillus oryzae* in ob/ob mice and primary mouse adipocytes. *Journal of the Science of Food and Agriculture*, *92* (9), 1833-1840.
- Kamiloglu, S., Sari, G., Ozdal, T., & Capanoglu, E. (2020). Guidelines for cell viability assays. *Food Frontiers*, *1* (3), 332-349.
- Kim, E., Lee, H. G., Han, S., Seo, K. H., & Kim, H. (2021). Effect of Surface Layer Proteins Derived from Paraprobiotic Kefir Lactic Acid Bacteria on Inflammation and High-Fat Diet-Induced Obesity. *J*

Agric Food Chem, 69 (50), 15157-15164.

- Lee, J., Jang, J. Y., Kwon, M. S., Lim, S. K., Kim, N., Lee, J., Park, H. K., Yun, M., Shin, M. Y., & Jo, H. E. (2018). Mixture of two *Lactobacillus plantarum* strains modulates the gut microbiota structure and regulatory T cell response in diet-induced obese mice. *Molecular nutrition & food research*, 62 (24), 1800329.
- Lee, M.-E., Jang, J.-Y., Lee, J.-H., Park, H.-W., Choi, H.-J., & Kim, T.-W. (2015). Starter cultures for kimchi fermentation. *Journal of Microbiology and Biotechnology*, 25 (5), 559-568.
- Lee, M., Song, J. H., Choi, E. J., Yun, Y.-R., Lee, K. W., & Chang, J. Y. (2021a). UPLC-QTOF-MS/MS and GC-MS Characterization of Phytochemicals in Vegetable Juice Fermented Using Lactic Acid Bacteria from Kimchi and Their Antioxidant Potential. *Antioxidants*, 10 (11), 1761.
- Lee, M., Song, J. H., Shim, W. B., & Chang, J. Y. (2020). DNAzyme-based quantitative loop-mediated isothermal amplification for strain-specific detection of starter kimchi fermented with *Leuconostoc mesenteroides* WiKim32. *Food Chem*, 333, 127343.
- Lee, S.-J., Jeon, H.-S., Yoo, J.-Y., & Kim, J.-H. (2021b). Some Important Metabolites Produced by Lactic Acid Bacteria Originated from Kimchi. *Foods*, 10 (9), 2148.
- Li, L., Zhang, Y., Speakman, J. R., Hu, S., Song, Y., & Qin, S. (2021). The gut microbiota and its products: Establishing causal relationships

- with obesity related outcomes. *Obesity Reviews*, 22 (12), e13341.
- Li, Q., Liu, Z., Huang, J., Luo, G., Liang, Q., Wang, D., Ye, X., Wu, C., Wang, L., & Hu, J. (2013). Anti-obesity and hypolipidemic effects of Fuzhuan brick tea water extract in high-fat diet-induced obese rats. *Journal of the Science of Food and Agriculture*, 93 (6), 1310-1316.
- Liu, R., & Nikolajczyk, B. S. (2019). Tissue immune cells fuel obesity-associated inflammation in adipose tissue and beyond. *Frontiers in immunology*, 10, 1587.
- Lopez-Illasaca, M., Crespo, P., Pellici, P. G., Gutkind, J. S., & Wetzker, R. (1997). Linkage of G protein-coupled receptors to the MAPK signaling pathway through PI 3-kinase γ . *Science*, 275 (5298), 394-397.
- Maere, S., Heymans, K., & Kuiper, M. (2005). BiNGO: a Cytoscape plugin to assess overrepresentation of gene ontology categories in biological networks. *Bioinformatics*, 21 (16), 3448-3449.
- Maha, I. F., Xie, X., Zhou, S., Yu, Y., Liu, X., Zahid, A., Lei, Y., Ma, R., Yin, F., & Qian, D. (2019). Skin metabolome reveals immune responses in yellow drum *Nibea albiflora* to *Cryptocaryon irritans* infection. *Fish & shellfish immunology*, 94, 661-674.
- Morais, S. G. G., Borges, G. d. S. C., dos Santos Lima, M., Martín-Belloso, O., & Magnani, M. (2019). Effects of probiotics on the content and bioaccessibility of phenolic compounds in red pitaya pulp. *Food Research International*, 126, 108681.

- Peters, A., Krumbholz, P., Jäger, E., Heintz-Buschart, A., Çakir, M. V., Rothmund, S., Gaudl, A., Ceglarek, U., Schöneberg, T., & Stäubert, C. (2019). Metabolites of lactic acid bacteria present in fermented foods are highly potent agonists of human hydroxycarboxylic acid receptor 3. *PLoS genetics*, *15* (5), e1008145.
- Pimentel, T. C., da Costa, W. K. A., Barão, C. E., Rosset, M., & Magnani, M. (2021). Vegan probiotic products: A modern tendency or the newest challenge in functional foods. *Food Research International*, *140*, 110033.
- Qayed, M., Michonneau, D., Socié, G., & Waller, E. K. (2021). Indole derivatives, microbiome and graft versus host disease. *Current Opinion in Immunology*, *70*, 40-47.
- Rajanikar, R., Nataraj, B. H., Naithani, H., Ali, S. A., Panjagari, N. R., & Behare, P. V. (2021). Phenyllactic acid: a green compound for food biopreservation. *Food Control*, *128*, 108184.
- Rocha, V. Z., & Libby, P. (2009). Obesity, inflammation, and atherosclerosis. *Nature Reviews Cardiology*, *6* (6), 399-409.
- Sanders, M. E., Merenstein, D. J., Reid, G., Gibson, G. R., & Rastall, R. A. (2019). Probiotics and prebiotics in intestinal health and disease: from biology to the clinic. *Nature reviews Gastroenterology & hepatology*, *16* (10), 605-616.
- Seo, M.-J., Lee, Y.-J., Hwang, J.-H., Kim, K.-J., & Lee, B.-Y. (2015). The inhibitory effects of quercetin on obesity and obesity-induced

inflammation by regulation of MAPK signaling. *The Journal of Nutritional Biochemistry*, 26 (11), 1308-1316.

Tang, C., Kong, L., Shan, M., Lu, Z., & Lu, Y. (2021). Protective and ameliorating effects of probiotics against diet-induced obesity: A review. *Food Research International*, 147, 110490.

Xie, W., Gu, D., Li, J., Cui, K., & Zhang, Y. (2011). Effects and action mechanisms of berberine and *Rhizoma coptidis* on gut microbes and obesity in high-fat diet-fed C57BL/6J mice. *PLoS one*, 6 (9), e24520.

Xu, J.-J., Sun, J.-Z., Si, K.-L., & Guo, C.-F. (2021). 3-Phenyllactic acid production by *Lactobacillus crustorum* strains isolated from naturally fermented vegetables. *LWT*, 149, 111780.

Yun, Y.-R., Lee, M., Song, J. H., Choi, E. J., & Chang, J. Y. (2022). Immunomodulatory effects of *Companilactobacillus allii* WiKim39 and *Lactococcus lactis* WiKim0124 isolated from kimchi on lipopolysaccharide-induced RAW264. 7 cells and dextran sulfate sodium-induced colitis in mice. *Journal of Functional Foods*, 90, 104969.

Zhu, K., Tan, F., Mu, J., Yi, R., Zhou, X., & Zhao, X. (2019). Anti-obesity effects of *Lactobacillus fermentum* CQPC05 isolated from Sichuan pickle in high-fat diet-induced obese mice through PPAR- α signaling pathway. *Microorganisms*, 7 (7), 194.

This chapter comprises articles, published in *Journal of microbiology and biotechnology* with minor modification as a partial fulfillment of Moeun

Lee's Ph.D. program

Chapter 5.

**Kimchi lactic acid bacteria starter culture: Impact on
fermented malt beverage volatile profile, sensory
analysis, and physicochemical traits**

Abstract

Starter cultures used during the fermentation of malt wort can increase the sensory characteristics of the resulting beverages. This study aimed to explore the aroma composition and flavor recognition of malt wort beverages fermented with lactic acid bacteria (*Levilactobacillus brevis* WiKim0194) isolated from kimchi, using metabolomic profiling and electronic tongue and nose technologies. Four sugars and five organic acids were detected using high-performance liquid chromatography, with maltose and lactic acid present in the highest amounts. Additionally, e-tongue measurements showed a significant increase in the sourness (AHS), sweetness (ANS), and umami (NMS) sensors, whereas bitterness (SCS) significantly decreased. Furthermore, 20 key aroma compounds were identified using gas chromatography-mass spectrometry and 15 key aroma flavors were detected using an electronic nose. Vanillin, citronellol, and β -damascenone exhibited significant differences in the flavor profile of the beverage fermented by WiKim0194, which correlated with floral, fruity, and sweet notes. Therefore, we suggest that an appropriate starter culture can improve sensory characteristics and predict flavor development in malt wort beverages.

Keywords: *Levilactobacillus brevis* WiKim0194, kimchi starter, fermented malt beverage, sensory evaluation, electronic tongue, electronic nose

5.1. Introduction

Cereal-based beverages crafted through lactic acid fermentation are attracting considerable attention due to their nutritional content and functional attributes, offering qualities such as low cholesterol, non-alcoholic, gluten-free, and functional properties (Yu & Bogue, 2013). These beverages hold potential as substrates for the development of synbiotic drinks, combining probiotics and prebiotics to synergistically promote gut health. Moreover, they function as readily accessible and cost-effective sources of energy, containing abundant prebiotic ingredients like dietary fibers and resistant starch, which efficiently facilitate microbial growth in the presence of moisture and hydrolytic enzymes (Kumar, Kaur, & Tomer, 2020). However, as consumers place greater emphasis on flavor enhancement, products must prioritize appealing taste and aroma, along with nutritional quality, to be selected in the market (Pswarayi & Gänzle, 2022).

Wheat and barley are the commonly used grains in the brewery industry. Wheat and barely contain many nutrients, including proteins and bioactive compounds. Following malting and mashing, which are necessary for wort production, fermentation by lactic acid bacteria (LAB) enhances nutrient availability and contributes to the development of attractive flavors (Hassani,

Procopio, & Becker, 2016). Prior to yeast fermentation, malting and lactic acid fermentation serve two purposes: enzymatic hydrolysis of the grain structure and enhanced flavor formation, potentially impacting the final beverage flavor (Arora, Jood, & Khetarpaul, 2010). In 2022, South Korea was the 17th largest beer consumer, and accounted for USD 3,716 million in sales (Statista, 2023). In recent years, consumers are turning to craft beer over mass-produced brands. Craft beer is typically produced by small, independent breweries that use traditional brewing methods and focus on creating beers with unique flavor and quality (Baiano, 2021). Hence, optimal malting and mashing conditions are necessary for the production of lactic acid-based beverages using various cereals.

LAB are prevalent in nature and widely employed as food-grade microorganisms in diverse fermentation industries. There is growing interest in the industrial applications of LAB, particularly their application as starter cultures; however, the quality of fermented products depends on the specific LAB species used in the fermentation process (Choi et al., 2020). The flavor profiles are affected by different LAB fermentation species. For example, *Lactobacillus* and *Pediococcus* are commonly associated with lactic acid production in sour beer (Bokulich & Bamforth, 2013). LAB are considered important for active metabolites beyond lactic acid. These metabolites include various organic acids such as acetic and formic acid, esters, aldehydes, and ketones, along with phenolic and non-phenolic compounds (Dysvik et al., 2019). In addition, LAB species *Lactobacillus brevis* (*L.*

brevis), *Lactobacillus Plantanum* (*L. plantanum*), and *Lactobacillus curvatus* (*L. curvatus*), that are commonly found in beer, have been identified in beer (Priest, 2011). Aroma composition and sensory acceptance have been reported for strains currently used in breweries (e.g., *L. amylolyticus*, *L. plantarum*) or in malt wort (e.g., *L. brevis*) (Dongmo, Sacher, Kollmannsberger, & Becker, 2017). Studies on LAB strains from various origins are necessary to enhance flavor and improve the characteristics of malt-based beverage production.

Kimchi, a traditional fermented food in Korea, is fermented using various LAB types that produce a range of metabolites, including lactic acid and acetic acid (imparting a sour taste), mannitol (providing cool sweetness), and acetoin (contributing to a unique fermentation aroma) (Lee, Song, Jung, Lee, & Chang, 2017). The optimal fermentation by specific LAB starters results in the formation of a diverse array of metabolites, contributing to the complex sensory properties of final products, including a savory taste (Lee, Song, Lee, Jung, & Chang, 2018). In this study, we aimed to characterize the growth properties of various LAB species isolated from kimchi and applied them to wort fermentation. Our focus was on characterizing their growth properties and evaluating the presence of metabolites that affect flavor and sensory properties.

5.2. Materials and Methods

5.2.1. Wort preparation and starter culture

A wort with a concentration of 12% was made by mixing 80% standardized barley malt with distilled water. Next, the mixture was autoclaved at 110°C for 10 minutes. After cooling, the debris was removed. Unhopped malt, employed as a base in the brewing experiment, was used to propagate and prepare the LAB starter culture, as well as for the microbial growth experiment. Eight previously identified and selected kimchi LAB strains were used in this study (Table 5.1). The isolated strains were cultured in de Man, Rogosa, and Sharpe (MRS) medium (BD Difco, Rockville, MD, USA) at 30 °C for 24 h. The LAB strains were activated in MRS broth for 24 hours and pre-cultured in wort for an additional 24 hours at 30°C prior to the experiment. Subsequently, the cells were pelleted at 6000 ×g, and 4°C for 10 minutes, and washed twice with sterile PBS. With each LAB strain, fermentation was conducted at laboratory scale under static conditions for 72 h at an inoculation rate of 1% (v/v). The fermented beverages were immediately stored at -20°C for sensory evaluation and at -80°C for aroma compound analysis.

Table 5.1. Lactic acid bacteria strains used in this study.

Strain	Gene bank ac no.	Code
<i>Lactococcus lactis</i> WiKim0124	MZ424472.1	WiKim0124
<i>Leuconostoc mesenteroides</i> WiKim32	NZ_CP037752.1	WiKim32
<i>Leuconostoc mesenteroides</i> WiKim33	CP021491.1	WiKim33
<i>Leuconostoc mesenteroides</i> WiKim0121	CP098784.1	WiKim0121
<i>Latilactobacillus curvatus</i> WiKim38	KU936208.1	WiKim38
<i>Latilactobacillus sakei</i> WiKim0176	-	WiKim0176
<i>Latilactobacillus sakei</i> WiKim34	OL638252.1	WiKim34
<i>Companilactobacillus allii</i> WiKim39	NR_159087.1	WiKim39
<i>Levilactobacillus brevis</i> WiKim0194	-	WiKim0194

5.2.2. Microbial growth

The growth experiments were conducted in 96-well microtiter plates, with each well containing a total volume of 200 μL . The strains were individually inoculated at approximately $6.0 \log_{10} \text{CFU mL}^{-1}$ in both MRS broth and wort, and then incubated at $30\text{ }^{\circ}\text{C}$ for 42 hours. To prevent evaporation, a sterile transparent film was used to cover the surfaces of the wells. Control samples (non-inoculated media) and each experimental trial were set up in triplicate and monitored using a microplate reader (Safire, Tecan, Maennedorf, Switzerland) to measure optical density (OD) at 600 nm every 3 hours. Prior to reading, the microtiter plate was shaken for 10 seconds.

5.2.3. Chemical analyses

pH of the LAB-fermented wort was determined using a pH meter (Orion 3-Star; Thermo Scientific, Waltham, MA, USA). Next, the samples were titrated with 0.1 N NaOH to achieve a pH of 8.3, facilitating the assessment of the titratable total acidity. Total acidity was calculated using a predefined equation (Lee, Song, Park, & Chang, 2019). Additionally, the total soluble solid content, measured as the $^{\circ}\text{Brix}$ value, was assessed for each sample using a digital refractometer (model WM-7, Atago Co., Ltd, Tokyo, Japan).

5.2.4. High-Performance Liquid Chromatography

The level of organic acids and sugars in the samples was assessed during the fermentation process using high-performance liquid chromatography (HPLC; Waters Alliance e2695; USA), as previously established protocols (Kim et al., 2022). Quantitative analysis of target compounds was performed using standard curves.

5.2.5. Electronic tongue analysis

Taste assessments of both fermented and non-fermented worts were conducted using electronic tongue analysis. This analysis employed an α -Astree II electronic tongue system (Alpha MOS, Toulouse, France), which featured a sensor array consisting of seven chemical sensors: AHS (sourness), NMS (umami), CTS (saltiness), ANS (sweetness), SCS (bitterness), and PKS, and CPS (comprehensive taste), in addition to an Ag/AgCl reference electrode. All tests were performed in triplicate.

5.2.6. Electronic nose analysis

Volatile compounds in both fermented and non-fermented wort were assessed using a rapid gas chromatography electronic nose system (Heracles II, Alpha M.O.S., Toulouse, France), as previously described (Rottiers et al., 2019), with minor adjustments. Two columns of different polarities were employed: a nonpolar MXT-5 (5% diphenyl) column and a moderately polar MXT-1701 (14% cyanopropylphenyl) column, each measuring 10 m in length and $180 \mu\text{m} \times 0.4 \mu\text{m}$. To extract volatile compounds from the sample

matrix, vials were incubated with continuous agitation (500 rpm) at 50°C for 20 minutes in a controlled thermostatic agitator. After incubation, 5 mL of the headspace was extracted using a syringe at 60°C and introduced into the GC system at 200 °C for 45 seconds at a flow rate of 125 µL/s, with hydrogen N7.0 as the carrier gas. Flame ionization detectors (FIDs) were maintained at a temperature of 260°C. Each test was repeated five times.

5.2.7. Statistical analysis

Principal component analysis (PCA) was conducted using the "prcomp" function within the "ggfortify" package of R software (v3.3.2; available at <https://www.r-project.org/>). Statistical analysis involved using a Student's t-test (utilized in PRISM) to compare groups. Results with *p*-values below 0.05 were deemed statistically significant.

5.3. Results and discussion

5.3.1. Strain selection

Growth kinetics, acidification rate, sugar utilization, and acid production were analyzed to determine the most suitable bacterial starters. Out of the eight isolates, WiKim0176 and WiKim0194 showed the highest optical density (OD) throughout the entire incubation period in MRS broth. These strains also exhibited the most rapid growth in malt wort at the end of the incubation period, with WiKim0194 reaching its maximum OD (Fig. 5.1A). In contrast, the remaining isolates demonstrated very weak growth compared to MRS broth. The pH of each culture was measured every 24 hours. As a general trend, a fast drop was observed within the first 24 hours of fermentation, followed by a mild decline thereafter. Similar pH values were observed until 72 h with the exception of *Leuconostoc* spp.. However, the highest acidification rate was observed with the WiKim0194 strain, throughout the malt wort fermentation process. Concurrently, there was a noticeable reduction in the sugar content of the total soluble solids (Fig. 5.1B). The degradation of carbohydrates in malt wort during fermentation leads to the generation of organic acids that influence its flavor profile and contribute to pH fluctuations (Nsogning Dongmo, Sacher, Kollmannsberger, & Becker, 2017). Screening for strains demonstrating adequate acidification

in malt wort led to the selection of WiKim0194. Acidification of malt wort by LAB is strain-dependent. Various fermentation types and metabolic characteristics (e.g. carbohydrates and proteins) of the strains may account for these results (Genet et al., 2023).

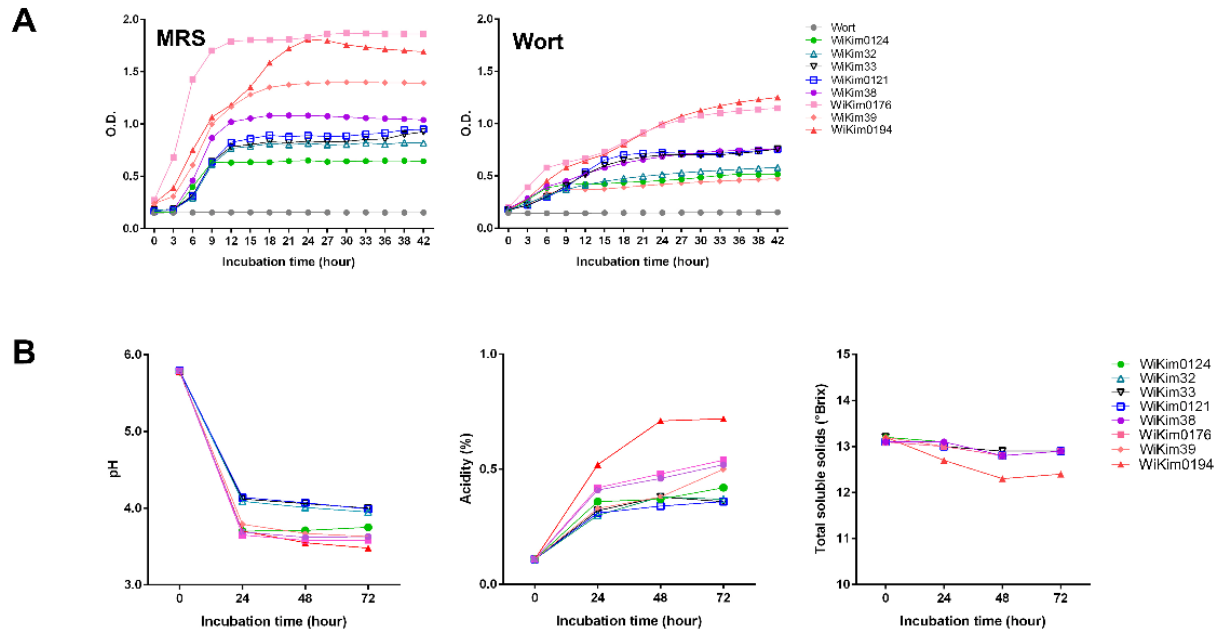


Fig. 5.1. Properties of malt wort beverages during fermentation using eight LAB strains. (A) Growth curves of the eight LAB strains were analyzed in two different media, MRS broth and wort. (B) pH profiles, titratable acidity, and total soluble solids. All experiments were conducted in triplicate.

5.3.2. Changes in sugar and organic acid concentrations throughout fermentation

Figure 5.2 illustrates the changes in the concentrations of sugars (maltose, glucose, raffinose, and mannitol) and organic acids (lactic, citric, succinic, malic, and acetic acids) during malt wort fermentation with different starter cultures. As shown in Figure 5.2A, raffinose concentrations declined steadily until 72 hours, with no significant variation between the strains. Maltose was the primary fermentable sugar in the malt wort, with other sugars making up a minor portion. During the early stages of growth, exhibited robust maltose utilization. Glucose levels declined by the 24-hour mark, indicating consumption, until it became undetectable. Subsequently, the glucose levels in sour wort increased with the use of all LAB strains, with variations among strains. Particularly the WiKim0194 strain showed highest increase. This increase in glucose production could be linked to the ability of the LAB strains to hydrolyze starch. A previous study reported the ability of LAB to break down sorghum starch, leading to an acidified end product, notably lactic acid, which lowers pH (Tano, Aka-Gbezo, Atchelouwa, & Koussémon, 2020). Their metabolic activity in metabolizing maltose into glucose enhances carbohydrate utilization capacity, influencing the microbial ecosystem (Woo et al., 2023). The production of organic acids is a result of sugar metabolism (Tkacz, Chmielewska, Turkiewicz, Nowicka, & Wojdyło, 2020). Lactic acid, citric acid, succinic acid, malic acid, and acetic acid are typical non-volatile acids

resulting from LAB-fermented foods and beverages (Yan et al., 2022). Fermentation can produce significant amounts of lactic acid, which serves as an excellent flavoring agent. Its moderate sourness lends a unique taste and has an appetite-enhancing effect (Wang et al., 2022). During sour wort production, lactic acid was the predominant compound produced (Fig. 5.2B). WiKim0194-fermented wort exhibited the highest lactic acid production (9.86 mg/mL at 72 h), followed by WiKim0176 (8.19 mg/mL at 72 h), which is consistent with the physicochemical findings. The citric, malic, and acetic acid levels increased in fermentations with all starters. Succinic acid, initially at 3.40 mg/mL, declined to undetectable level post-fermentation with WiKim0176, WiKim39, and WiKim0194. Succinic acid can serve as a metabolic intermediate utilized or produced during fermentation. While it is typically formed by yeast, its presence tends to decrease in beverages undergoing LAB fermentation (Han, Su, & Du, 2023). Acetic acid, while slightly irritating, can soften food when found in low concentrations; hence, a moderate level of acetic acid can enhance the sourness of food (Cai et al., 2021). However, in this study, acetic acid was present in fermentations with all starter strains at 72 hours, without notable differences between strains. Based on these results, the taste and aroma characteristics were further analyzed in the WiKim0194 starter, which exhibited the most rapid and effective fermentation.

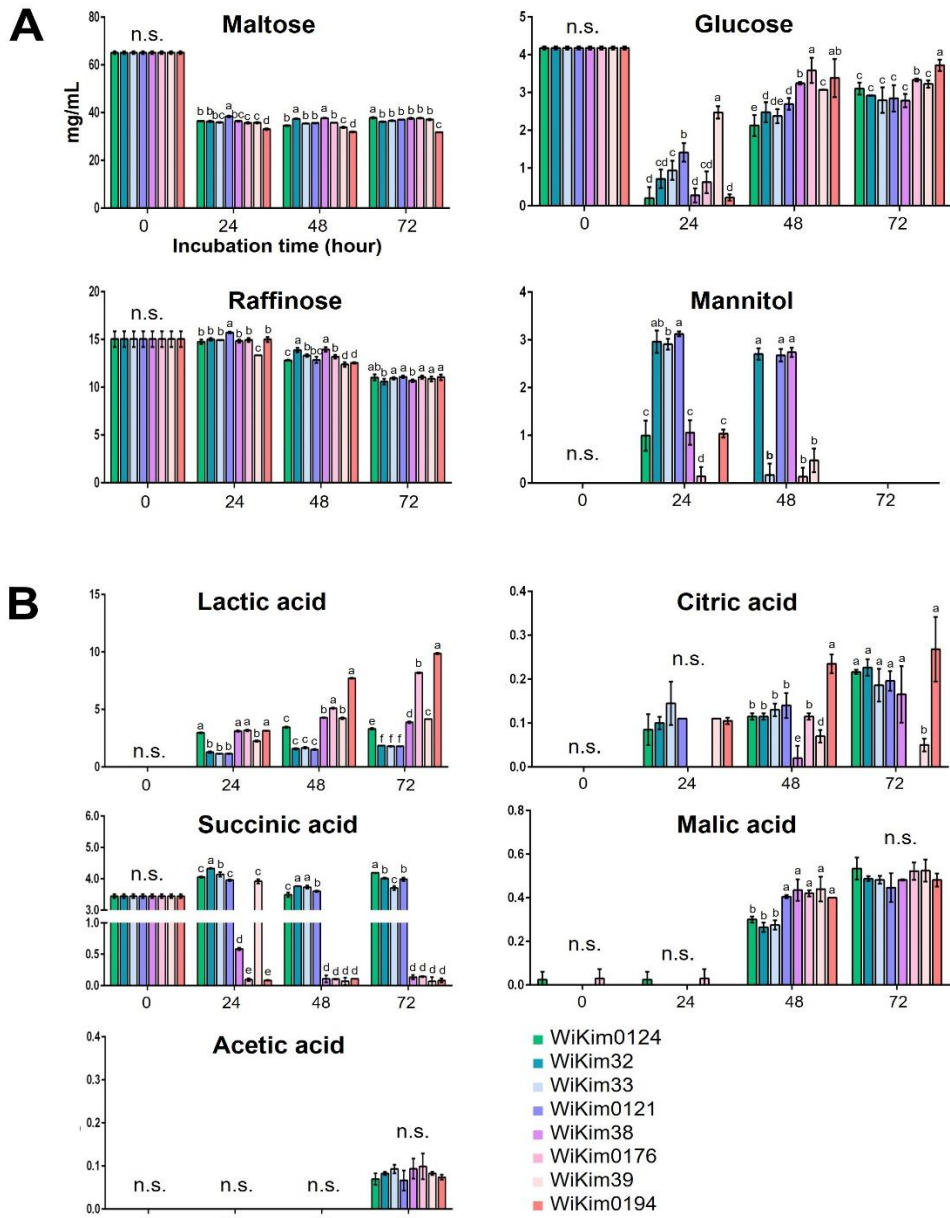


Fig. 5.2. Metabolomic profiles of malt wort beverages. (A) Sugar content. (B) Organic acid contents. All experiments were conducted in triplicate. Different letters denote significant differences ($p < 0.05$, ANOVA with Tukey-HSD post hoc test).

5.3.3. Sensory characteristics of fermented malt beverage

5.3.3.1. E-tongue analysis

The E-tongue is an electronic equipment that converts electrical signals into taste perception, facilitating an unbiased evaluation of food taste. It has high sensitivity and eliminates subjective elements inherent in conventional sensory assessments (Zhang, Hu, Wang, Kong, & Chen, 2021). Figure 5.3 illustrates the response values of the sensory characteristics of the fermented malt beverage, including sourness (AHS), bitterness (SCS), saltiness (CTS), umami (NMS), and sweetness (ANS), as obtained from E-tongue analysis. Significant changes in signal values were detected during the fermentation of malt wort, and the major sensory difference detected was an increase in sourness. This is likely due to lactic acid fermentation, in which lactic acid is the primary product of WiKim0194. The second major sensory difference was a decrease in bitterness. The significant decrease in perceived bitterness was associated with the generation of other intensely flavored compounds that enhance taste attributes. These compounds may help obscure the unsavory bitter taste, with organic acids, including lactic acid, detected at higher levels in the fermented malt wort, possibly contributing to this effect (Jaeger, Nyhan, Sahin, Zannini, & Arendt, 2024). Sweetness decreased by 0.6-fold, likely contributing to the carbohydrate metabolism of WiKim0194, which is consistent with the decrease in sugar content. Sugars and organic acids play a role in flavor formation. However, various secondary metabolites like amino acids, flavonoids, and alkaloids are also essential

contributors to flavor (Cao et al., 2022). Given that flavor perception is collectively determined by sugars, acids, and other metabolites, which can undergo changes and alterations within and among these chemicals (Zhou et al., 2023), further study is necessary to employ omics-based techniques like metabolomics. This will enable a more precise identification of flavor-related chemical components that might impact e-tongue analysis.

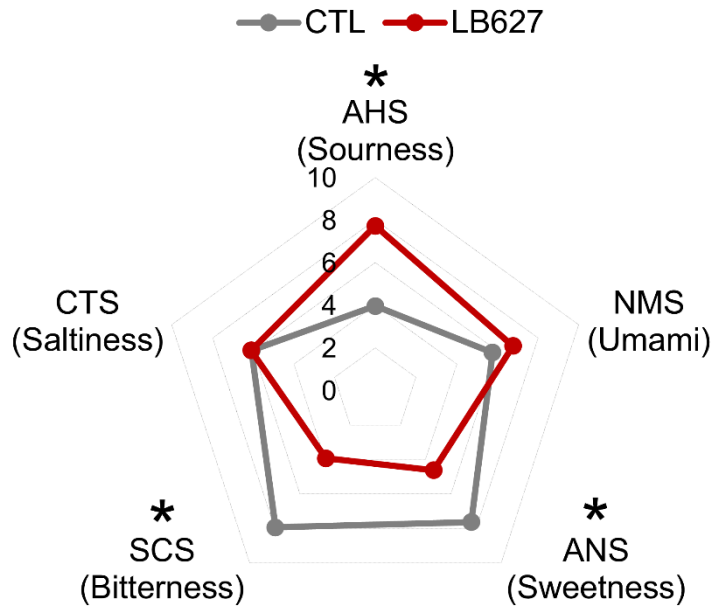


Fig. 5.3. Sensory attribute profiles of WiKim0194-fermented malt wort constructed by e-tongue. SCS, bitterness; CPS, comprehensive taste; CTS, saltiness; NMS, umami; ANS, sweetness; AHS, sourness. Statistical significance was analyzed by Student's t-test ($*p < 0.05$). All experiments were conducted in triplicate.

5.3.3.2. Key aroma compounds

The comprehensive flavor profile is influenced by the distinct contributions of each essential aromatic compound. To identify the key odor-active compounds that contribute the most to the final flavor of the fermented malt wort, GC-MS and an E-nose system were utilized. The principal component analysis (PCA) plot explains the correlation between each beverage produced by fermentation, the corresponding aroma compounds (Fig. 5.4A), and sensory descriptors (Fig. 5.4B). The plot of the GC-MS profiles revealed a 63.24% variation in the sample set, enabling the identification of two sample groups and characteristic aroma compounds. The beverages fermented with WiKim0194 were distinctly different from each other and from those fermented by CTL. Large variations were observed among the aromatic compounds in the hydrocarbon and acid categories. Meanwhile, the plot of the e-nose profiles revealed a 45.07% variation in the sample set. Beverages fermented with WiKim0194 exhibited relatively attractive flavor notes such as vanilla, fruity, floral, citrus, lemon, and sweet. However, beverages from the CTL group had relatively less attractive flavor notes, such as bitter or unclassified. This observation is consistent with the relatively high levels of key aroma compounds recorded during the GC-MS analysis (Fig. 5.4C). Acetic acid accounted for 16.54% of the variation in WiKim0194-fermented malt wort, as indicated by GC-MS results. Recognized for its sourness and vinegar-like flavors, acetic acid significantly affects the sensory characteristics. Additionally, the quality of

the 'sour odor,' distinct from acidic taste, often presents as a refreshing and well-balanced scent (Dysvik et al., 2020). The increase in fruity and floral aromas was probably due to the generation of intense aromatic compounds during lactic acid fermentation (Jaeger et al., 2024). Several unidentified compounds (decamethylcyclopentasiloxane, 3-methyl-4-oxo-pentanoic acid, and octamethyl-cyclotetrasiloxane) were detected, along with potential fruity and floral aromatic compounds, such as 3-methyl-butanal (Smit, Engels, & Smit, 2009) and 1-pentanol (Zhang et al., 2018). This is also consistent with the fact that the positive flavor attributes in WiKim0194-fermented malt wort were ethyl cyclohexanecarboxylate (Yao et al., 2023a), vanillin (Yao et al., 2021), citronellol (Elsharif & Buettner, 2017), (Z)-citral (Yao et al., 2023b), and beta-damascenone (Shen et al., 2023), with floral, fruity, and sweet flavor notes, respectively, recorded during e-nose analysis (Fig. 4.4D). The bitter odor and off-flavor of WiKim0194-fermented malt wort are thought to have decreased due to a reduction in the compounds responsible for the bitter flavor, such as chlorobenzene (Matsushita et al., 2017) and 2-acetylpyridine (Kiyomichi et al., 2023).

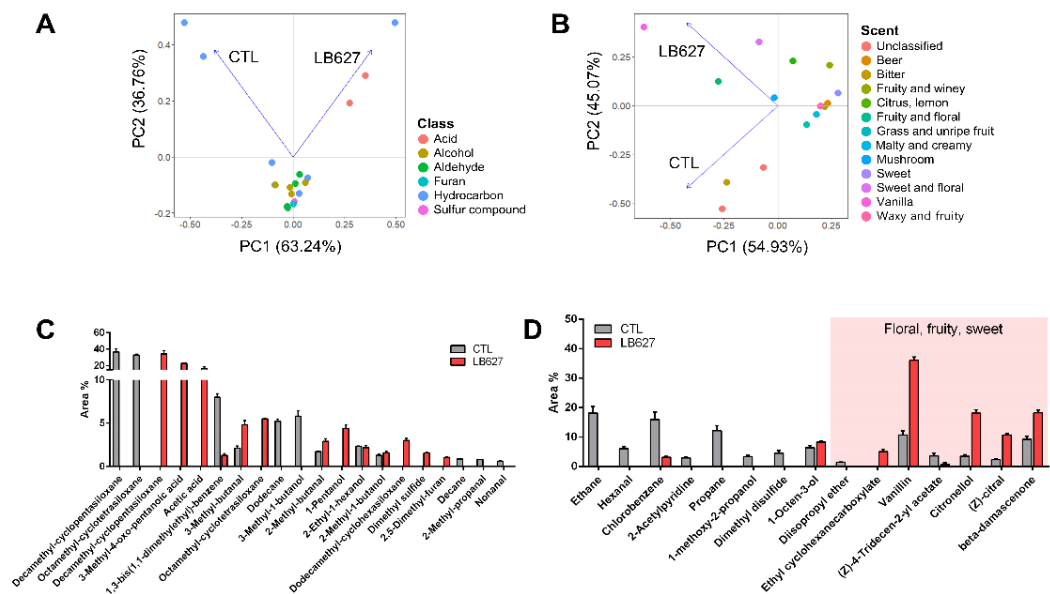


Fig. 5.4. Comparison of aroma compounds—e-nose signal values in WiKim0194-fermented malt wort. (A) The PCA scores constructed based on the composition of aroma compounds obtained from GC-MS. (B) The PCA scores constructed based on the composition of e-nose signal value profiles. (C) Key fermentative aroma compounds in fermented malt wort obtained from GC-MS. (D) Key fermentative aroma compounds based on e-nose signal values. All experiments were conducted in triplicate.

5.4. Conclusion

Our results indicate that the addition of a specific starter significantly affects the sensory properties of LAB-fermented malt wort beverages, particularly in terms of sourness, bitterness, and sweetness perception, as revealed by e-nose and e-tongue analyses. Additionally, our findings offer valuable insights into the multitude of metabolites that affect the flavor, fragrance, and overall sensory perception of these beverages. These insights enrich our understanding of LAB starters in sour beer production.

5.5. References

- Arora, S., Jood, S., & Khetarpaul, N. (2010). Effect of germination and probiotic fermentation on nutrient composition of barley based food mixtures. *Food Chemistry*, *119* (2), 779-784.
- Baiano, A. (2021). Craft beer: An overview. *Compr Rev Food Sci Food Saf*, *20* (2), 1829-1856.
- Bokulich, N. A., & Bamforth, C. W. (2013). The microbiology of malting and brewing. *Microbiology and Molecular Biology Reviews*, *77* (2), 157-172.
- Cai, W., Wang, Y., Hou, Q., Zhang, Z., Tang, F., Shan, C., Yang, X., & Guo, Z. (2021). Rice varieties affect bacterial diversity, flavor, and metabolites of zha-chili. *Food Research International*, *147*, 110556.
- Cao, K., Wang, B., Fang, W., Zhu, G., Chen, C., Wang, X., Li, Y., Wu, J., Tang, T., Fei, Z., Luo, J., & Wang, L. (2022). Combined nature and human selections reshaped peach fruit metabolome. *Genome Biol*, *23* (1), 146.
- Choi, I. S., Ko, S. H., Kim, H. M., Yang, J. E., Jeong, S.-G., Chang, J. Y., Lee, K. H., Qi, S.-B., Xin, Q., & Cui, C.-B. (2020). Coffee residue as a valorization bio-agent for shelf-life extension of lactic acid bacteria under cryopreservation. *Waste Management*, *118*, 585-590.

- Dongmo, S. N., Sacher, B., Kollmannsberger, H., & Becker, T. (2017). Key volatile aroma compounds of lactic acid fermented malt based beverages—impact of lactic acid bacteria strains. *Food Chemistry*, *229*, 565-573.
- Dysvik, A., La Rosa, S. L., Liland, K. H., Myhrer, K. S., Østlie, H. M., De Rouck, G., Rukke, E.-O., Westereng, B., & Wicklund, T. (2020). Co-fermentation involving *Saccharomyces cerevisiae* and *Lactobacillus* species tolerant to brewing-related stress factors for controlled and rapid production of sour beer. *Frontiers in microbiology*, *11*, 279.
- Dysvik, A., Liland, K. H., Myhrer, K. S., Westereng, B., Rukke, E. O., De Rouck, G., & Wicklund, T. (2019). Pre-fermentation with lactic acid bacteria in sour beer production. *Journal of the Institute of Brewing*, *125* (3), 342-356.
- Elsharif, S. A., & Buettner, A. (2017). Influence of the chemical structure on the odor characters of β -citronellol and its oxygenated derivatives. *Food Chemistry*, *232*, 704-711.
- Genet, B. M., Xiao, H., Christensen, L. F., Laforce, I. N., Mohammadifar, M. A., Bang-Berthelsen, C. H., & Hansen, E. B. (2023). Selection of proteolytic LAB starter cultures for acidification of soy based dairy alternatives. *LWT*, *184*, 115082.
- Han, Y., Su, Z., & Du, J. (2023). Effects of apple storage period on the organic acids and volatiles in apple wine. *LWT*, *173*, 114389.
- Hassani, A., Procopio, S., & Becker, T. (2016). Influence of malting and

lactic acid fermentation on functional bioactive components in cereal-based raw materials: a review paper. *International Journal of Food Science & Technology*, 51 (1), 14-22.

Jaeger, A., Nyhan, L., Sahin, A. W., Zannini, E., & Arendt, E. K. (2024). Lactic Acid Fermentation as a Valorising Agent for Brewer's Spent Yeast—Improving the Sensory Quality and Nutritional Potential. *Fermentation*, 10 (1), 54.

Kim, S., Kim, H. M., Seo, H. J., Yeon, J., Park, A. R., Yu, N. H., Jeong, S. G., Chang, J. Y., Kim, J. C., & Park, H. W. (2022). Root-Knot Nematode (*Meloidogyne incognita*) Control Using a Combination of *Lactiplantibacillus plantarum* WiKim0090 and Copper Sulfate. *J Microbiol Biotechnol*, 32 (8), 960-966.

Kiyomichi, D., Franc, C., Moulis, P., Riquier, L., Ballestra, P., Marchand, S., Tempère, S., & de Revel, G. (2023). Investigation into mousy off-flavor in wine using gas chromatography-mass spectrometry with stir bar sorptive extraction. *Food Chemistry*, 411, 135454.

Kumar, A., Kaur, A., & Tomer, V. (2020). Process optimization for the development of a synbiotic beverage based on lactic acid fermentation of nutriceals and milk-based beverage. *LWT*, 131, 109774.

Lee, M., Song, J. H., Jung, M. Y., Lee, S. H., & Chang, J. Y. (2017). Large-scale targeted metagenomics analysis of bacterial ecological changes in 88 kimchi samples during fermentation. *Food Microbiol*, 66, 173-

183.

Lee, M., Song, J. H., Lee, S. H., Jung, M. Y., & Chang, J. Y. (2018). Effect of seasonal production on bacterial communities in Korean industrial kimchi fermentation. *Food Control*, *91*, 381-389.

Lee, M., Song, J. H., Park, J. M., & Chang, J. Y. (2019). Bacterial diversity in Korean temple kimchi fermentation. *Food Res Int*, *126*, 108592.

Matsushita, T., Sakuma, M., Tazawa, S., Hatase, T., Shirasaki, N., & Matsui, Y. (2017). Use of gas chromatography–mass spectrometry–olfactometry and a conventional flask test to identify off-flavor compounds generated from phenylalanine during chlorination of drinking water. *Water research*, *125*, 332-340.

Nsogning Dongmo, S., Sacher, B., Kollmannsberger, H., & Becker, T. (2017). Key volatile aroma compounds of lactic acid fermented malt based beverages - impact of lactic acid bacteria strains. *Food Chem*, *229*, 565-573.

Priest, F. G. (2011). Rapid identification of. *Brewing Microbiology*, 305.

Pswarayi, F., & Gänzle, M. (2022). African cereal fermentations: A review on fermentation processes and microbial composition of non-alcoholic fermented cereal foods and beverages. *International Journal of Food Microbiology*, *378*, 109815.

Rottiers, H., Tzompa Sosa, D. A., Van de Vyver, L., Hinneh, M., Everaert, H., De Wever, J., Messens, K., & Dewettinck, K. (2019). Discrimination of cocoa liquors based on their odor fingerprint: A

- fast GC electronic nose suitability study. *Food Analytical Methods*, *12*, 475-488.
- Shen, S., Wu, H., Li, T., Sun, H., Wang, Y., & Ning, J. (2023). Formation of aroma characteristics driven by volatile components during long-term storage of An tea. *Food Chemistry*, *411*, 135487.
- Smit, B. A., Engels, W. J., & Smit, G. (2009). Branched chain aldehydes: production and breakdown pathways and relevance for flavour in foods. *Applied microbiology and biotechnology*, *81*, 987-999.
- Statista. (2023). Revenue of the beer market worldwide by country in 2023.
- Tano, M. B., Aka-Gbezo, S., Atchelouwa, C. K., & Koussémon, M. (2020). Use of lactic acid bacteria as starter cultures in the production of Tchapalo, a traditional sorghum beer from Côte d'Ivoire. *Am. J. Food Sci. Health*, *6*, 23-31.
- Tkacz, K., Chmielewska, J., Turkiewicz, I. P., Nowicka, P., & Wojdyło, A. (2020). Dynamics of changes in organic acids, sugars and phenolic compounds and antioxidant activity of sea buckthorn and sea buckthorn-apple juices during malolactic fermentation. *Food Chemistry*, *332*, 127382.
- Wang, G., Song, X., Zhu, L., Li, Q., Zheng, F., Geng, X., Li, L., Wu, J., Li, H., & Sun, B. (2022). A flavoromics strategy for the differentiation of different types of Baijiu according to the non-volatile organic acids. *Food Chem*, *374*, 131641.
- Woo, S.-H., Park, J., Sung, J. M., Choi, E.-J., Choi, Y.-S., & Park, J.-D.

- (2023). Characterization of Lactic Acid Bacteria and Yeast from Grains as Starter Cultures for Gluten-Free Sourdough. *Foods*, 12 (23), 4367.
- Yan, Y., Chen, H., Sun, L., Zhang, W., Lu, X., Li, Z., Xu, J., & Ren, Q. (2022). The changes of microbial diversity and flavor compounds during the fermentation of millet Huangjiu, a traditional Chinese beverage. *PLoS One*, 17 (1), e0262353.
- Yao, H., Su, H., Ma, J., Zheng, J., He, W., Wu, C., Hou, Z., Zhao, R., & Zhou, Q. (2023a). Widely targeted volatileomics analysis reveals the typical aroma formation of Xinyang black tea during fermentation. *Food Res Int*, 164, 112387.
- Yao, H., Su, H., Ma, J., Zheng, J., He, W., Wu, C., Hou, Z., Zhao, R., & Zhou, Q. (2023b). Widely targeted volatileomics analysis reveals the typical aroma formation of Xinyang black tea during fermentation. *Food Research International*, 164, 112387.
- Yao, L., Mo, Y., Chen, D., Feng, T., Song, S., Wang, H., & Sun, M. (2021). Characterization of key aroma compounds in Xinjiang dried figs (*Ficus carica* L.) by GC–MS, GC–olfactometry, odor activity values, and sensory analyses. *LWT*, 150, 111982.
- Yu, H., & Bogue, J. (2013). Concept optimisation of fermented functional cereal beverages. *British Food Journal*, 115 (4), 541-563.
- Zhang, L., Hu, Y., Wang, Y., Kong, B., & Chen, Q. (2021). Evaluation of the flavour properties of cooked chicken drumsticks as affected by sugar

smoking times using an electronic nose, electronic tongue, and HS-SPME/GC-MS. *LWT*, *140*, 110764.

Zhang, M., Chen, X., Hayat, K., Duhoranimana, E., Zhang, X., Xia, S., Yu, J., & Xing, F. (2018). Characterization of odor-active compounds of chicken broth and improved flavor by thermal modulation in electrical stewpots. *Food Res Int*, *109*, 72-81.

Zhou, J., Yang, S., Ma, Y., Liu, Z., Tu, H., Wang, H., Zhang, J., Chen, Q., He, W., Li, M., Lin, Y., Zhang, Y., Wu, Z., Zhang, Y., Luo, Y., Tang, H., Wang, Y., & Wang, X. (2023). Soluble sugar and organic acid composition and flavor evaluation of Chinese cherry fruits. *Food Chem X*, *20*, 100953.

Conclusions

This study highlights the significant potential of LAB strains isolated from kimchi in enhancing the health-promoting properties of fermented products. The antioxidant activity of these LAB strains was confirmed through various assays, including DPPH, ABTS, and OH radical scavenging activities. The LAB strains also demonstrated strong reducing potential, lipid peroxidation inhibitory effects, and enhanced antioxidant enzyme activity. Transcriptomic and proteomic analyses indicated that these strains activate cellular processes and intracellular metabolism to combat oxidative stress, thus supporting their role in oxidative damage mitigation.

Furthermore, the health-promoting effects of LAB-fermented VJ were examined by analyzing the metabolites generated through LAB fermentation. Using advanced metabolite profiling techniques, significant metabolite changes were observed in the LAB-fermented VJs, with a notable positive correlation between these compounds and their antioxidant capacities. Six functional active ingredients, including organic acids, phenols, and amino acids, were identified, indicating the beneficial effects of LAB fermentation on antioxidant activities. Specifically, *C. allii* WiKim39 and *L. lactis* WiKim0124 strains were found to be promising for the development of probiotic beverages due to their enhanced antioxidant properties.

In addition to antioxidant benefits, VJ fermented with WiKim39 and WiKim0124 effectively reduced fat accumulation *in vitro* and *in vivo*. The study proposed ILA, PLA, and LA as potential bioactive compounds with lipid accumulation inhibitory effects. These findings suggest that these kimchi LAB strains can be used as functional starters for plant-based foods, providing a foundation for developing probiotic beverages aimed at preventing obesity progression.

Moreover, sensory analysis of LAB-fermented malt wort beverages revealed that the addition of specific starters significantly affects the sensory properties, including sourness, bitterness, and sweetness perception. Insights from e-nose and e-tongue analyses underscored the multitude of metabolites influencing flavor and aroma formation, enriching the understanding of LAB starters in sour beer production.

In summary, these studies collectively support the use of kimchi LAB strains as functional starter cultures to enhance the antioxidant properties, sensory attributes, and overall health benefits of various fermented foods. Future research should focus on further elucidating the underlying mechanisms, optimizing fermentation processes, and exploring the full spectrum of health benefits these LAB strains can offer.

국문초록

프로바이오틱스는 식물성 식품, 음료, 시리얼과 같은 식품에 응용될 수 있으며 소비자들에게 프로바이오틱스를 제공하는 대체 수단으로 새로운 선택지를 제공함과 동시에 건강학적 이점을 제공할 수 있다. 프로바이오틱스에 대한 관심 연구 분야는 특정 2차 대사 산물을 식별하고 유용성분을 규명하는 방향으로 확장되고 있다. 이러한 포스트바이오틱스는 식품 가공, 저장 과정 및 위장관 내 소화 과정을 견디며 다양한 생리적 이점을 제공한다. 이에 따라 건강 증진 효과를 갖춘 프로바이오틱스 강화 제품에 대한 수요가 증가하고 있다. 그러나 과학적으로 개발된 프로바이오틱스 제품은 맛과 향미가 감소하여 감각적 수용도가 낮아지는 문제가 발생할 수 있으며, 이는 소비자의 기호도 감소로 이어질 수 있다.

본 연구의 구체적인 목표는, 1) 김치유래 유산균의 항산화 효과를 조사하고, 과산화수소에 노출되었을 때 산화 스트레스에 저항하는 잠재적 메커니즘을 전사체와 단백질체 수준에서 탐구, 2) 유산균 발효 과채 주스(VJ)의 대사산물 규명: 초고성능 액체 크로마토그래피-사중극자 비행시간형 질량분석기(UPLC-

QTOF-MS)와 가스 크로마토그래피-질량분석기(GC-MS)를 이용한 발효 VJ에 존재하는 파이토케미컬 분석 및 이 대사산물과 향산화 특성 간의 상관관계 비교, 3) 발효된 VJ가 체내 지방 축적에 미치는 영향을 시험관 내(*in vitro*) 및 생체 내(*in vivo*)에서 검증 및 그 유용성분 규명, 4) 대사체 프로파일 결과와 전자 혀 및 전자 코 기술을 활용하여 유산균으로 발효된 맥아 음료의 맛 인식 패턴, 향미 구성 및 관능품질특성을 조사하는 것이다.

김치는 한국 전통 발효식품으로, 그 기능적 특성은 널리 보고되어 왔다. 저장 기간 동안 김치 내 유산균은 발효를 통해 김치에 함유된 성분을 변화시켜 독특한 풍미와 건강에 유익한 생리 활성 화합물을 생성한다. 따라서 김치 유래 유산균은 김치의 다양한 건강 기능성과 밀접한 관련이 있다.

전국에서 수집한 김치를 발효하며 분리한 35,000여 종의 유산균 중, 식품에 적용할 때 우점화 가능성이 높은 5종의 균주를 사전에 선별하여 실험에 사용하였다.

김치 유산균 5종의 잠재적인 향산화 활성을 비교한 결과 *Latilactobacillus curvatus* WiKim38, *Companilactobacillus allii* WiKim39, 그리고 *Lactococcus lactis* WiKim0124는 더 높은 환원력, 지질 과산화 억제 효과, 및 향산화 효소 활성을

나타내었다. 과산화수소수에 노출된 유산균을 대상으로 RNA 시퀀싱을 이용한 전사체 데이터와 2차원 겔 전기영동으로 단백질체 프로파일 분석을 수행하였다. 그 결과 유산균이 산화 스트레스에 대응하여 세포막, 세포 내 대사, 그리고 세포 과정을 활성화하는 것을 확인하였다. 이를 통해 유산균의 항산화 특성에 대한 잠재적 원천으로 김치 유산균의 온전한 세포, 세포 추출물, 및 그 대사산물에 있는 것으로 추정하였다. 따라서, 프로바이오틱 유산균의 항산화 활성 메커니즘에는 자체 항산화 효소 및 항산화 대사산물의 생성, 세포벽 단백질 내 항산화 과정을 조절 또는 조절 경로 활성화, 그리고 활성산소종 생성 효소의 하향 조절이 포함될 수 있음을 예측하였다.

이를 통해 항산화 효능이 가장 우수한 두 종류의 김치 유산균, WiKim39와 WiKim0124를 최종 선정하고, 이를 기능성 유산균으로 발효식품에 적용하는 연구를 수행하였다.

4가지 작물 품종을 혼합하여 만든 음료에 유산균을 첨가하여 제조한 프로바이오틱 VJ의 발효 대사산물과 그 항산화 특성을 조사하였다. 이전에 확인된 두 가지 균주(WiKim39와 WiKim0124)가 VJ에 접종되었으며, 이들의 특성은 비표적 UPLC-QTOF-MS 및 GC-MS를 사용하여 분석을 수행하였다. 또한, 발효물에서 라디칼 소거 활성 등 항산화 활성을 평가하였다.

발효된 VJ는 총 페놀 화합물의 증가와 함께 향상된 항산화 능력을 나타내었다. 발효 과정에서 d-류신산(LA), 인돌-3-유산(ILA), 3-페닐유산(PLA) 수치가 크게 증가하였다. 이러한 대사산물은 상관관계 분석에서 항산화 특성과 유의미한 양의 상관관계를 나타내었다. 이러한 결과는 유산균 발효 VJ가 가질 수 있는 건강상의 이점과 밀접한 관련이 있으며, WiKim39와 WiKim0124로 발효된 VJ는 생리활성에 유리한 효과를 나타낼 것으로 예측하였다.

항산화 특성은 활성산소를 감소시켜 염증과 지방 축적을 억제함으로써 항비만 효과를 촉진한다. 이에 따라, 다음 연구에서는 항산화 활성이 우수한 WiKim39와 WiKim0124 균주가 항비만 효능도 나타내는지 조사하였다. 유산균 단독으로 또는 발효 VJ 형태로 식품 매트릭스와 함께 섭취하였을때의 효능을 비교하였으며 *in vitro* 및 *in vivo*에서 활성을 평가하였다. 이 균주들은 염증성 사이토카인의 유전적 발현을 자극하여 면역 기능을 향상시키고 지질 축적을 효과적으로 억제하는 것으로 관찰되었다. 또한, 발효된 VJ는 유산균을 단독으로 섭취한 경우보다 효능이 뛰어나, 식품 매트릭스에서 유산균 발효를 통해 생성된 대사산물의 생체 이용률이 확대된 것으로 예측하였다. 특히, 발효된 VJ의 유용 대사산물인 LA, ILA, PLA는 인간 중간엽

줄기세포에서 지질 축적이 개선된 것을 확인하였다.

다음으로, 관능 품질이 개선된 발효 음료를 개발하고자 하였다. 이를 위해 식물성 식품이 발효 과정 중 화합물 구성 변화가 감각적 특성에 미치는 영향을 탐구하였다. 실험에는 사전에 선발된 우점화 가능성이 높은 김치 유산균 5종에 발효 속도 증진용 유산균 2종을 추가하여 사용하였다. 그 결과, 맥아 음료에서 우점화와 발효 속도 증진에 탁월한 *Levilactobacillus brevis* WiKim0194 유산균이 선발되었다. 이후 WiKim0194로 발효된 맥아 음료의 향 구성과 풍미 인식을 조사하는 것을 최종 목표로 하였다. 연구 방법으로는 고성능 액체 크로마토그래피와 GC-MS를 통한 대사체 프로파일링, 전자 혀(e-tongue) 및 전자 코(e-nose) 기술을 사용하였다. 전자 혀로 감지된 주요 미각의 차이는 신맛의 증가와 쓴맛의 감소로 관찰되었다. 발효된 맥아 음료에서 WiKim0194의 주요 산물인 젖산을 포함한 유기산은 불쾌한 쓴맛의 인식을 억제하는 것으로 예측하였다. 전자 코로 감지된 WiKim0194 발효 맥아 음료의 긍정적인 향미 특성은 각각 꽃 향기, 과일 향기, 달콤한 향기(Vanillin, citronellol, and β -damascenone)로 확인되었다. 또한, WiKim0194 발효 맥아 음료의 쓴 냄새와 불쾌한 맛은 쓴맛을 유발하는 휘발성 화합물들(chlorobenzene, 2-acetylpyridine)의 감소로 인해

쓴맛에 대한 감각적 인지도 함께 감소된 것으로 추정하였다.

본 연구를 통해 도출된 결과는 김치 유래 유산균의 건강 증진 효과를 검증하고 식품 산업에서 응용하기 위한 기초를 마련하였다. 적합한 유산균은 식품 발효에서 발효 주도용 종균으로 사용될 수 있으며, 생리활성 메커니즘과 대사 경로에 영향을 미치고, 건강 기능성 개선 또는 향상된 관능품질 특성을 통해 제품 품질을 종합적으로 향상시킬 수 있을 것으로 사료되었다. 따라서 본 연구는 발효 식품 산업에서 프로바이오틱 유산균 제품으로 응용하기 위해 종균으로 적합한 균주 선택의 중요성을 제시했다는 점에서 그 의의가 크다고 할 수 있다.

주제어: 프로바이오틱스, 종균, 기능성 식품, 대사체학, 관능평가

학번: 2021-38950